Modal analysis of bottom founded offshore wind structures via the creation of a FE model

Emeric Descourtieux

Technische Universiteit Delft

TUDelft

Modal analysis of bottom founded offshore wind structures via the creation of a FE model

by

Emeric Descourtieux

to obtain the degree of Master of Science
at the Delft University of Technology,
to be defended publicly on Tuesday July 31, 2018 at 4:30 PM.

Student number:	4509404	
Project duration:	July 26, 2017 – July 31, 2018	
Thesis committee:	Ir. P. G. F. Sliggers	TU Delft
	Ir. P. van der Male	TU Delft
	Dr. Ir. K. N. van Dalen	TU Delft

TU Delft

Acknowledgements

This master thesis is the conclusion of three years of study at the Technical University of Delft. This represents a huge success for me and an extreme satisfaction. During these three years, I had to learn how to work in English, evolve in a very international environment and constantly try to improve myself. I could not have done it alone, so I would like to thank the people who helped me in any way.

First of all, I want to thank my supervisors, Pim van der Male and Frank Sliggers, who helped me in my thesis, showing me the right direction when I was stuck in my work and always being there to answer to my questions. I would like to thank my friends from TU Delft, who helped me to go through the master. Coffee breaks have always been a good time between two intensive periods of work. A big thank you also to my fellow dancers of Rock'n Delft, it was nice to release the pressure once a week and cut me a few moments from the thesis. And at last, I would like to thank my family for supporting me and encouraging me during these three years and so much more. Thank you all.

I would like to dedicate this report to my text editor software, which decided to stop working two weeks before the deadline of this report. Thank you for this perfect timing.

Emeric Descourtieux
Delft, July 2018

Abstract

Offshore wind energy is a developing industry. One way to implement the wind turbine in the sea is to use lattice structures. Since these structures are placed offshore, they must be able to withstand all kinds of loads. One aspect of the design must take into account the natural frequencies. It is essential that the eigenfrequencies of the support structure do not correspond to the passing frequencies of the blades and any other dynamic actions. To avoid this, the natural frequencies of the structure should be estimated during the design. The objective of this MSc study is the development of an easy to use finite element model to perform the modal analysis of an offshore wind support structure. It was built based on relevant inputs, defining the possible design of the lattice structure. Based on these parameters, the model can be adjusted and a high number of designs can be tested easily.

The model is built in Matlab and consists of several modules, each one representing a different part of the design. The program is named OwjEma, for Offshore wind jacket - Eigenvalues & modes analysis. The block diagram of OwjEma is presented on Figure 1.

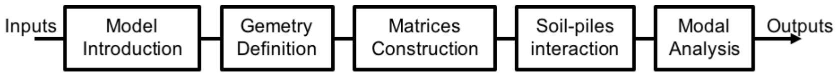

Figure 1: OwjEma block diagram

The user has access to a main script to enter all necessary inputs. Then the program starts and a second function, named FE_model_builder.m, takes over. This second function is considered as the brain of the program, in the sense that it gives orders to the other scripts and does not create outputs strictly speaking. FE_model_builder.m is divided into five parts. The first, the definition of the geometry, creates the nodes and elements composing the structure. Then, nodes are added to take into account the marine growth thickness and visualize the local modes. The second part concerns the creation of matrices characterizing the model. Each element is associated with two matrices: a local element mass matrix and a local element stiffness matrix. Each is computed in a local frame of reference, then rotated and assembled into two global matrices, representing the complete structure. To these two matrices, the effect of the environment is added: the corrosion effect, the marine growth weight and the impact of the flooded elements. Once the two matrices have been obtained, the equivalent stiffness characterizing the soil-pile interaction is calculated in the third part. This calculation is based on the p-y curves and the t-z curve model. Depending on the pile size and the soil properties, the equivalent stiffness is determined. Once the matrices completely describe the model, eigenvalues and mode shapes are calculated in the fourth part. From these outputs, the user can check whether or not the natural frequencies correspond to the passing frequencies of the blades and other dynamic loads. The fifth part of the function is the plotting of the structure.

The functionalities of the Matlab tool have been validated and thoroughly checked. Firstly by comparing the analytical and numerical results of a simplified structure (a clamped beam), and secondly using a complete structural model by comparing the outputs of the program with the outputs of the professional software *Bladed*. All key results are verified such as the geometry, the mass of the structure, the stiffness matrix, the implementation of the soil stiffness, the mass matrix, the effect of flooded members and the influence of marine growth. From these verifications, it can be concluded that the characterizing matrices of the structure are correctly defined and that the model correctly represents the modal behaviour of a lattice structure.

The tool is ready to be used for sensitivity studies to verify which parameters most affect natural frequencies. The model can also be used as a pre-design tool to quickly obtain and test different scenarios for an offshore wind support structure. This is done for a structure with three legs and four legs. Both concepts are modelled with the same parameters, in the same environment. Then, the natural frequencies of the four-legged structure are calculated. This represents the reference configuration. The inputs of the three-legged

structure are modified to obtain similar first natural frequency in both scenarios. Both models are then compared. Cost, fabrication, installation process and load resistance are estimated in both cases. In conclusion, the three-legged structure appears to be more effective than the four-legged design for these specific environmental conditions. However, this is only true for this particular case.

The tool has some limitations such as the restricted number of possible designs/configurations, the assumption that the transition piece is a rigid body, the use of the p-y curves that can overestimate the stiffness of the soil, the non-linearity of the system that does not take into account the variation in time, the axial force in the members affecting the stiffness no accounted for. Recommended future work may address these issues. Also, since the model is built with different modules, it is possible to add new features such as a dynamic response analysis section or a stress and fatigue calculation function.
The final conclusion is that the tool does what it is meant to do (i.e. quick and accurate modal analysis) and that it can be further extended by adding new functions.

Contents

List of Figures

List of Tables

Nomenclature

$\eta_{damp,i}$	Viscous damping of element i
ν_i	Poisson's coefficient of element i
ν_{soil}	Soil Poisson coeffiencient
ϕ	Soil internal friction angle [deg]
ρ_{fluid}	Fluid density [kg·m^{-3}]
σ_a	Reference pressure [Pa]
$\sigma_i(t)$	Stress of element i
σ_v	Vertical effective stress [Pa]
ε_c	Vertical strain
ε_i	Strain of element i [m]
α	Batter angle [rad]
$\alpha_{Rayleigh}$	Rayleigh mass damping coefficient
$\beta_{Rayleigh}$	Rayleigh stiffness damping coefficient
η_i	Dimensionless displacement in y - direction
γ	Soil density [kg·m^{-3}]
ω	Natural frequencies [rad·s^{-1}]
$\Phi_{y,i}$	Shear deformation parameter in the y direction of element i
$\Phi_{z,i}$	Shear deformation parameter in the z direction of element i
ρ_i	Density of element i [kg·m^{-3}]
ξ_i	Dimensionless displacement in x - direction
$\xi_{mod,i}$	Damping of mode i
ζ_i	Dimensionless displacement in z - direction
A_i	Cross section area of element i [m^2]
A_{static}	Factor for static loading
$\mathrm{a}_{local,i}$	Matrix of local displacement
$\mathrm{A}_{s,i}$	Cross sectional area effective in stress of element i [m^2]
b_1	Bottom horizontal member lenght [m]
b_{Nb}	Top horizontal member lenght [m]
C_a	Added mass coefficient
C_d	Drag coefficient

c^{*}_{ii}	Diagonal term of the modal damping matrix
c^{cr}_{ii}	Critical damping of mode i
$C_{KV,i}$	Kelvin-Voigt damping matrix
$C_{Rayleigh}$	Rayleigh damping matrix
$C^{*}_{Rayleigh}$	Modal Rayleigh damping matrix
D_{ω}	The diagonal matrix of the natural frequencies
D_{i}	Diameter of element i [m]
D_{leg}	Leg diameter [m]
D_{pile}	Pile diameter [m]
E_{anode}	Anode potential [V]
E_{i}	Young's modulus of element i [Pa]
E_{steel}	Steel potential [V]
$E^{*}_{i}(\omega)$	Complex dynamic modulus of element i
G_{0}	Initial shear modulus of the soil [Pa]
G_{i}	Shear modulus of element i - [Pa]
h0	Distance between seabed and bottom horizontal member [m]
I_{cur}	Current's intensity [A]
$I_{z,i}$	Second moment of area in the z direction of element i [m^4]
J_{i}	Polar moment of area of element i [m^4]
Jh	Jacket height [m]
k_{ii}	Shear deflection factor of element i
k_{i}	Roughness of element i [m]
k_{mod}	Initial modulus of subgrade reaction [$Pa \cdot m^{-1}$]
K_{total}	Total stiffness matrix, without the boundaries conditions
K^{*}	Modal stiffness matrix
$K_{global,i}$	Global element stiffness matrix of element i
K_{glob}	Global stiffness matrix, with the boundaroes conitions
$K_{local,i}$	Local element stiffness matrix of element i
Kc	Keulen Carpenter number
L_{bottom}	Jacket base width [m]
L_{top}	Jacket top width [m]
l_{i}	Lenght of element i [m]
M	Pile bending moment [Nm]
m_{anode}	Anode's mass [kg]

M_{total}	Total mass matrix, without the boundaries conditions
M^*	Modal mass matrix
m^*_{ii}	Diagonal term of the modal mass matrix
m_{bay}	Bay ratio of the lattice structure
$M_{global,i}$	Global element mass matrix of element i
M_{glob}	Global mass matrix, with the boundaries conitions
$M_{local,i}$	Local element mass matrix of element i
Nb	Number of bay
OCR	Soil over-consolidation ratio
p	Lateral soil resistance [N]
p_u	Static ultimate resistance [N]
q	Distributed load along the pile [N]
Q_A	Axial force on the pile [N]
Q_{cur}	Current's capacity of the anode [A.h.kg^{-1}]
Q_L	Lateral force on the pile [N]
$q_{analytical}$	The analytitcal static deformtation
$q_{numerical}$	The numerical static deformtation
q_{tip}	Pile tip resistance [Pa]
r_f	Curve lifting factor
R_{pile}	Pile radius [m]
S	Local scour depth [m]
S_t	Local scour depth at instant t [m]
s_u	Undrained shear strength [Pa]
T_i	Transfer matrix of element i
t_i	Matrix of the local frame of reference of element i
t_{mg}	Marine growth thickness [m]
$t_{protection}$	Duration of the protection [h]
T_p	Wave peak period [s]
$t_{skin,max}$	Maximum pile skin resistance [Pa]
t_{skin}	Pile skin resistance [Pa]
TPL	Distance between top horizontal member and transition piece [m]
u_{anode}	Anode efficiency factor ≈ 0,85
u_{rms}	Velocity standard deviation at seabed
u_{fluid}	Fluid velocity [m·s^{-1}]

$u_{mod,i}$	The modal displacement i
V_{ω}	The eigenmatrix
$V_{attachement,i}$	The Bladed attachement mode i
V_i	Volume of element i [m^3]
z_{eq}	Equivalent depth of the soil layer [m]
z_{if}	Dimensionless zone of influence around the pile

1
Introduction

1.1. Wind energy objective

Wind energy has been used for centuries, as evidenced by the thousands of fourteenth-century Dutch windmills. However, the first wind turbine used to produce electricity was built in 1887 by Charles Francis Brush [1849 - 1929], with a capacity of 12 kW. Today, wind turbines can reach a production of 8 MW, with a rotor diameter of 164 m (Vestas 164 - 8MW) [5]. The wind energy market has grown steadily in recent decades and will continue to grow in the coming years.
In 2015, global electricity consumption was 21.36 trillion kWh [1]. Values have increased over the last century and will continue to grow as shown in Figure 1.1. To meet the demand, new methods of energy production must be developed in a sustainable way. As of December 15, 2015, 196 countries have signed the Paris Cop 21 agreement, which aims to reduce the world to 1.5°C by reducing greenhouse gas emissions. One way to converge towards this goal is to increase the share of renewable resources in energy production.

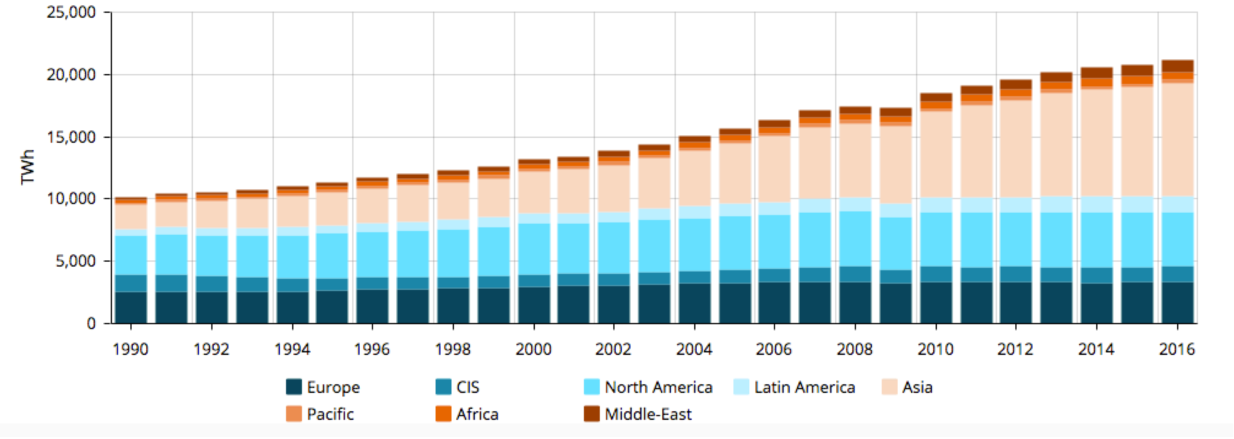

Figure 1.1: World electricity consumption - source : www.enerdata.net

The increase in wind electricity production also responds to a logic of independence from oil resources and its fluctuating prices. The price of wind energy is easier to predict in the long term since the wind is technically unlimited.

1.2. Why going offshore

Wind energy is already developed on land since it is easier to build a wind turbine onshore than at sea. Nevertheless, offshore wind has some advantages. The main reason is there is more space offshore than on land. With increasing rotor size, wind farms need larger area to be fully effective.
Another reason is visual pollution. A wind turbine in the sea will not create visual pollution of the landscape, disturbs the environment with the noise and diminish the value of the property for the inhabitants. In addition, it is safer to have no one around a wind turbine (due to collapse or falling ice from the blades).
Another aspect is that wind resources are much higher offshore than on land. Therefore, going offshore also responds to a logic of reducing the cost of the kW/h. Building a single offshore wind turbine makes no sense economically. But implementing a whole wind farm in the sea will significantly reduce the cost of production and is competitive with the onshore wind turbines.

1.3. Monopile vs Jacket

There are several types of offshore wind turbine foundations. It can be floating or structure based foundation. This report focuses only on this last category. Two concepts mainly used are the monopile and the jacket foundation type. The monopile consists of a single tubular element connected to the wind turbine through a transition piece.
The jacket is a multi-member structure, connected to the wind turbine by a transition piece. The foundation piles of the structure are driven through the legs. However, a similar structure called "tower" (not to be confused with the wind turbine's tower) has foundations attached to the legs by sleeves. Both structures are often merged into the single-term *jacket*. This is the case for this report.
If the monopile structure is used for most of the offshore wind turbine, the concept of the jacket should not be neglected. Indeed, the jacket concept is more effective than the monopile foundation in deeper waters.
However, since both structures are offshore, the design of each of them must withstand offshore conditions, such as corrosion or hydrodynamic loads.

1.4. Modal analysis objective

The modal analysis is the evaluation of the structures' eigenfrequencies and modes. These represent how the structure is deformed at a given frequency.
The foundations of offshore wind turbines must be designed in accordance with rotor and blade frequencies. The rotor rotates with a certain frequency range. This range is named 1P. As the rotor is composed of three blades (in most cases), the frequency range 3P corresponds to the frequency of passage of the blades. In order to avoid resonance, the eigenfrequencies of the structure must not be in these two ranges, 1P and 3P, as shown in Figure 1.2.

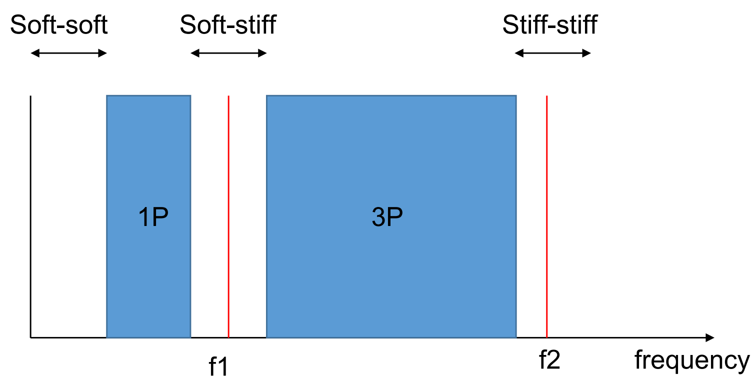

Figure 1.2: Example of rotor and blade range of frequencies

The two red lines f1 and f2 represent the first two natural frequencies of the structure. These values are supposed to be located in regions called "soft-soft", "soft-stiff" or "stiff-stiff" in order to avoid resonance with the rotor's frequency and the blades' passing frequency. Modal analysis is also used to estimate the dynamic

behaviour of a structure, depending on the modes shape and the eigenfrequencies calculated. The stress and fatigue of the structure's members can be estimated from this operation.
Therefore, modal analysis is one of the first steps in designing a structure, since its outcome influences the rest of the study.

1.5. FE model definition

The finite element method is a way of discretizing the elements of a model. This method solves the problem only for a finite number of points. As shown in the figure 1.3, a continuous element is discretized with a finite number of nodes. These nodes interact with each other according to the mathematical expressions implemented in the matrices. These matrices define the model and since they are finite, they can be implemented in a numerical algorithm.

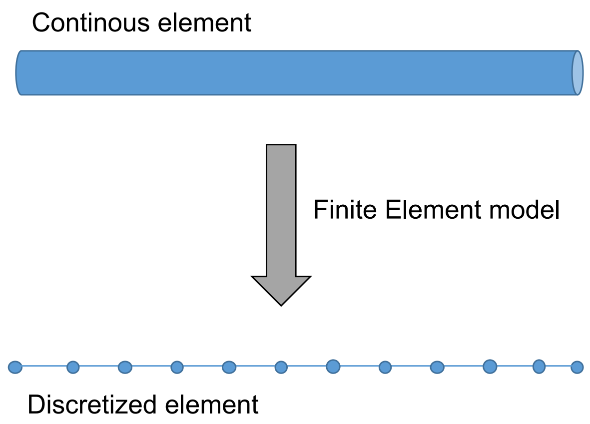

Figure 1.3: Finite element model definition

Since the model is discretized, the accuracy of the results is lower compared to an analytical method. The choice of method depends on the purpose of the model. In this case, the model's objective is to calculate the modal behaviour of an offshore wind turbine jacket. Consequently, it is more efficient to use a finite element method since we are interested in the general behaviour of the structure, and not in a specific part. In addition, the jacket is a complex structure, with many different elements. It would be too difficult and time consuming to use a continuous system for the model.
The output of such a model is the behaviour of the nodes used to discretize the elements, not the behaviour of the element itself. However, if the distance between two nodes is sufficiently small compared to the length of the element, the behaviour of the member can be approximated.

1.6. FE model objective

The finite element model developed in this report is the model of an offshore wind turbine jacket. The point of this model is to return the structure's modal behaviour, in other words, the modes shape and the associated natural frequencies. With this model, the user should have a rough idea of the final design. This model should be used to check if the structure is properly designed for the 1P rotor frequency and the 3P blade frequency. If the natural frequencies obtained are not satisfactory, the user can easily modify the model's inputs to increase or decrease the eigenvalues.
The second goal of the model is to be user-friendly, which means it must be easy to understand and use. The user must be able to customize the structure as much as possible. The idea is that anyone with little knowledge of the offshore wind industry can use this finite element model without spending too much time trying to understand it.
Finally, the model element FE, program with the software Matlab, must require a small computation effort. This means avoiding as much as possible the Matlab functions that require a lot of resources and the creation of unnecessary outputs.

1.7. Master thesis objectives

The objective of the Master thesis is to design and program on *Matlab* a finite element model of an offshore jacket that can be used to perform modal analysis. The program must return the structure's modes shape and the eigenfrequencies, but also the parameters characterizing the model such as the matrices of mass and stiffness, or the list of nodes and elements. Based on these results, the user should be able to conduct modal analysis and to get a preview of a jacket design. The second objective of the thesis is to make the model user-friendly, so it can be used and improved by someone other than the one who coded it. Inputs must be relevant, clear to everyone and easy to edit. The program must explain the calculation steps in real time, so the user knows what is happening and why during the operating time. Finally, the model must be built with different modules, which can allow an external person to modify and improve the code. Therefore, other functions can be added to the program.

This report is divided into four parts. Part I, the literature review, focuses on existing finite element models, how they work, how they are related to the offshore wind industry, and what their limitations are. Models similar to the one built in this report already exist in the offshore industry, such as Bladed, a software, developed by DNV GL. However, this program can be difficult to use and does not return the exact modes shape and eigenvalues of the offshore wind support structure. It is more a tool to optimize the design of the wind turbine. This is the subject of Chapter 2. Then, Chapter 3 of Part I details the possible inputs of a finite element model representing an offshore wind support structure. A selection among these inputs is made and implemented in the model.
After defining the relevant entries for the model, the program is constructed. Part II explains how the model is built and how the various functions of the program work. This part can also be considered as the user manual because it details the inputs, outputs and internal logic of each component of the program. The specificity of the model developed in this report is the ability to customize the structure with a finite number of entries. The geometry does not need to be calculated separately and added to the program. In this model, geometry construction and modal analysis are part of the same algorithm.
Before being used, the model must be verified. This is the subject of Part III. The different functions created are tested and compared to another finite element model: *Bladed*. This part evaluates the model by checking the results first with a clamped beam then with a multi-member structure. Several operations are performed to check the program, such as the comparison of the analytical and numerical results, the verification of the static response, the modal behaviour, the total mass and the additional mass of the structure.
Part IV details the comparison between a four-legged and a three-legged structure. This study is carried out with the previously developed program. A four-legged structure is established as a reference model. Then, a three-legged structure is modelled with the same inputs as in the reference design. The parameters of the three-legged structure are modified to obtain a similar first natural frequency in both cases. The purpose of this section is to evaluate the most appropriate design, based on cost, installation, fabrication and load resistance.

Once the model has been designed, created, and tested, it can be used by other users to perform sensitivity studies, modal analyses, or to implement new functions in the model.

I

Literature review

2

Existing models

The goal of this thesis is to create a finite element model of a wind turbine support structure. The model should be easy to use and offer the ability to customize the concept design. However, some models have already been designed. Before starting to look at how to develop a finite element model, it would be wise to check how other models work, what they offer and what their limitations are. In this chapter, several finite element modelling programs will be studied. Two are commercial software (*Bladed* and *Ansys*), while the others have been developed for a specific research project.

2.1. Bladed

The model created in this report has been designed in accordance with the DNV codes. This company has also released a software to design a wind turbine, named *Bladed*. It's a professional program with a lot of possibilities for the user. It can be used to model the rotor, the nacelle and the support structure. The part of the rotor and the nacelle is quite accurate and the large number of inputs can model precisely this element of the wind turbine.

The software has existed for twenty years, so it can be assumed that the outputs are correct and accurate. This could be a good basis for checking the validity of the finite element model design in this report.

The program wants to be able to represent any type of wind turbine support structure. Therefore, it is possible to model a monopile or multi-member structure, an onshore or offshore wind turbine, or even a floating structure. But the consequence of this large amount of possibility is that there is no quick option for pre-designing a structure. The way elements of a structure are entered in the software makes impossible to create the design without external tools. Since each element must be entered individually, modelling any type of wind turbine structure takes a long time. Bladed is a tool for once a pre-design of the structure is established. It should be used to optimize the design.

Another aspect of Bladed is the amount of possible outputs. Since the software is used to adjust the design, it must return a lot of information to the user. However, the downside is that Bladed acts as a black box, in the sense the calculations implemented in the code of the software are not explained. As a consequence, it can sometimes be difficult to understand how to modify the parameters that influence the results.

The aspect of Bladed directly related to the subject of this thesis is the modal analysis. In Bladed, among the possible outputs we can find the modes and the associated frequencies of the support structure. However, these modes are not the natural modes of the structure. The Bladed User's Manual states: "*The tower modes are not the natural modes of vibration of the tower. They are split into attachment modes which involve the response to a unit load in one of six directions at the nacelle attachment; and normal modes which involve no motion of the nacelle attachment node*". The modes calculated in Bladed are used to estimate the dynamic response of the structure. But strictly speaking, the eigenfrequencies and the associated deformation are not correct. This will have two consequences on the model design in this report. First, the outputs of the modal analysis should represent the actual deformation of the model corresponding to a certain natural frequency. Secondly, in order to verify the model, a specific function must be created to compute the same type of modes and frequencies as Bladed. Otherwise, comparing the two programs makes no sense.

As discussed earlier in this section, defining the geometry of the structure in Bladed can be complicated. Then, some of the outputs of the model can be the inputs for the Bladed geometry. The idea is to create a pre-design with the model,and, based on the results, implement it in Bladed for optimization.

2.2. Ansys

Ansys is a company specialized in numerical simulations, mainly with finite element models. Therefore, Ansys is not a finite element model properly speaking, but a software used to create finite element models. Nevertheless, as it is a major software in numerical simulation, and since it is used in the offshore wind industry, it makes sense to spend time learning from it.
Several options are proposed in Ansys, such as the representation of fluid dynamics, dynamic structure, thermodynamic or electromagnetic behaviour. However, with the scope of the master thesis, this section will focus on the dynamic part of the structure.
This software is a professional engineering program and it can be safely considered that the results are accurate (implying a correct use of the software). There are two ways to implement a structure: with Ansys classic or with Ansys Workbench. The first possibility helps to the design of simple structure. Consequently, it does not apply to a jacket wind support structure. The Ansys workshop is more relevant for such work, although it requires programming knowledge. Since Ansys is a general software, not specific to the offshore wind industry, many options are present, and not all are relevant to the model. Consequently, it is difficult to model a jacket quickly and easily as it is in Bladed.
Ansys can model a structure and define a mesh to simulate it. The consequence of this is accurate results. However, the mesh of a structure like a jacket can take a lot of time, and even more for the calculation. For this reason, with the objectives of designing a wind support structure, this software should be used once the pre-design has been established. Then, it can be used to model a specific part of the structure, such as the foundations or the transition piece.

2.3. Model created for a specific project

The two previous software presented are used to create models. But a lot of models of an offshore wind support structure have been developed for specific research projects. This section gives an overview of these models and what can be learn from them in the design of a finite element model of a lattice structure.
The Stabil toolbox is a list of functions developed in Matlab by the Structural Mechanic Department of the Katholieke Universiteit Leuven. This pack has been developed to assist in the creation of finite element models. It is easy to adjust and use because it is composed of different parts. The idea to create the model with different modules is helping, since it allows to program to be extended in the future. An other person can simply add a new module to the code to improve it.
In 2014, Kok Hon Chew, E.Y.K. Ng and Kang Tai [13] have created a finite element model to study the influence of the number of legs on the structure's behaviour. This parameter can be added to the model to estimate its importance.
In the Upwind report, by Wybren de Vries [15], several concepts are studied for use in deep water. For the Jacket concept, a model is created in Bladed to perform a sensitivity and cost analysis. The structure focuses on various parameters, including the impact of the type of foundation (rigid or rigid) on natural frequencies. These type of parameters can be included into the model since they seem to have an influence on the final design.

2.4. Why a new model

The conclusion of the previous section is that a finite element model alone does not mean anything. A model is created to represent something in particular. In this report, the model is created to perform a modal analysis of an offshore wind support structure. Consequently, the inputs in this model must be relevant for a modal analysis. According to the studies [15] and [13], the number of legs or the type of foundation can be an example of such inputs.
Based on the commercial software, Bladed, the model should be made specifically for the offshore wind industry, and be easy to custom. The user should be able to understand and easily access the program code. The goal is not to create a black box, but a program that can ve used by anyone with a little knowledge of the offshore wind industry.
The idea of this model is not to replicate exactly the structure, but to create a tool to established the pre-designed concept, which can be optimized in a more complex software.

3
Inputs definition

Before starting building the model, a thought must be given on which inputs and outputs are relevant for the study. So, in this chapter, different inputs are going to be defined in order to obtain an extended list of realistic offshore wind turbine support structure. This review of the entries will focus on the exciting and potential concepts of multi-member support used in the offshore wind industry. Potential because if some of the concepts are already in service, other presented in this chapter are just the combination of different brace pattern, foundation and lattice structure that have never been experienced. This part won't give an absolute overview of all the concepts, but will try to represent as much as possible the reality of this industry. The concepts will be defined with the elements presented on the Figure 3.1. In the section 3.2, the various components of the multi-member structure concepts will be detailed, such as the batter inclination, the bracing and the variation of the leg diameter. Section 3.3 will present the elements of the foundation model, which are the type of foundation, the piling procedure and the number of piles.

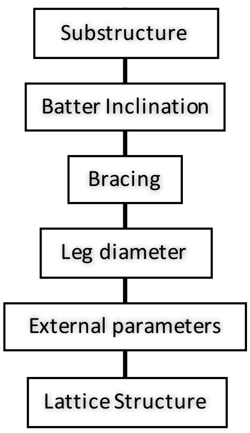

(a) Lattice Structure Overview

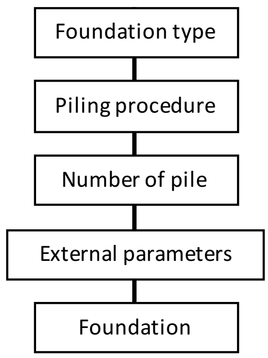

(b) Foundation Overview

Figure 3.1: Multi-Member Structure Concept Overview

In Section 3.5 of this chapter, the external parameters affecting the structure's modal behaviour will be developed (added mass, marine growth, corrosion, sacrificial anode, coating, corrosion allowance, flooded members, scour effect and soil properties). The idea is to show how the eigenvalues will be modified, and what the governing equations of these phenomena are. However, it should be noted that the presented parameters won't all be considered as inputs for the program, since they may be judged irrelevant to the study or not representative of the offshore wind industry. The idea of this chapter is to create a list of potential inputs that can be added to the model in the future. The objective is also to explain to the user what the inputs mean and how they should be used.

3.1. Terminology

Jacket: the term "jacket" relates to a certain type of foundation, where piles are driven through the legs. If the piles are connected to the substructure with a pile sleeve, the correct term to be used is tower. However, in this report the term "tower" refers to a wind turbine tower. Therefore, the term of "jacket" refers as well for the jacket and the tower substructure.
Tower: the term "tower" refers to the wind turbine tower.
Brace pattern: this term designates the layout of the non-leg members in the lattices structure. Usually it is associated to a letter representing its shape. This term is detailed in Section 3.2.3.

3.2. Substructure

3.2.1. Multi-member structure

The first step of the concept design is to choose an appropriate substructure shape. Each of them has its advantages and inconvenients. A concept should be selected based on several parameters, such as the water depth, the environmental conditions, the lifetime or the total cost. Five different options are detailed in this section. Since this report is only about multi-member structure, the monopile foundation is not considered.

The lattice structure term describes several concepts. Among them are the full truss, the jacket or the tower substructure. Each of these concepts can be conceived with three or four legs. The lattice structure is made of tubular steel elements. The wind turbine tower is connected to the substructure via a transition piece, which transfers the loads to the substructure, mainly in the axial direction.
For a **jacket** substructure, the piles are driven through the legs and then used as foundations. So, the legs must be straight and with a constant diameter to allow the passage of the foundations.
The **tower** substructure concept (not the wind turbine tower) represents a lattice structure in which the foundations are attached to the structure at the seabed. Then, the legs can be angled and offer a diameter variation.
In the **full truss** concept the rotor is directly connected to the lattice structure. Ergo, a wind turbine tower is not present in this model. A transition piece is placed at the top allowing the nacelle to rotate. This type of substructure will increase the weight and the cost of the wind turbine since it uses more steel than a *regular* lattice structure. In the three cases, the large base of the structure increases the resistance to overturning. Examples of these lattice structures are presented on Figure 3.2.

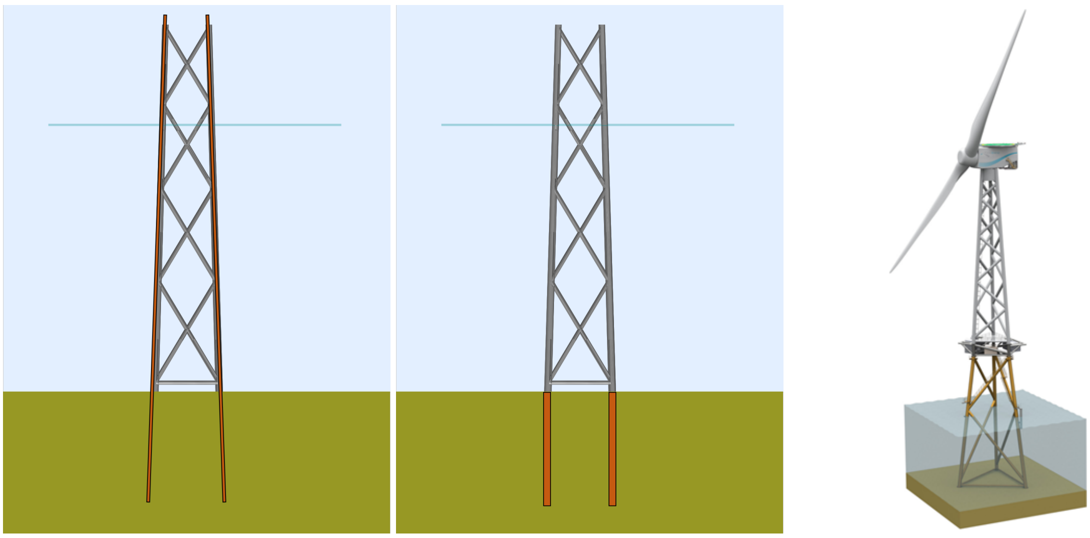

(a) Jacket concept example

(b) Tower concept example

(c) Full truss concept example

Figure 3.2: Lattice structures examples

The **tripod** [7] (see Figure 3.3) is a three-legged structure, using a small number of tubular elements. A central vertical element of large diameter transfers the load from the tower to the substructure. Relatively lightweight, the piles are driven into the seabed from 10 to 20 meters. The tripod can be used only in water depths larger than 7 meters as the steel frame prevents the vessel from approaching [2]. The loads are transfer in the axial direction and, as for the previous lattice structures, its large base prevent it from overturning. It uses less steel and nodes than a traditional substructure. However, the welding and the design are complex, which doesn't necessarily reduce the manufacturing cost. This model has been used on the wind farm *Alpha Ventus*, *Borkum*, *Global Tech 1* and *MEG Offshore 1*.

Figure 3.3: A tripod in Bremerhaven

The **twisted jacket**. The legs of this structure are twisted with an angle from 0 to 90 degrees [19], which reduce the amount of steel used and the number of nodes. This new type of substructure can reach a water depth of 60 meters. It has been installed on the wind farm *Hornsea*.

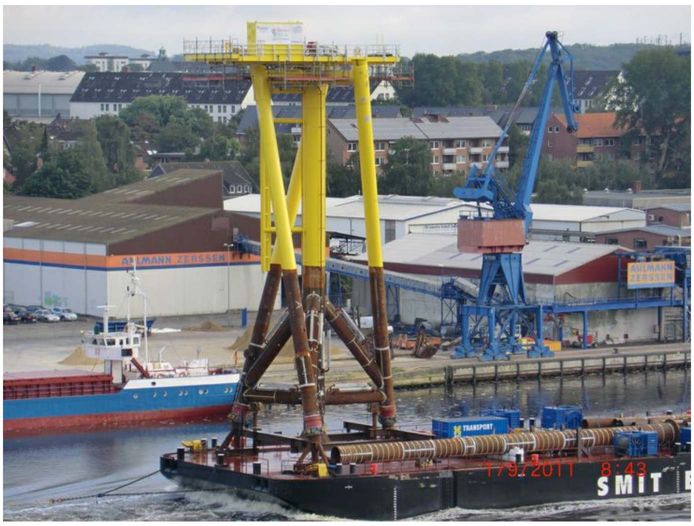

Figure 3.4: Twisted Jacket for the wind farm Hornsea

3.2.2. Batter angle

The batter angle is defined as the angle between the legs and the horizontal axis. In the case of a jacket, the batter angle should remain the same to allow the pile passing through the legs. But in the other cases, the batter angle doesn't have to be constant, which give the opportunity to build higher substructure.

3.2.3. Brace pattern

The brace pattern is defined as the configuration of the vertical, diagonal and horizontal elements between the legs. The bracing transfers the loads from the top to the base. Several type of basic bracing can be considered such as the X - brace pattern, the diagonal brace pattern and the K - brace pattern (as shown on Figure 3.5). However, the final lattice structure can be a combination of all.

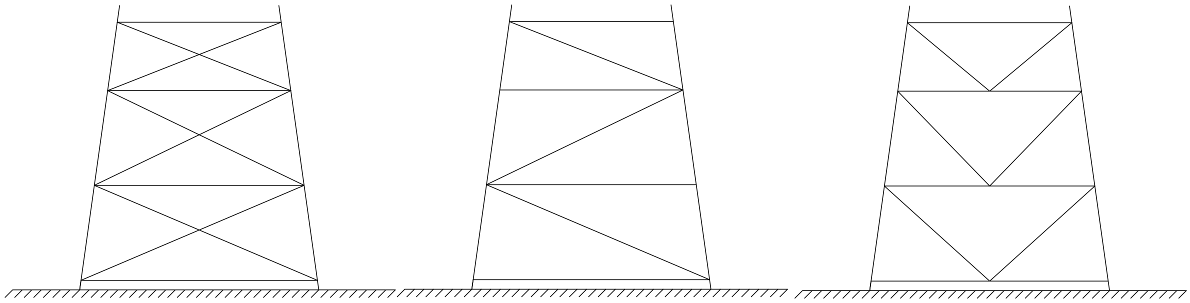

(a) X - bracing (b) Diagonal bracing (c) K - bracing

Figure 3.5: The three type of bracing

The X - brace pattern can be with or without horizontal member. The diagonal brace pattern also has some variations, presented on the Figure 3.6. The optimum bracing is the X - brace pattern and the diagonal brace pattern convergent 2, as they transfer the loads in the most efficiency way. However, other bracings exist and their influence on the structure dynamics should be tested in this report.

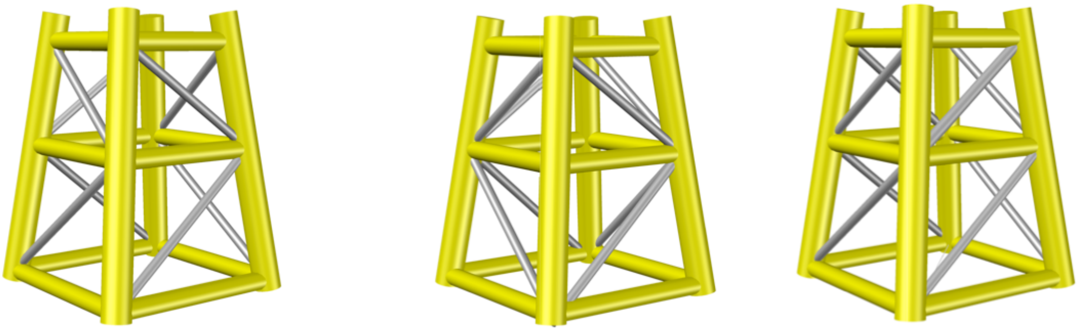

(a) Diagonal bracing convergent 2 (b) Diagonal bracing convergent 4 (c) Diagonal bracing parallel

Figure 3.6: Different type of diagonal bracing

3.2.4. Leg Diameter

In the case of very high lattice structure, the legs can be designed with a non-constant diameter. This will increase the stability without increasing too much the amount of steel used. However, this is valid only for foundations other than jackets, since the piles must be driven through the legs.

3.3. Foundation

3.3.1. Foundation type

In this report, three categories of foundation are presented: the tower foundation, the jacket foundation and the suction bucket foundation.

The tower foundation consists of using sleeve attached to the corner of each leg [10], into which the piles are driven. This can be done before (pre-piling) or after the substructure positioning (post-piling). In the case of the jacket foundation, the piles are drive into the seabed through the legs. In consequence, the batter angle should never exceed 1:6, to avoid operational problem and should also be constant.

The suction bucket, or caisson foundation represents the third foundation family in this report. It fixes the structure to the soil by pumping out the sand and the water during the installation. For this reason, there is no need to drive pile into the seabed, which reduces the noise for the marine life. This method decreases the weight of the structure and make the decommissioning easier.

3.3.2. Piling procedure

The piling procedure here is related to the tower foundation. It corresponds to the pre-piling and the post-piling.
The post-piling process consists of inserting the pile once the substructure is on the seabed, while the pre-piling consists of inserting the foundation in the soil before positioning the substructure on it. With this technique, the piling and the substructure installation can be done on different days, which will lead to a reduction in cost and to an increase in safety. However, the pre-piling requires a very accurate positing of the pile. To achieve that, a template is used. This method has been used on the wind farms *Alpha Venturis*, *Thornton Bank*, *Ormonde* and *Nordsee Ost* [3].

3.3.3. Number of piles per leg

The sleeve can be used to insert one or several piles, which will affect the structure's dynamics and stability. It should also be noted that, once in the soil, each pile has a zone of influence. Therefore, if adding several pile increase the stability of the structure, they can interact with each other, which can have unexpected consequences.

3.4. Top transition

The transition piece is placed between the substructure and the tower. It must be resistant to the bending, the loads and the shear stress throughout the lifetime of the wind turbine. The choice of the transition piece concepts depends on the type of substructure. For a tripod, it is similar to a monopile transition piece, and for the other concepts, it is similar to a classic jacket transition piece.
However, since the idea of the report is to represent the global behaviour of the structure and not only of the transition piece, it should be model as a rigid element with a mass. Different way of representing it are shown on Figure 3.7.

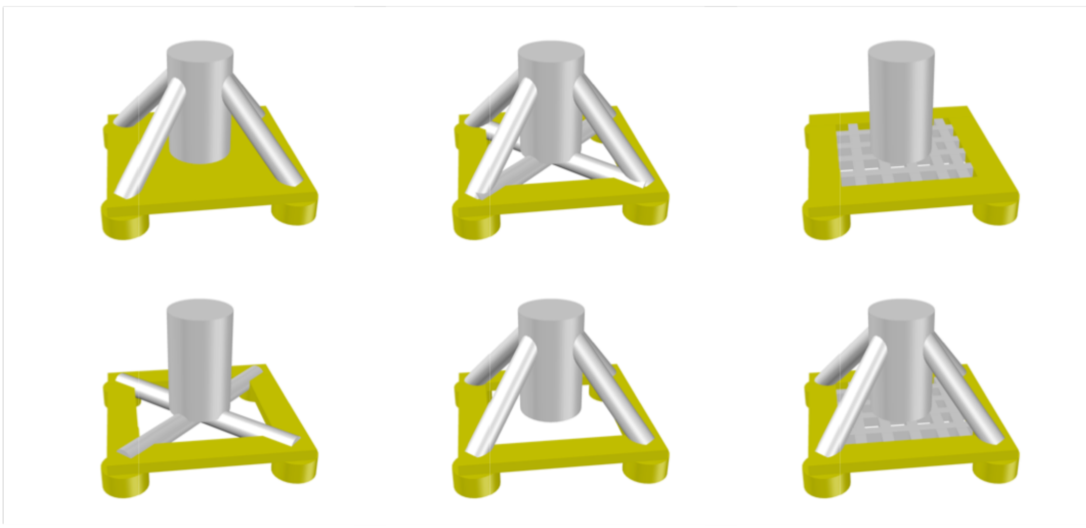

Figure 3.7: Different transition piece modelization

3.5. External parameters

3.5.1. Flooded members

Members below the sea level can be flooded or not flooded, which will change their buoyancy and mass. The legs and the brace members can be flooded separately. When flooded, the mass of the elements increases, reducing the natural frequencies. Additionally, the load exercised on the foundation won't be the same, and the dynamic of the system will be changed.

3.5.2. Material properties

The structure is mainly composed of steel, which is characterized by the yield stress, the tensile strength and the elongation before breaking, given by the DNVGL-OS-B101 and presented in Table 3.1 [8]. Steel is divided into three categories : normal strength steel, high strength steel and extra high strength steel, each defined by the previous parameters and by their chemical composition.

Type of steel	Yield stress - MPa	Tensile strength - MPa	Elongation at break - %
Normal Strength Steel	235	400 - 520	22
High strength Steel	265 - 390	400 - 660	20 -22
Extra high strength Steel	420 - 690	530 - 940	14 - 18

Table 3.1: Steel characterisation

The yield stress is related to the Young's modulus, which is used to characterize the elements of the structure. Each of them is represented with two nodes, the diameter, the thickness, the Young's modulus, the density and the Poisson's coefficient of the material. The values recommended by the DNVGL-RP-C204 [9] are presented on Table 3.2.

Material	Young's Modulus - GPa	Density - kg·m^{-3}	Poisson coefficient
Steel	210	7860	0,3

Table 3.2: Steel properties

3.5.3. Added mass

The added mass represents the inertia of the system caused by the water displacement around the structure. This added mass depends on the relative acceleration and on the added mass coefficient C_A. It can be determined using the equations provided by the DNVGL-RP-C205 [6]. This coefficient is dependant of the Keulen-Carptenter number and of the drag coefficient. If KC < 3, then $C_A = 1$. However, if KC ≥ 3, the added mass coefficient is calculated using the Equation (3.1).

$$C_A = max \begin{cases} 1 - 0,044 \cdot (KC - 3) \\ 0,6 - (C_D - 0,65) \end{cases} \tag{3.1}$$

C_D represents the drag coefficient, which can be calculated using the DNVGL-RP-C205 [6]. It depends on the element's size and on the surface's roughness, which is also given in the DNVGL-RP-C205 and presented on Table 3.3.

Material	roughness - meters
Uncoated steel	$5\cdot10^{-5}$
Painted steel	$5\cdot10^{-6}$
Highly corroded steel	$3\cdot10^{-3}$
Marine growth	$5\cdot10^{-3}$ - $5\cdot10^{-2}$

Table 3.3: Surface roughness

3.5.4. Marine growth

Every submerged structures will face marine growth. In order to correctly model the wind turbine support structure, some parameters related to marine growth must be taken into account. First, the marine growth should be considered soft (grassy type material) or hard (layers of shell) [11]. These two types will have a different density. The hydrodynamic loads will also be impacted, since the surface roughness won't be the same. The drag coefficient will be changed, and thus the added mass, as explain in Section 3.5.3. The density and the thickness of the marine growth will differ depending on the emplacement and the depth of the lattice structure, but also with the current, food supply, water temperature, salinity, Ph value, oxygen content and cathodic protection [12]. Their is an infinity of marine growth type, however, some typical thickness values depending on the region are given in the DNVGL-0S-J101: Design of Offshore Wind Turbine Structures [10] and are presented on Table 3.4. According to the DNVGL-RP-C205 the marine growth thickness is assumed to increases linearly for two years until reaching its final value [6].

	Thickness [mm]					
Water Depth	Central & Northern North Sea	Norwegian Sea	Southern North Sea	Central & Southern California	Gulf of Mexico	West Africa
-10 meters	100	60	150	200	38	100
-20 meters	100	60	100	200	38	100
-30 meters	100	60	100	200	38	100
-40 meters	100	60	100	200	38	100
-50 meters	50	30	50	200	38	100

Table 3.4: Typical marine growth thickness

In West Africa, the marine growth can reach 300 mm in the splash zone. The density of the marine growth is approximately 1325 kg.m^{-3} [10]. However, this value is just an estimation, and this report should use a larger interval when modelling the impact of marine growth.
Biofouling increases the mass of the structure and influences the drag and added mass coefficient. As a result, the damping and the added mass of the structure will be modified. [6]. Still, it won't affect its stiffness, causing a reduction in the natural frequencies [12].

3.5.5. Corrosion

As the multi-member structure is made of steel and placed in the sea, corrosion must be taken into account with a protection which will reduce the risk of failure. The splash zone and the underwater part are subject to corrosion [9] and must be protected. Sacrificial anodes, coating or corrosion allowance can be used to prevent this phenomena.
Typical corrosion rate values for uncoated steel in seawater are given in Table 3.5 [17]. In freshwater, the corrosion rate is divided by two.

Zone	Corrosion rate - mm/year
Splash zone	0,15
Submerged zone	0,07
Abrasive sediment zone	0,3

Table 3.5: Typical Corrosion rates

The splash zone is the external structure's surface periodically inside and outside the water. Its size can be approximated as the wave height with a return period of 100 years [24]. This part of the structure should be carefully monitored as it is the most exposed area to corrosion.
This phenomenon must be represented carefully in the finite element model since it is not homogeneous. A member won't be corroded the same way everywhere.

3.5.6. Sacrificial anodes

A sacrificial anode is an alloy of zinc and aluminium. The interest of this protection is to be consumed instead of the steel structure. This will happen if the potential of the anode is lower than the potential of the steel.

$$E_{anode} < E_{steel} \tag{3.2}$$

Each sacrificial anode is designed for a period of time. Once the anode is completely consumed, the seawater will begin to corrode the steel structure. Therefore, the mass of the sacrificial anode must be large enough to withstand several years. The anodic mass is determined using Equation 3.3 [25].

$$m_{anode} = \frac{I_{cur} \cdot t_{protection}}{u_{anode} \cdot Q_{cur}} \tag{3.3}$$

Where:
m_{anode}: mass of the anode - kg
$t_{protection}$: duration of the protection - h
I_{cur}: current intensity - A
Q_{cur}: current capacity of the anode - A.h.kg^{-1}
u_{anode}: efficiency factor ≈ 0,85

Usually, the anode mass is between 500 kg and 1000 kg, for a design of 25 years. Each of them must be at least one meter below sea level and one meter above the seabed. At least one anode must be present per member [9]. This will lead to additional mass on the structure, which affect modes and eigenvalues.

3.5.7. Corrosion allowance

The corrosion allowance is the additional steel layer supplied to the element in the splash zone, where the sacrificial anodes are ineffective. It is designed so the members have a normal dimension at the end of the structure's life, and are able to withstand loads and stresses. However, corrosion allowance will lead to an increase in the mass and the stiffness of the members. It will also increase the global structure surface, which will modified the drag and inertia forces. All these aspects must be considered during the design of the offshore wind turbine.
The corrosion allowance is based on a minimum rate of 0,10 mm/year [9]. Consequently, for a 25 years design it should be larger than 2,5 mm.

3.5.8. Coating

Another method to prevent corrosion is the coating. The members are covered by several layers of different materials, in order to isolate them from the sea. These layers can have different compositions, as the one propose by Ramesh Singh in *Corrosion Control for Offshore Structures* [24] and presented on Table 3.6.

n°	Layer	Thickness	Density
1	EPOXY	300 μm	1,44 $g.cm^{-3}$
2	Adhesive	300 μm	
3	Solid polypropylene	8,4 mm	0,895 - 0,92 $g.cm^{-3}$
4	Solid polypropylene	30 to 40 mm	0,895 - 0,92 $g.cm^{-3}$
5	Polypropylene shield	4 to 5 mm	
6	Polypropylene foam	30 mm	0,31 - 0,35 $g.cm^{-3}$
7	Polypropylene outer shield	5 mm	

Table 3.6: Exemple of coating layer

However, this composition seems to be extreme, usually the coating thickness don't exceed a few millimetres. It might be interesting to investigate on the impact of such a protection on the structure.

3.5.9. Scour effect

The scour effect is caused by the moving water. It represents the hole in the soil appearing around a submerged body. Its intensity is related to the structural design and the soil properties. The pile diameter and the distance between the legs will have a large influence.

The scour effect is broken down in two parts:
- the **local scour** around each pile. It is caused by a horseshoe vortex, generated by a change in the surface elevation [7]. The piles' diameter and the Keulen-Carptenter number have a direct impact on the scour intensity.
- the **global scour** around the complete structure. It is caused by the variation of the flow velocity and the turbulence generated by the piles [26]. So, it depends on the chosen concept. The more "transparent" the structure is, the smaller the scour effect will be. The number of piles and their configuration is then taken into account.

The scour effect generates a hole around the piles and the structure, which reduces its stability and may even leads to a structural failure. This risk is important and should be taken into account during the design process.
According to the DNVGL-ST-0126 [7], the local scour effect is related to the Keulen-Carpenter number KC, such as :

$$KC = \frac{1,41 \cdot u_{rms} \cdot T_p}{D_{leg} + t_{mg}} \tag{3.4}$$

Where u_{rms} the standard deviation of velocity at seabed, T_p the wave peak period, D_{leg} the leg diameter and t_{mg} the marine growth thickness.
If KC $\geqslant$ 6, the scour depth is expressed as:

$$S = 1,3 \cdot (D_{leg} + t_{mg}) \cdot (1 - e^{-0,03 \cdot (KC-6)}) \tag{3.5}$$

If KC < 6, no scour effect is observed, since no horseshoe vortex is formed.
The local scour effect doesn't appear suddenly, but develops over the years. The time development of the scour effect is given by Equation 3.6.

$$S_t = S \cdot (1 - e^{-\frac{t}{T_1}}) \tag{3.6}$$

Where T_1 is a coefficient calculated with the DNVGL-ST-0126 [7].

3.5.10. Soil properties

The foundations of the substructure are assumed to be vertical piles in this report. They are modelled as beam with a constant cross section and their interactions with the soil are calculated by the use of p-y and t-z curves. This represents the non-linear stiffness of the soil and it depends on the soil's type (sand or clay), the internal friction angle, the vertical strain and the untrained shear strength. An appropriate way to define the p-y and t-z curves is described in *DNVGL-OS-J101 Design of Offshore Wind Turbine Structures* [10].
Since the soil can be composed of several layers, the effect of one on the other is incorporated to the model, as explain by Lymon C. Reese and Willem van Impe [23]. The model of the pile-soil interaction can be viewed on Figure 3.8.

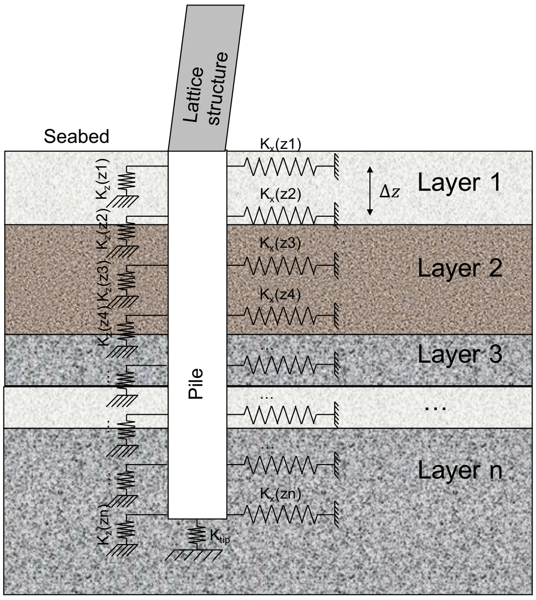

Figure 3.8: Example of pile-soil interaction in a multilayer soil

3.6. Inputs overview

Once all the inputs are identified, the lattice structure and the foundations are defined. Figure 3.9 and Figure 3.10 present all the possible combinations. It should be remembered that in the case of a jacket foundation, the batter angle and the legs diameter must be constant, otherwise the piles won't be able to pass through the legs. These two figures do not represent the actual possibility of the model, but what can be done by the addition of extra features. Moreover, this list of inputs is not exhaustive and can be completed by the user.

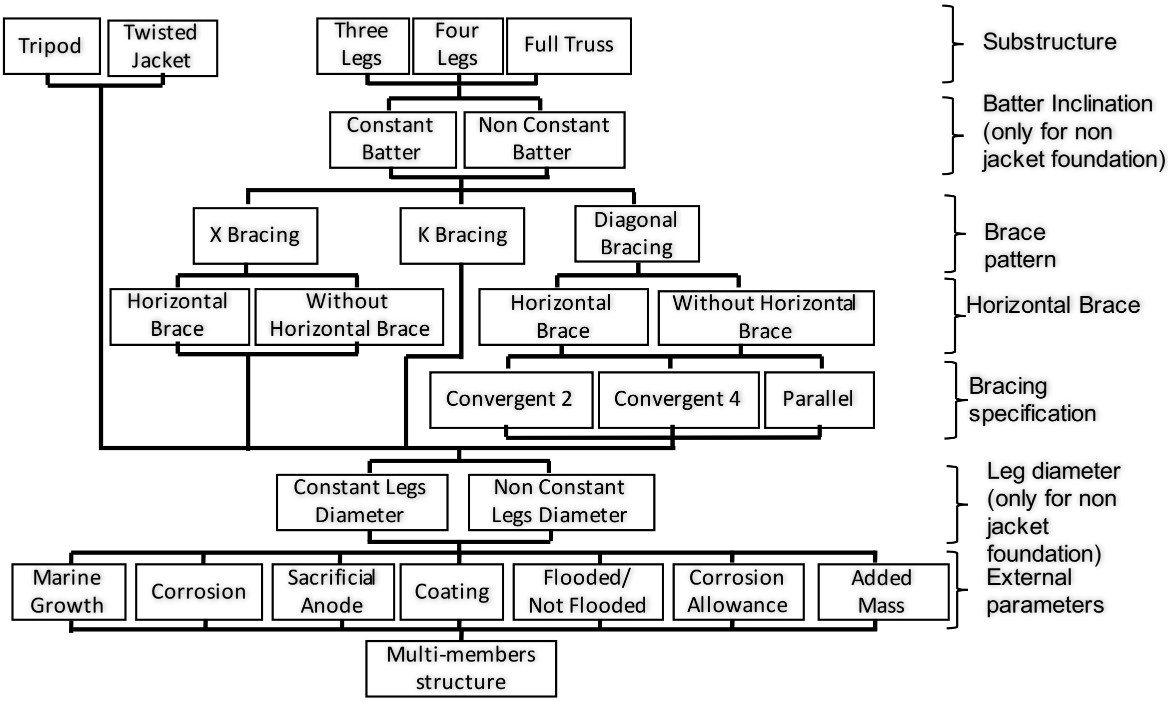

Figure 3.9: Overview of the lattice structure possibility

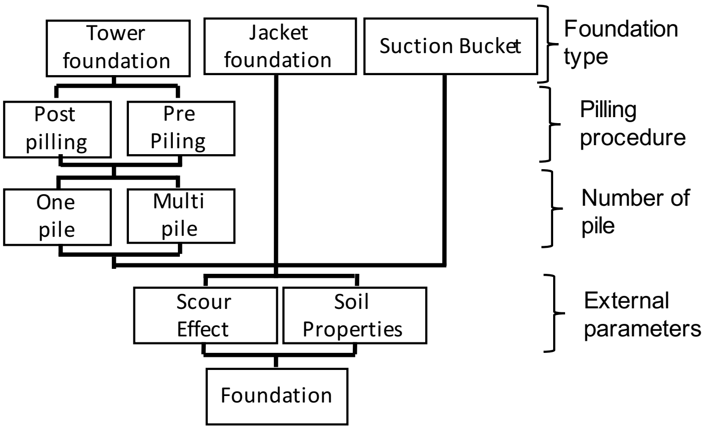

Figure 3.10: Overview of the foundation possibility

The model design in this report is based on the possibilities presented in Figure 3.9 and Figure 3.10. However, it has been decided to exclude for now the concepts of tripod and twisted jacket as they are less representative of the offshore wind industry than the three legs and four legs structures. The full truss concept has been rejected for the same reason. The simplified list of inputs is presented on Figure 3.11. It has also been decided to consider for now to only vertical pile foundation.

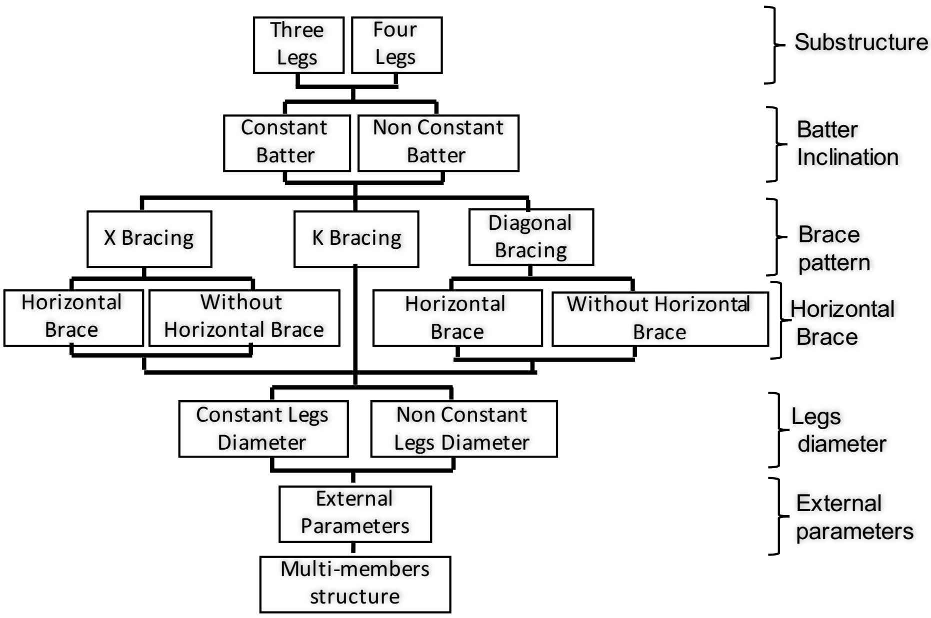

Figure 3.11: Model final inputs overview

II

Finite Element Model Construction

4

Model Introduction

In Part I, relevant inputs to a finite elements model of of wind turbine jacket have been identified, such as geometric, material, environmental and soil properties inputs. While not all these parameters are going to be used by the program (as explained in Section 3.6), this gives an idea of the kind of wind support structure that can be designed. This second part explains how the program, named OwjEma (for **O**ffshore **w**ind **j**acket - **E**igenfrequencies & **m**odes **a**nalysis), is constructed in Matlab and how the different scripts interact with each other. It describes the logic behind the algorithms and details the different functions. This first chapter gives an overview of the model architecture and a short description of the functions.These functions are described more in detailed in the next chapters.

4.1. Terminology

- *Model*: this term designates the interpretation of the reality, under which scope it is defined and how it can be numerically represented.
- *Finite Element Model*: this specifies that the model is constructed with a finite element logic. It implies discretized structure's elements.
- *Algorithm*: The algorithm is composed by all the logical steps taken by the model.
- *Program*: The program is the numerical interpretation of the algorithm, where all the steps are written in a language that can be interpreted by a software. It this case, the software is Matlab.
- *Script*: In the same way the program is the numerical interpretation of the algorithm, the scripts are the numerical interpretation of the logical steps of the algorithm.
- *Function*: It has a more global definition than the script. It is composed of a script that returns outputs for given inputs.
- *Matlab functions*: The Matlab functions are the functions already implemented in Matlab and not build for this program.
- *Model architecture*: It is the way the program is constructed, how the functions interact with each other and in which order. It can be considered as the "road" the model is taking.

4.2. Model Architecture

The model architecture is shown on Figure 4.1. It represents the path taken by the program. This figure is composed of six orange squares, each one representing a different part of the program. These parts are associated to different chapters: the geometry definition (Chapter 5), the matrices construction (Chapter 6), the soil-pile interactions (Chapter 7), the modal analysis (Chapter 8) and the response analysis (Chapter 9). The first part, *model introduction* is treated in the present chapter. The blue square symbolizes the functions, with the inputs and outputs of each one.

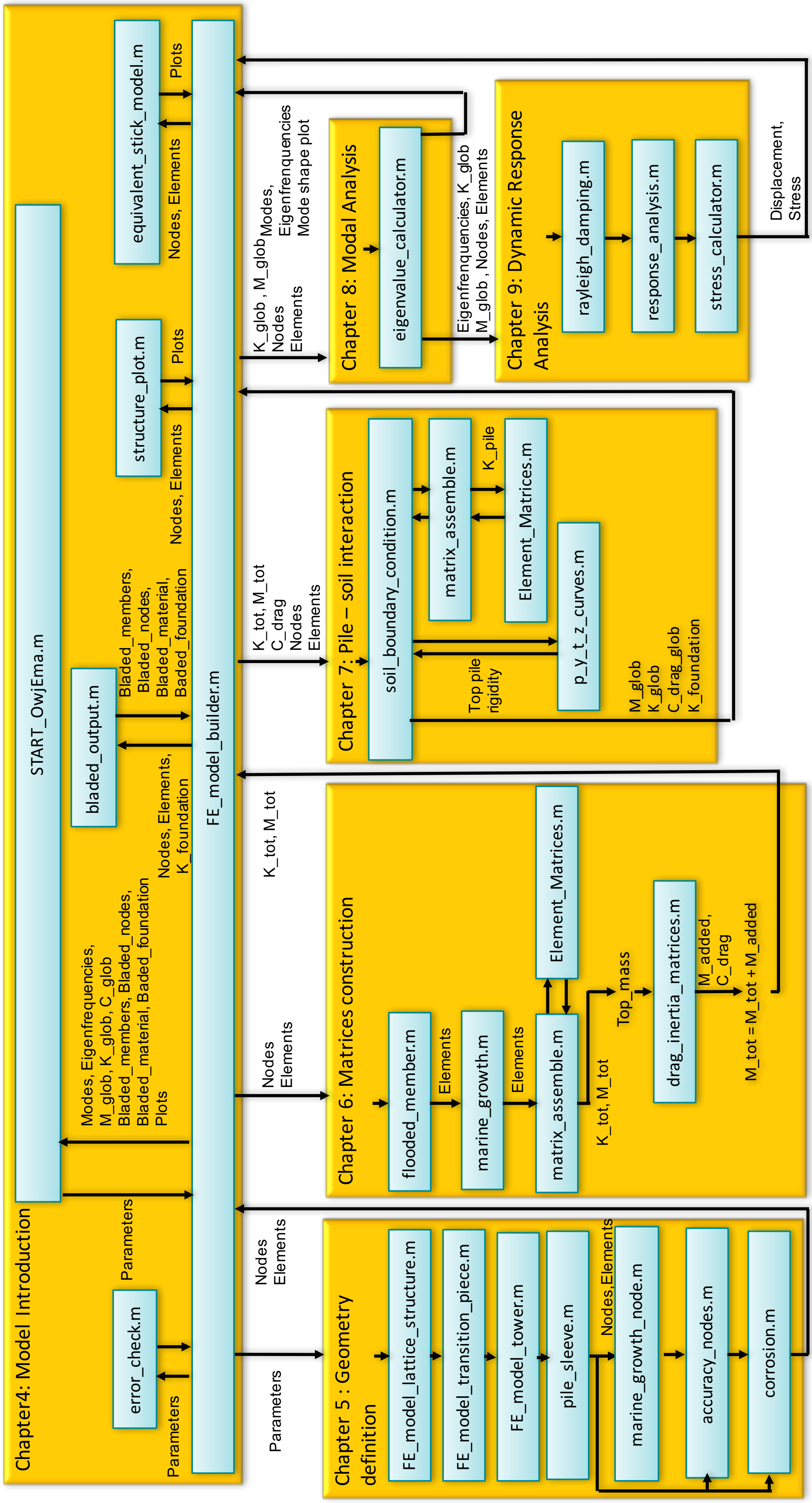

Figure 4.1: OwjEma architecture

4.3. List of the functions

This section presents the list of the function developed for OwjEma (except for the function *cone.m* which has been coded by Waldemar Swiercz and downloaded from the website mathworks.com [4]). This list briefly describes the goal of the functions. Each of them are detailed in the next chapters.

Function	**Description**
accuracy_nodes.m	Creates extra nodes and elements in order to increase the model accuracy
bladed_output.m	Returns files that can be copied and pasted in the software Bladed
cone.m	Constructs a cylinder connecting two centers points. (coded by Waldemar Swiercz and downloaded from the website mathworks.com [4])
corrosion.m	Reduces the members wall thickness caused by the corrosion
drag_inertia_matrices.m	Calculates the added mass and the drag coefficients
eigenvalue_calculator.m	Calculates the modes and the eigenvalues of the model.
Element_Matrices.m	Returns the mass matrix and the stiffness matrix of one tubular element
equivalent_stick_model.m	Calculates the equivalent stick model and plots the results
error_check.m	Checks if the inputs are correctly entered by the user
FE_model_builder.m	Executes all the scripts related to the finite element model
FE_model_lattice_structure.m	Creates a finite element model of the lattice structure
FE_model_tower.m	Creates a finite element model of the tower
FE_model_transition_piece.m	Creates a finite element model of the transition piece
flooded_member.m	Calculates the buoyancy of the structure according to the flooded option selected by the user. It adds to the mass matrix the water's weight
marine_growth.m	Adds the mass relative to the marine growth in the total mass matrix.
marine_growth_node.m	Creates extra nodes and elements to take into account the marine growth
matrix_assemble.m	Transforms the elements matrices from the local frame of reference to the global frame of reference. Then the total mass matrix and the total stiffness matrix are assembled.
p_y_t_z_curves.m	Calculates the piles displacement according to the structure weight and the statics forces applied on the top of the pile.
pile_sleeve.m	Creates the members representing the effect of the pile sleeves.
rayleigh_damping.m	Defines the Rayleigh damping matrix
response_analysis.m	Determines the response to an harmonic load applied on the rotor
soil_boundary_condition.m	Includes the soil stiffness in the total stiffness matrix and create the global mass matrix and the global stiffness matrix
START_OwjEma.m	This is the main script, the one used to enter the inputs
stress_calculator.m	Calculates the stress and the fatigue associated to the selected nodes
structure_plot.m	Creates the figures in 3D of the complete structure

Table 4.1: List of the functions created for OwjEma

4.4. START_OwjEma.m

The user only uses the main function: START_OwjEma.m. It is where all the inputs are defined. A copy of the script START_OwjEma.m showing all the inputs can be found in Appendix A. The entries can be divided into five categories: environmental (Table 4.2), material properties (Table 4.3), geometric (Table 4.6), soil characteristics (Table 4.4 and Table 4.5) and the plot options. Each category is represented by a different section in START_OwjEma.m, to avoid confusion for the user.

Input	**Description**	**Unit**
msl	Mean sea level	meter
rho_w	Sea water density	kg.m^{-3}
splash_zone	Amplitude of the splash zone. The splash zone is defined in Section 3.5.5.	meter
u_current	Current velocity	m.s^{-1}
current_dir	Current direction	rad
T	Wave period	s
wave_a	Wave amplitude	meter
wave_dir	Wave direction	rad
mg_region	Geographical region (for the marine growth)	-
mg	Marine growth thickness. If the region is unknown, the average marine growth is entered here. Otherwise it should be entered 'N'	meter
rho_mg	Marine growth density	kg.m^{-3}

Table 4.2: Environmental inputs description

Input	**Description**	**Unit**
rho_s	Steel density	kg·m^{-3}
E_s	Steel Young's modulus	Pa
nu_s	Steel Poisson's coefficient	-
rho_TP	Transition piece density	kg·m^{-3}
E_TP	Transition piece Young's modulus. It should be noted that, in order to make the transition piece rigid, its Young modulus is higher than the one of the rest of the structure.	Pa
nu_TP	Transition piece Poisson's coefficient	-

Table 4.3: Material inputs descriptions

The soil is considered to be made of different layers of sand and clay. Therefore, the parameters are entered by the user in a table, where each line represents a layer. An example of it is shown on Table 4.4. In addition, to the soil parameters, the foundation inputs are defined in Table 4.5.

Layer ID	Top layer type	Layer depth [m]	γ [kg·m^{-3}]	ϕ [deg]	s$_u$ [Pa]	ε [-]	ν [-]
1	2	0	8000	0	25000	0.02	0.3
2	1	2	8000	30	0	0	0.3
3	2	4	10000	0	100000	0.005	0.3

Table 4.4: Example soil parameters inputs

Where:
- Layer type: represents the nature of the layer, sand = 1, clay = 2
- Layer depth: represents the depth at which the top of the layer is - meter
- γ: represents the layer density - kg·m^{-3}
- ϕ: represents the layer friction angle - degree (for sand only)
- c$_u$: represents the layer undrained shear strength - Pascal (for clay only)
- ε: represents the layer verticals strain (for clay only)
- ν: represents the layer Poisson coefficient

Input	Description	Unit
Lf	Pile length	meter
Df	Pile outer diameter	meter
t_fun	Pile wall thickness	meter
Delta_z	Step interval for the p-y and t-z curves computation. It has to be kept in mind that the value of Delta_z needs to be smaller than the smallest layer thickness. Otherwise, the model won't take into account all the layers to estimate the soil equivalent stiffness.	meter
F_x	Static load at the top of each pile in the x direction	N
F_y	Static load at the top of each pile in the y direction	N
stiffness_type	Specifies how the equivalent pile stiffness is calculated: rigid foundation = 0, linear stiffness = 1 and tangential stiffness = 2. If *stiffness_type* = 0, all the soil parameters are disregarded.	-
Pile_sleeve	Specifies the presence of pile sleeve or not ('Y' or 'N')	-
Pile_sleeve_mass	Represents the pile sleeve mass	kg
Pile_excentricity	Represents the pile sleeve distance form the leg	meter

Table 4.5: Foundation pile inputs description

The geometric inputs are summarized in Figure 4.2 and Table 4.6. However, this figure represents only the case when the batter angle is constant. If not, the lattice structure is defined as shown on Figure 4.3.

Input	Description	Unit
lifetime	Designate the lifetime of the structure, used to calculate the corrosion	year
L_max	Maximum length of each element	meter
NL	Number of legs. Can be 3 or 4	-
Dl_bottom	Outer leg diameter at the sea bed	meter
Dl_top	Outer leg diameter at the top	meter
tl_bottom	Leg wall thickness at the sea bed	meter
tl_top	Leg wall thickness at the top	meter
Fl_leg	Specifies if the legs are flooded or not ('Y' for yes, 'N' for no)	-
Fl_brace	Specifies if the brace members are flooded or not ('Y' for yes, 'N' for no)	-
BA	Specifies if the batter angle is constant or not ('Y' for yes, 'N' for no)	-
Bay_inter	Represents the number of bays in the lower part of the structure if the batter angle is not constant	-
Dt_bottom	Outer tower diameter at the transition piece	meter
Dt_top	Outer tower diameter at the top	meter
Tt_bottom	Tower wall thickness at the transition piece	meter
Tt_top	Tower wall thickness at the top	meter
M_nacelle	Mass of the nacelle	tons
M_rotor	Mass of the rotor	tons
Rotor_inertia	Rotor moment of inertia	$kg.m^2$
Yaw_inertia	Yaw moment of inertia	$kg.m^2$
Nacelle_length	Nacelle length (for visualization only)	meter
Nacelle_height	The nacelle length (for visualization only)	meter
Nacelle_width	Nacelle length (for visualization only)	meter
blade_size	Length of the blades (for visualization only)	meter
Bracing_type	Defines the type of bracing(X , Z or K, see section 3.2.3) by entering 'X', 'Z' or 'K'.	-
Nb	Represents the number of bays	-
Horizontal_member	Defines the presence or not of horizontal members between each bay with the value 'Y' for yes and 'N' for no	-
D_brace	Outer brace members diameter	meter
t_brace	Brace members thickness at the top	meter

Table 4.6: Geometric inputs description

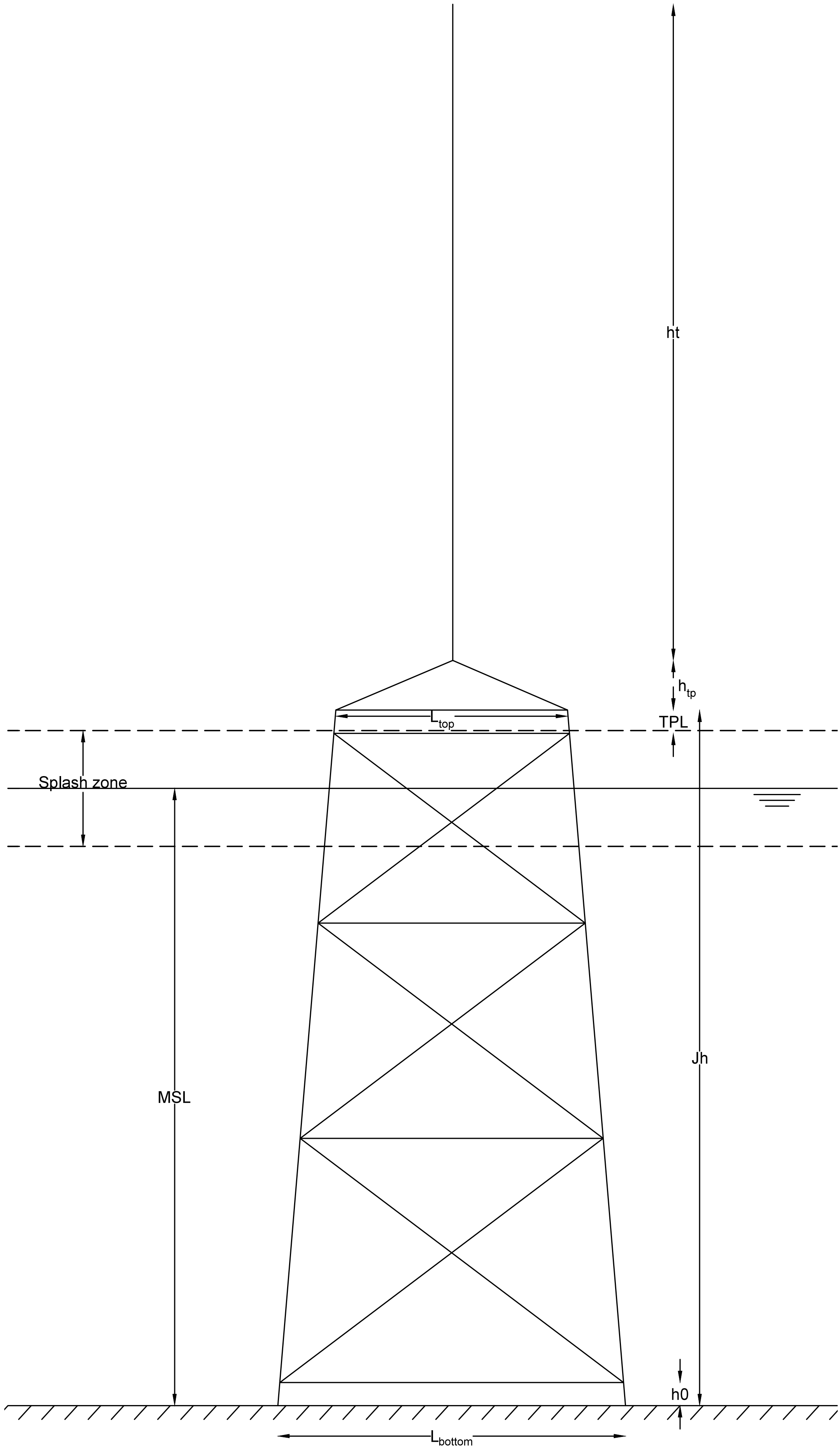

Figure 4.2: Lattice structure inputs geometry parameters

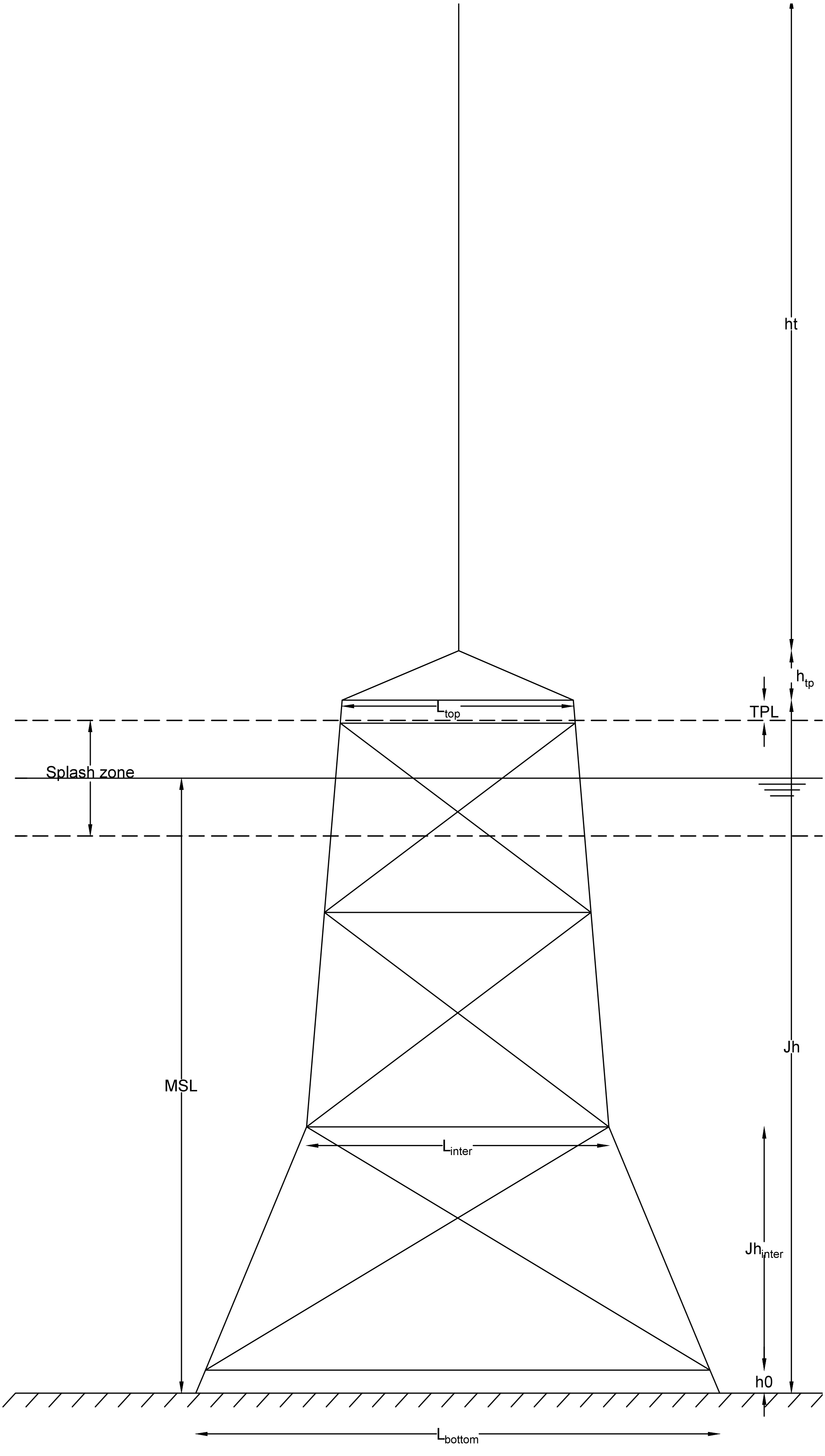

Figure 4.3: Lattice structure inputs geometry parameters with non constant batter angle

The plot options inputs consist in asking the user which modes shape should be plotted, if the structure should be plotted and if yes if it should be plotted with lines or with volumes.

4.5. FE_model_builder.m

Once the user launches the program, the script FE_model_builder.m takes over. It can be described as the brain of the program. This function activates the scripts related to the inputs and saves the outputs. All the inputs defined in START_OwjEma.m are saved in a file named *Inputs*. This file is transmitted to the different functions of the program.
The first step of the function is to check the inputs. This is detailed in Section 4.6. Then the function activates the scripts related to the geometry (Chapter 5),such as FE_model_lattice_structure.m, FE_model_transition_piece.m, FE_model_tower.m, marine_growth_node.m, accuracy_nodes.m and corrosion.m. The result of this operation is the creation of two outputs: the list of the nodes and the list of the elements, which are detailed in Section 5.8. These two lists are then transferred to the relevant functions.
Then the FE_model_builder.m script activates the global matrices construction (Chapter 6) with the functions Element_Matrices.m, matrix_assemble.m, flooded_member.m, marine_growth. In this part two new outputs are created, the global mass matrix and the global stiffness matrix. The drag_inertia_matrices.m script creates the added mass matrix and the hydrodynamic damping matrix. These two are also returned to the user and are used in the response analysis section. These outputs are part of the ones returned to the user after being updated to account for the soil stiffness.
The soil-pile interactions (Chatper 7) are represented by an equivalent soil stiffness at the top of each foundation pile. Such an operation is done by using the function soil_boundary_condition.m. This function activates three other functions: the matrix_assemble.m and the Element_Matrices.m to establish the foundation stiffness matrix and the p_y_t_z_curves.m script to calculate the soil resistance. This part of the FE_model_builder.m script updates the mass, stiffness and damping matrices, which are now the definitive versions shown to the user and also the ones used for the modal analysis.
After the computation of the nodes, the elements and the matrices, FE_model_builder.m activate the eigenvalue_calculator.m script (Chapter 8). This function uses the Matlab function *eig* to calculate the mode and the eigenfrequencies. However, the main part of that script is the plotting of the selected mode shapes. In this part, new outputs are created for the user : the eigenmatrix, the eigenfrequencies and the mode shapes plots.
All the previous section were the core of the program, the user cannot disable them. It is not the case of the next part, the response analysis. If the input modal_displacement_analysis = 'N', the scripts rayleigh_damping.m , response_analysis.m and stress_calculator.m are not activated. Otherwise, based on the choice of the user, the program will determined the displacement, the loads and the stress exercising on the selected nodes in the selected directions.
The last part of FE_model_builder.m concerns the activation of the scripts bladed_output.m (Section 4.7) and structure_plot.m (Section 4.8).
The outputs of FE_model_builder.m are the outputs of the program: a list of nodes, material, elements, the matrix of the equivalent soil stiffness, the eigenfrequencies, the eigenmatrix and the global mass, stiffness and damping matrices of the system.

4.6. error_check.m

Before starting building the model, the inputs have to be checked, in order to verify if they have been correctly entered by the user. This is done with the function *error_check.m*. If an input is wrongly enter (such as a negative value, an impossible combination of parameters or a typo) the function stops the program and returns an error message indicating which parameter is incorrect and which value should be entered. The *error_check.m* function doesn't have a proper output, it is only used to ensure that the program doesn't crash during the running, which could lead to a waste of time for the user. The other objective is to obtain accurate results by making sure the inputs are correct.

4.7. bladed_output.m

This objective of the script is to rewrite the outputs (the list of nodes, the list of elements and the soil equivalent stiffness) in a Bladed compatible form. The new outputs can be copied and pasted in Bladed and are easier to understand for the user. An example of the nodes output is presented on Table 4.7.

Node	Height - m	Local x - m	Local y - m	Point mass - kg	Foundation
1	-50	-6	-6	0	Rigid
2	-48	-5,94	-5,94	0	-
3	-29,06	-5,40	-5,40	0	-
4	-11,86	-4,91	-4,91	0	-
5	3,78	-4,46	-4,46	0	-
:	:	:	:	:	:
144	90	0	0	0	-

Table 4.7: Example of the output Bladed_nodes

The bladed_member output is presented on Table 4.8. Each member is defined by two lines in the bladed_member output table, each one representing one extremity of the element. The "sealed" column specifies if the member is sealed or not. It influences the structure's buoyancy. In the same way, the "flooded" column specifies if the member is flooded or not.

Member	Node	Diameter - m	Wall - mm	Material Id	Flooded	Marine thickness - mm	Sealed
1 (End 1)	1	1,28	53,70	1	N/A	100	Yes
1 (End 2)	2	1,28	53,05	1	N/A	100	Yes
2 (End 1)	2	1,27	51,77	1	N/A	100	Yes
2 (End 2)	3	1,28	53,7	1	N/A	100	Yes
:	:	:	:	:	:	:	:
466 (End 1)	142	0,73	20	2	N/A	0	Yes
466 (End 2)	143	0,73	20	2	N/A	0	Yes
467 (End 1)	143	0,73	20	2	N/A	0	Yes
467 (End 2)	144	0,73	20	2	N/A	0	Yes

Table 4.8: Example of the output Bladed_members

The column "Material Id" of Table 4.8 directly refers to an other outputs of bladed_output.m: the Bladed_material. It associated to an ID all the material properties. An example is shown on Table 4.9.

Material Id	Density[$kg{\cdot}m^{-3}$]	Young modulus [$N{\cdot}m^2$]	Shear modulus [$N{\cdot}m^2$]
1	8500	2.10E11	8.07E10
2	8500	2.10E13	8.07E12

Table 4.9: Example of the output Bladed_material

The column "Foundation" of Table 4.7 refers to the soil stiffness. In the case of rigid foundation (if stiffness_type = 0), no soil stiffness matrix are created since the degrees of freedom of the piles are constrained. In the other cases, the foundation equivalent stiffness is named "Sand1" and the matrix associated is presented on Table 4.10.

	Δx	Δy	Δz	θx	θy	θz
Fx	5,44E8	0	0	0	0	0
Fy	0	5,44E8	0	0	0	0
Fz	0	0	6,41E8	0	0	0
Mx	0	0	0	0	0	0
My	0	0	0	0	0	0
Mz	0	0	0	0	0	0

Table 4.10: Example of output Bladed_stiffness_foundation

4.8. structure_plot.m

This function creates 3D plots of the structure. Based on the temporary lists of nodes and elements, the outputs of this section can be visualized on Figure 4.4. It can be noticed from Figure 4.4a that the nodes due to the marine growth and the splash zone are correctly implemented. Figure 4.4a represents the skeleton of the structure, the location of the nodes and the definition of the elements. On the other hand, Figure 4.4b is here only for visualization, since the lines plotted on Figure 4.4a can be difficult to distinguish from each other. However, Figure 4.4b takes more time to draw since it uses 3D elements. It is advisable to not use it when performing several simulations in the row. It should be used only for final visualization.

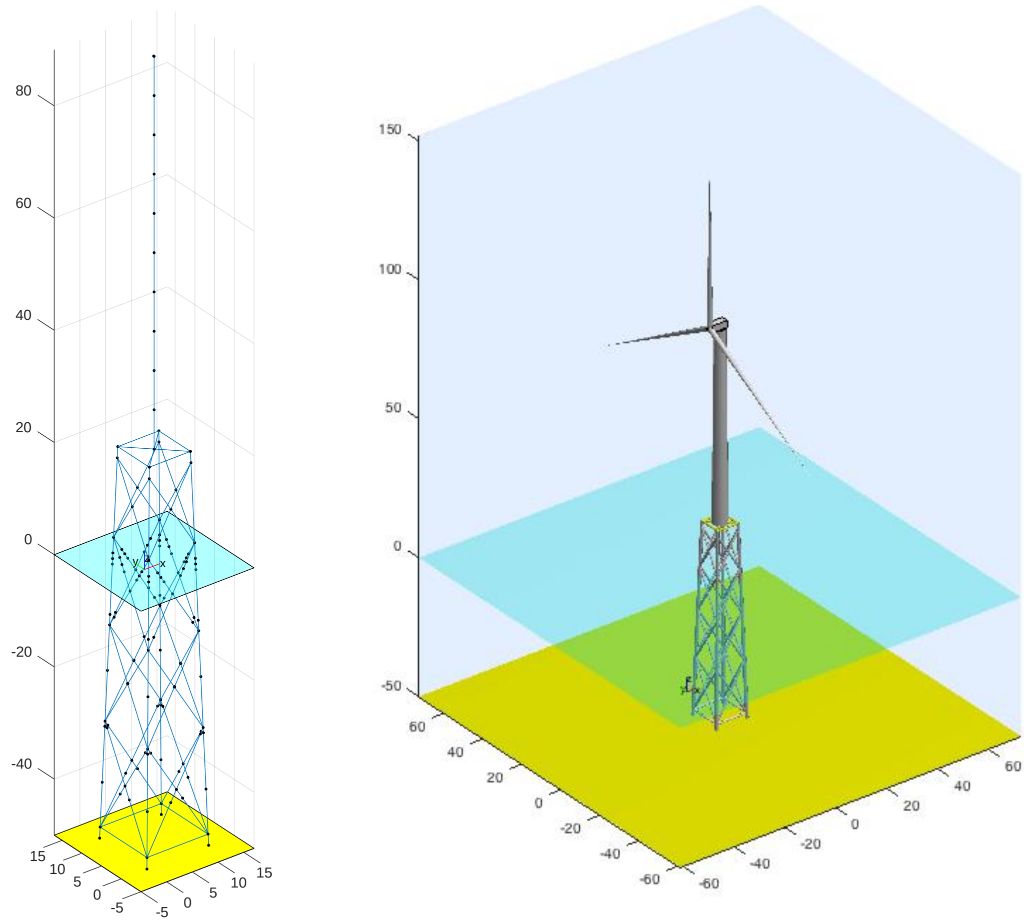

(a) Structure with nodes and elements as line

(b) Structure represented with cylinders

Figure 4.4: Geometry outputs - visualization

4.9. equivalent_stick_model.m

To estimate the transparency of the structure and calculate the hydrodynamic forces applied to the structure, the model of the equivalent stick is computed. Although this operation is outside the scope of the study, it is considered as the next step in the design process. The equivalent stick model returns the equivalent drag and inertia diameters at each depth. These values are used in the Morison equation. An example of an equivalent stick model is shown in Figure 4.5.

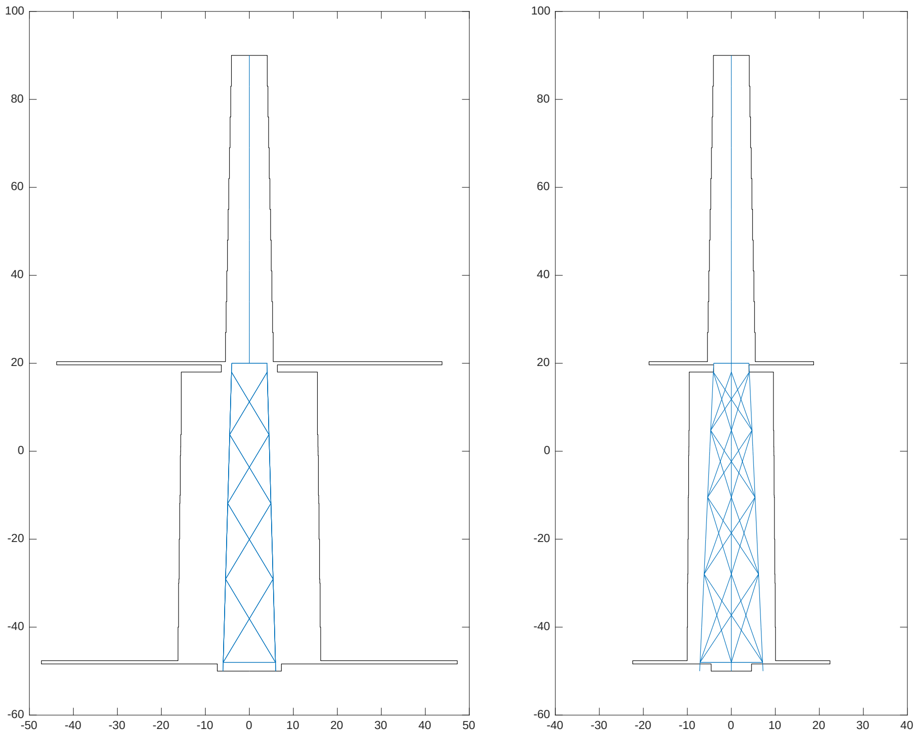

(a) Equivalent inertia diameter

(b) Equivalent drag diameter

Figure 4.5: Example of equivalent stick model

The equivalent diameters are based on the diameter, length and inclination of the elements. The direction of the hydrodynamic loads is also taken into account. However, it should be remembered that this equivalent stick model is an estimate and therefore, the results of the Morison equation are approximations.

5
Geometry Definition

The first step of the program is to define the geometry of the structure. This corresponds to the creation of the nodes and elements.
This chapter deals with the structure geometry definition. It details how the program interprets the inputs related to the lattice structure, the transition piece and the tower. The structure is geometrically built by the functions described in this chapter, which are:
- FE_model_lattice_structure.m
- FE_model_transition_piece.m
- FE_model_tower.m
- pile_sleeve.m
- marine_growth_node.m
- accuracy_nodes.m
- corrosion.m
The construction of the scripts associated to the geometry has been designed carefully to optimize the calculation and to reduce the computational effort. Figure 5.1 shows how these different functions interact with each other.

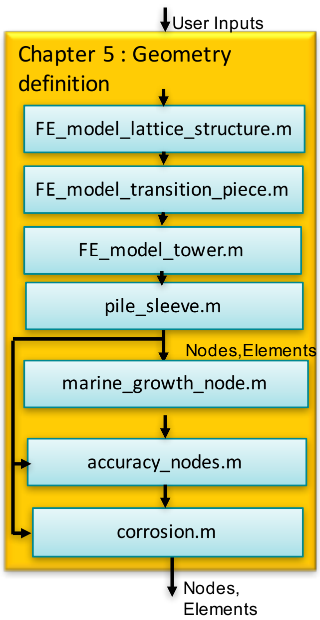

Figure 5.1: Geometry definition section

The nodes and the elements of the model are defined with the functions FE_model_lattice_structure.m,

FE_model_transition_piece.m, FE_model_tower.m and pile_sleeve.m. Then the nodes corresponding to the marine growth are added to the model with script marine_growth_node.m. The function accuracy_nodes.m adds extra nodes to the different members, to allow the computation of the local modes shape. The last step of this part is to reduce the elements wall thickness according to the corrosion effect.
The temporary outputs of this section are named Nodes and Elements, which correspond to a list of nodes and elements describing the structure. These outputs are saved in the memory of FE_model_builder.m function in order to be used as inputs in other program's functions.

5.1. FE_model_lattice_structure.m

This function defines the lattice structure geometry. In order to reduce the computational effort, only one face of the lattice structure is calculated. Then the symmetries are used to reproduce this face and model the complete jacket.

5.1.1. Batter angle

The batter angle, as defined in section 3.2.2, is the angle between the legs and the horizontal axis. The following demonstration is made for a constant batter angle, but the logic is the same for a structure with a non constant batter angle. The only difference is that two m ratios will have to be calculated.
According to the inputs notation, the batter angle is:

$$\alpha = \frac{L_{bottom} - L_{top}}{2 \cdot Jh} \tag{5.1}$$

This value is used to define the length of the top and of the bottom member. Nb is the number of bay.

$$b_1 = L_{bottom} - 2 \cdot h_0 \cdot tan(\alpha) \tag{5.2}$$

$$b_{Nb} = L_{bottom} - 2 \cdot (Jh - TPL) \cdot tan(\alpha) \tag{5.3}$$

5.1.2. m ratio

The lattice structure is defined according to a ratio m_{bay}. Each bay height is a multiple of this ratio. It is based on the number of bays, the jacket height and the width of the top and bottom. The m_{bay} ratio is defined as follow: the dimensions of each bay are equal to the dimensions of the previous one multiply by the m_{bay} ratio.
In other words, $dim_n = m_{bay} \cdot dim_{n-1}$. Then, if Nb number of bays are present:
$dim_2 = m_{bay} \cdot dim_1$
$dim_3 = m_{bay} \cdot dim_2$
:
$dim_{Nb} = m_{bay} \cdot dim_{Nb-1}$
Consequently, the first and last bay dimension can be related with the following equation:

$$dim_{Nb} = m_{bay}^{Nb} \cdot dim_1 \tag{5.4}$$

If we replace dim_{Nb} by b_{Nb} and dim_1 by b_1, the m_{bay} ratio can be determined.

$$m_{bay} = (\frac{b_{Nb}}{b_1})^{\frac{1}{Nb-1}} \tag{5.5}$$

So, the heigh of each bay can be express with m :
$h_2 = m_{bay} \cdot h_1$
$h_3 = m_{bay} \cdot h_2$
:
$h_{Nb} = m_{bay} \cdot h_{Nb-1}$
Since the sum of all the bays height is known (in this case it is J_h - h_0 - TPL), all the dimensions of the structure can be easily calculated:

$$\sum_{i=1}^{Nb-1} h_i = \sum_{i=1}^{Nb-1} m_{bay}^i h_1 = J_h - h_0 - TPL \tag{5.6}$$

$$h_1 = \frac{\sum_{i=0}^{Nb-1} m_{bay}^i}{Jh - h_0 - TPL} \tag{5.7}$$

5.1.3. Legs definition

Now that each bay height is found, the coordinates of each node in the first leg are calculated. The nodes are located at each junction between a brace member and the leg. This list of nodes is then used to describe the elements. Each member is represented by an identification number, two nodes, the diameter and the wall thickness at each node, the Young's modulus, the Poisson's coefficient, the material density and the material ID. Other parameters will be added latter, such as the marine growth and the added mass coefficient.
Once this first leg is defined, it is duplicated and rotated to create the other legs of the jacket. This operation reduces the computational time, although its impact is not very significant.

5.1.4. Braces definition

The brace pattern is defined according to the value of Brace_pattern (X, Z or K) and Horizontal_member ('Y' or 'N') entered by the user, the diameter and the wall thickness. Here again, only the bays of the first face are calculated. In the case of an X bracing, an additional node must be added to each bay. It represents the junction between the two diagonal members.
This section offers five possibilities to customised the brace pattern, which are presented in Figure 5.2. It can be noticed that the top and bottom horizontal members are always present. The input Horizontal_member only concerns the horizontal members between the braces.

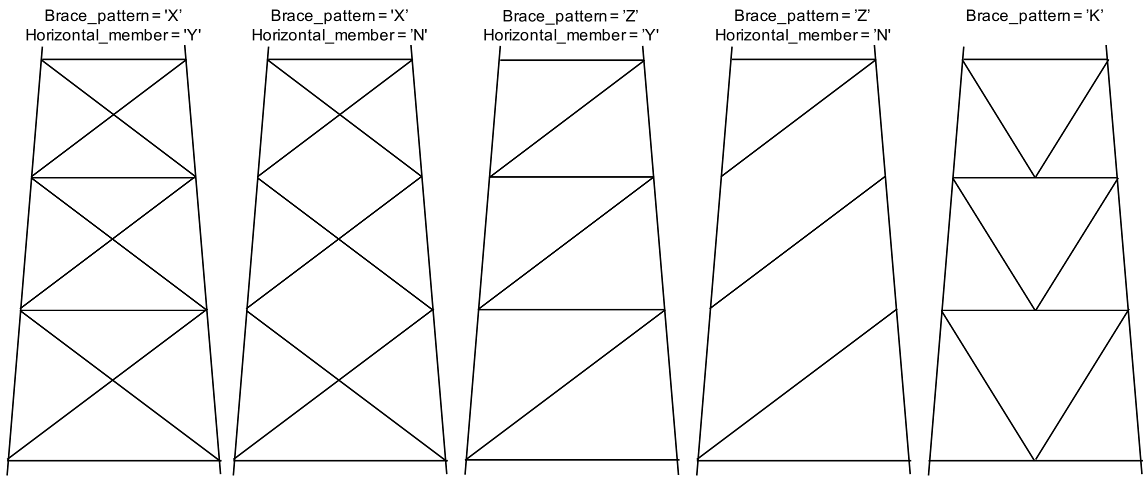

Figure 5.2: Brace patterns

5.2. FE_model_transition_piece.m

The complete structure is defined from the seabed to the top. Therefore, after the jacket definition, the transition piece (between the substructure and the tower) is calculated. However, the goal is not the represent the exact behaviour of this part, but the overall displacement. As a result, the transition piece is defined as extremely rigid compared to the rest of the structure. This is done by increasing the Young modulus of the transition piece, which the user can do by modifying the input E_TP. This value should be high enough compare to the Young modulus of the rest of the structure, represented by the input E_s. As an example, if E_s = 2,10e11 Pa and E_TP = 2,10e13 Pa, the transition piece is considered as extremely rigid.
The transition piece is composed of four horizontal members (three in the case of a three legs structure) between the upper nodes of each leg, and four (three) diagonals members between the upper nodes of each leg and the node at bottom of the tower(named transition piece node). It is represented by the yellow elements on Figure 5.3.

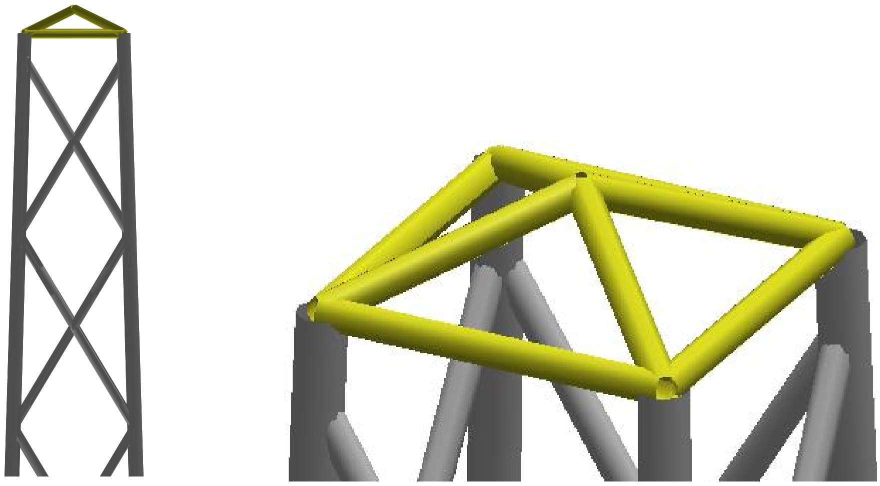

(a) Transition piece and lattice structure

(b) Zoom on the transition piece

Figure 5.3: Transition piece representation

5.3. FE_model_tower.m

The tower is the last part of the structure to be defined. It is composed of cylinders and supports the rotor, the nacelle and the turbine. Nevertheless, the wind turbine is not modelled geometrically, it is represented by a top mass directly added to the mass matrix. Hence, the wind turbine plotted on the 3D figure is there only for visualization. It doesn't have a physical impact on the mode and the eigenfrequencies.
The tower is modelled as a vertical element between the transition piece node and the top node (which is an additional output of this function since it is used to implement the top mass into the model). However, this doesn't make any sense for a modal analysis. For this reason, the tower is divided into a least 10 elements to have a better representation of the modes shape. The interpretation of the tower is shown on Figure 5.4.

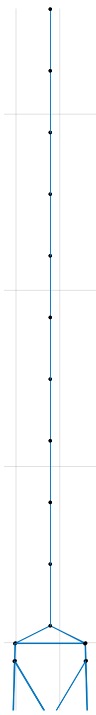

Figure 5.4: Model of the tower

5.4. pile_sleeve.m

The function pile_sleeve.m defines which nodes are connected to the foundation piles. If the rigid foundations option is selected, the nodes located at the seabed are constrained. But if the foundations are considered as stiff, the user has a choice. He can decide whether to connect the foundation piles directly to the legs, or to use a pile sleeve between the piles and the legs. This choice is characterised by the input Pile_sleeve which can be 'Y' for yes and 'N' for no.
As for the transition piece, the pile sleeves are modelled as rigid elements, in order to represent the structure's overall behaviour. The pile sleeves are represented as horizontal members, with a mass and a length defined by the user. This leads to an eccentricity between the legs and the foundation piles. This distance influences the structure's natural frequencies.

5.5. marine_growth_node.m

As for every submerged structure, the marine growth must be taken into account. As explained in section 3.5.4, the thickness of marine growth varies every 10 meters. As a result, additional nodes are added every 10 meters, from 0 to -50 meters. A visual explanation of this function is given on Figure 5.5. It can be noticed that the element numbers change thought the process although the nodes ID remain the same. It improves the computation time since the identification numbers of the nodes and the elements are equal to their line number. In consequence, it won't be necessary to use the Matlab function *find*, which significantly increases the running time. In the same way, extra nodes are added to represent the influence of the splashzone, defined in section 3.5.5.

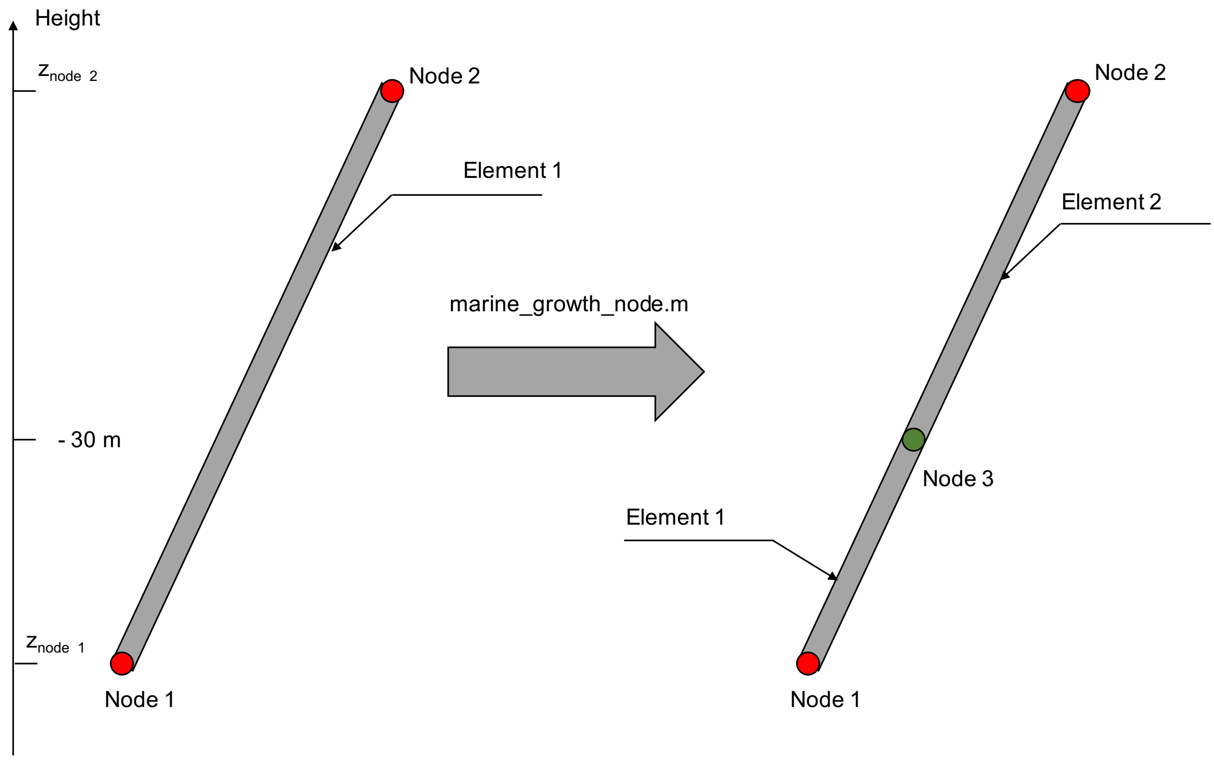

Figure 5.5: marine_growth_node.m explanation

5.6. corrosion.m

As explained in Section 3.5.5, the corrosion is an important factor in the design of an offshore structure. After a certain time, the elements' wall thickness is reduced due to the corrosion. It is represented in the model by the corrosion rates relative to the splash zone and the submerged zone presented in Table 3.5.
The model represents the state of the elements after a certain period. This is defined by the input *Lifetime* (in year). Ergo, if the user doesn't want to model the corrosion, he should enter *Lifetime = 0*. If *Lifetime*>0,

the script corrosion.m removes a thickness of $t_{corrosion}$ = *Lifetime· corrosion rate* to all the elements in the submerged zone. If $t_{corrosion} > 0{,}5 \cdot D_{element}$, the program stops and returns an error message. This message encourages the user to reduce the lifetime or to increase the elements' wall thickness.

5.7. accuracy_nodes.m

If the user chooses it, the accuracy of the model can be improved. This is quantified by L_{max}, the maximum length of each element. If the size of one member is larger than L_{max}, it is divided into two elements by adding an additional node in the middle. If these two new members still have a length higher than L_{max}, the function is applied a second time, until reaching a length smaller than the one defined by the user. The algorithm of this function is shown on Figure 5.6.

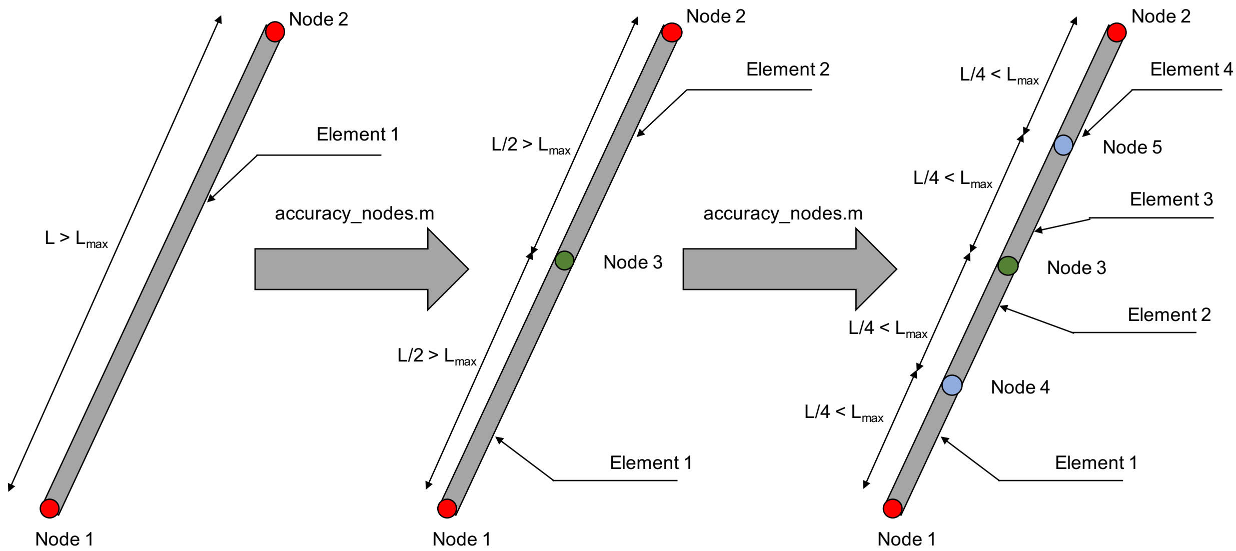

Figure 5.6: accuracy_nodes.m explanation

This function has a short running time. However, this operation will increase the computation effort later in the model, especially regarding the eigenvalues computation. For each new node, the matrices will be increased by 6 lines and 6 columns, which can slow down the calculation by several minutes. The idea of this function is to divide the members into small elements in order to be able to calculate the local modes, which is impossible if a member is only characterized by two nodes.

5.8. Geometry outputs

The outputs of this geometric construction are the lists of all the nodes and elements in the lattice structure, transition piece and tower. These lists are not the ones returned to the user. They are reassembled to be Bladed compatible and more comprehensible. This is done by the function bladed_output.m (4.7). An example is given in Table 5.1 for the list of nodes and in Table 5.2 for the list of elements.

Node ID	x coordinate [m]	y coordinate [m]	z coordinate [m]
1	0	0	-50
2	0.5	1.2	-48
:	:	:	:
144	6	6	90

Table 5.1: Example of the nodes list

ID	Node1	Node2	D1	D2	t1	t2	E	ρ	ν	C_a	C_d	mg	Type	ID_{mat}	Fl
1	1	2	1,289	1,284	0,053	0,053	2.1E11	8500	0.3	2,13	0.1	0.1	1	1	1
2	2	3	1,284	1,265	0,053	0,050	2.1E13	8500	0.3	2,13	0.1	0.1	1	2	1
:	:	:	:	:	:	:	:	:	:	:	:	:	:	:	:
467	143	144	4,15	4	0,021	0,020	2.1E11	8500	0.3	0	0	0	0	1	0

Table 5.2: Example of the element list

Where:

- ID: An unique number associated to the members. This value is used to access to the element information
- Node 1: The ID of the node at the first extremity of the element. It corresponds to the Node ID of Table 5.1
- Node 2: The ID of the node at the second extremity of the element. It corresponds to the Node ID of Table 5.1
- D1: The diameter of the element at the first extremity - meter
- D2: The diameter of the element at the second extremity - meter
- t1: The wall thickness of the element at the first extremity - meter
- t2: The wall thickness of the element at the second extremity - meter
- E: The Young modulus of the element - Pascal
- ρ: The material density of the element - kg·m^{-3}
- ν: The material Poisson coefficient of the element
- C_a: The added mass coefficient associated to the element and calculated by the function drag_inertia_matrices.m
- C_d:The drag coefficient associated to the element and calculated by the function drag_inertia_matrices.m
- mg: The marine growth thickness associated to the element - meter
- Type: This value determines which part of the structure the element represents : lattice structure = 1 , transition piece =2, tower = 3. This parameter is used by the function flooded_member.m to determined if the member is flooded or not. It has been created since the brace members and the legs can be independently flooded or not. Therefore they had to be distinguished.
- ID_{mat}: The ID of the element material. The parameter is relevant for the function bladed_output.m. The value corresponds to the first column of Table 4.9
- Fl : it specifies whether the element is flooded or not with 1 for yes and 0 for no

The parameters C_a, C_d and mg are not defined in that Chapter. The list of elements is updated by the functions marine_growth.m and drag_inertia_matrices.m in Chapter 6.
The last outputs of this Chapter are the top node ID, which correspond to the node attached to the nacelle, and the foundation nodes ID, which are the nodes connected to the seabed. These outputs are important since they are used to compute the boundary conditions of the model, developed in Chapter 6 and Chapter 7.

6

Matrices construction

In the previous chapter, the elements were defined as lines between two nodes and characterized by the temporary lists of nodes and elements shown in Section 5.8. This Chapter 5 concerned the definition of the geometry. The second part of the FE_model_builder.m script (Section 4.5), is described in this chapter, and is associated to the functions:
- Element_Matrices.m
- matrix_assemble.m
- flooded_member.m
- marine_growth.m
- drag_inertia_matrices.m
The structure of this part of the program is shown on Figure 6.1.

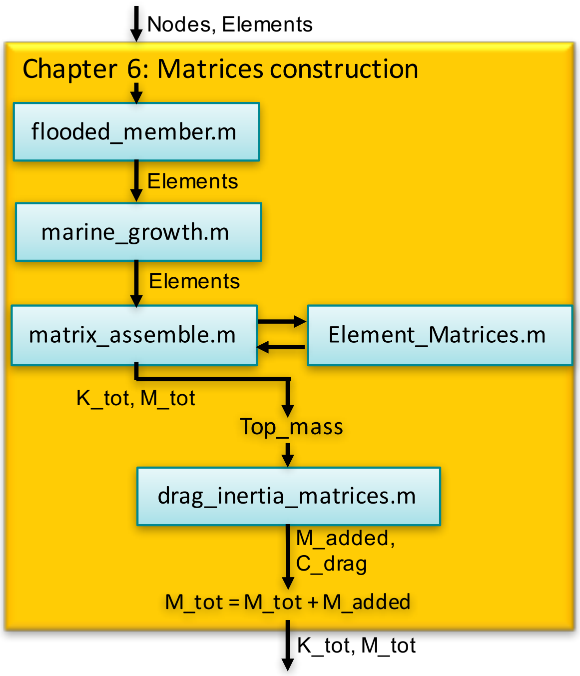

Figure 6.1: Matrices construction section

This chapter describes the physical construction of the structure, with the material properties taken into account. To each element is added a mass and a stiffness. Both parameters are characterized by two matrices: the element mass matrix and the element stiffness matrix. Later, a damping matrix will also be added to the

model. These matrices describe the interactions between the two nodes of one element. Each matrix is defined in a local frame of reference. Then a rotation is applied to both matrices to express them in a global frame of reference. After this operation, the matrices can be assembled into two global matrices which characterized the modal behaviour of the structure.
These two global matrices are independent of the environment. To model the impact of the water and the biofouling on the structure, the functions flooded_member.m, marine_growth.m and drag_inertia_matrices.m are used. The top mass is added to the global mass matrix at the end of this section.
The outputs of this part are named M_{tot} and K_{tot}. However, to describe completely the modal behaviour of the model, the soil boundary conditions need to be added to the stiffness matrix. This is the subject of Chapter 7.

6.1. flooded_member.m

With the functions Element_Matrices.m and matrix_assemble.m, the mass and stiffness matrices of the model are calculated. Still, these parameters represent the structure but not the environment. The function flooded_member.m is based on the inputs *Fl_leg* and *Fl_brace*, which specify whether the legs members and the brace members are flooded or not. This affects the model's buoyancy but also adds an extra mass to the submerged members. This mass is the amount of water present in the elements. It corresponds to the element inner volume multiplied by the sea water density.
The script flooded_member.m has two outputs :
- the updated list of elements, where the value 1 or 0 in column "Flooded" specifies if the member is flooded or not
- the buoyancy force, which is used in Chapter 7.

The activation of this script leads to a decrease in the natural frequencies, since the mass of the model is increased but not the stiffness.

6.2. marine_growth.m

The marine growth can be defined in two different way by the user: either by specifying a geographical area with the input *mg_region*, or by entering an average value of the marine growth thickness with the input *mg*. The first option is based on the nodes created by the function marine_growth_node.m (Section 5.5) and the values of the marine growth thickness given in the DNVGL-RP-C205 [6] and shown in Table 3.4. The weight of the marine growth corresponding to the element is calculated based on a biofouling density of 1325 kg·m^3 [10], but, the user can change this value in START_OwjEma.m.
If the user chooses to enter an average value for the marine growth thickness, all the submerged members will be associated to the same value of marine growth weight.
In both cases, the temporary output Elements (defined in Section 5.8) is updated with the column 13 replaced by the values of the marine growth thickness. This column is reused by the function bladed_output.m (Section 4.7). Another output of this function is the total weight of the marine growth, which is used by the script soil_boundary_condition.m (Chatper 7).
As for the function flooded_member.m, the function marine_growth.m reduces the natural frequencies of the model since it increases the mass without influencing the stiffness.

6.3. Element_Matrices.m

In the model, to each element is associated two matrices : an element mass matrix and an element stiffness matrix. The two matrices are based on the work of JS Przemieniecki [1985] [22]. To compute these two matrices, he assumed an element to be a beam with a constant cross section and without variation of temperature. (It should be noted that in the case of non-constant diameter for the legs, the elements should be small enough to account for this variation). Since the elements (presented on Figure 6.2) are composed of two nodes, each one with six degrees of freedom (three translations and three rotations), the element stiffness matrix and the element mass matrix have a dimension of 12 by 12. Each matrix is calculated in a local frame of reference with the local x-axis defined as the axial axis of the beam.

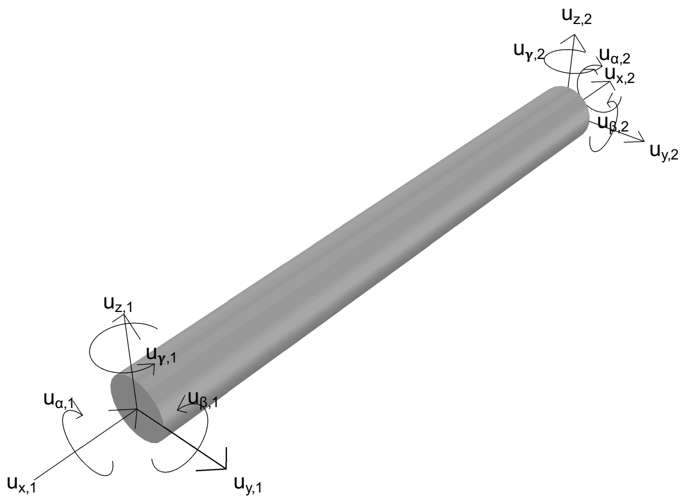

Figure 6.2: Beam element

To determine the element stiffness matrix, JS Przemieniecki [1985] [22] applied forces to the element at each extremity: axial forces, shearing forces, bending moments and torsional moments. The element mass matrix is calculated with Equation 6.1, where V_i represents the element volume and $a_{local,i}$ the matrix of local displacement. The following demonstration is made for the element i.

$$M_{local,i} = \int_{V_i} \rho_i a^t_{local,i} a_{local,i} dV_i \tag{6.1}$$

According to JS Przemieniecki, the matrix $a_{local,i}$ is expressed as:

$$a^t_{local,i} = \begin{pmatrix} 1-\xi_i & 0 & 0 \\ 6(\xi_i-\xi_i^2)\eta_i & 1-3\xi_i^2+2\xi_i^3 & 0 \\ 6(\xi_i-\xi_i^2)\zeta_i & 0 & 1-3\xi_i^2+2\xi_i^3 \\ 0 & -(1-\xi_i)l_i\zeta_i & -(1-\xi_i)l_i\eta_i \\ (1-4\xi_i+3\xi_i^2)l_i\zeta_i & 0 & (-\xi_i+2\xi_i^2-\xi_i^3)l_i \\ (-1+4\xi_i-3\xi_i^2)l_i\eta_i & (\xi_i-2\xi_i^2+\xi_i^3)l_i & 0 \\ \xi_i & 0 & 0 \\ 6(-\xi_i+\xi_i^2)\eta_i & 3\xi_i^2-2\xi_i^3 & 0 \\ 6(-\xi_i+\xi_i^2)\eta_i & 0 & 3\xi_i^2-2\xi_i^3 \\ 0 & -l_i\xi_i\zeta_i & -l_i\xi_i\eta_i \\ (-2\xi_i+3\xi_i^2)l_i\zeta_i & 0 & (\xi_i^2-\xi_i^3)l_i \\ (2\xi_i-3\xi_i^3)l_i\eta_i & (-\xi_i^2+\xi_i^3)l_i & 0 \end{pmatrix} \tag{6.2}$$

Where l_i is the length of the element i and the columns 1, 2 and 3 represent respectively the x displacement, the y displacement and the z displacement. ξ_i, η_i and ζ_i are non dimensional parameters:

$$\begin{aligned} \xi_i &= \frac{x}{l_i} \\ \eta_i &= \frac{y}{l_i} \\ \zeta_i &= \frac{z}{l_i} \end{aligned} \tag{6.3}$$

Element mass matrix and element stiffness matrix are presented respectively in Equation 6.4 and Equation

6.5, where the matrices coefficients are expressed as a function of the diameter, the wall thickness, the Young's modulus, the density and the Poisson's coefficient of the material:

- E_i: the Young's modulus of the element i - Pascal

- l_i: the length of the element i - meter

- A_i: the cross section area of the element i - m^2

- $I_{z,i}$: the second moment of area in the z direction of the element i - m^4

- $I_{y,i}$: the second moment of area in the y direction of the element i - m^4

- J_i: the polar moment of area of the element i - m^4

- k_{ii}: the shear deflection factor of the element i

- ν_i: the Poisson's coefficient of the element i

- ρ_i: the density of the element i - $kg{\cdot}m^{-3}$

- $\Phi_{y,i} = \dfrac{12 \cdot E_i I_{z,i}}{G_i A_{s,i} \cdot l_i^2}$: the shear deformation parameter in the y direction of the element i
- $\Phi_{z,i} = \dfrac{12 \cdot E_i I_{y,i}}{G_i A_{s,i} \cdot l_i^2}$: the shear deformation parameter in the z direction of the element i
- $G_i = \dfrac{E_i}{2 \cdot (\nu_i + 1)}$: the shear modulus of the element i - Pascal
- $A_{s,i} = k_{s,i} \cdot A_i$: the cross sectional area effective in stress of the element i - m^2

These matrices are associated with the degrees of freedom presented on Figure 6.2. The associated vector can be written as: $[u_{x,1}, u_{y,1}, u_{z,1}, u_{\alpha,1}, u_{\beta,1}, u_{\gamma,1}, u_{x,2}, u_{y,2}, u_{z,2}, u_{\alpha,2}, u_{\beta,2}, u_{\gamma,2}]^t$.
The script Element_Matrices.m computes the element matrices based on the outputs Nodes and Elements defined in Section 5.8. This function is not activated by the function FE_model_builder.m but by the function matrix_assemble.m (detailed in Section 6.4). This script transfers the element matrices from a local frame of reference to a global frame of reference. The local element matrices are calculated, rotated and assemble one after the other. The objective is to avoid saving all the element matrices, which consume memory resources and slow down the program.

$$K_{local,i} = \begin{pmatrix}
\frac{E_iA_i}{l_i} & & & & & & & & & & & \\
0 & \frac{12E_iI_{z,i}}{l_i^3(1+\Phi_{y,i})} & & & & & & & & & & \\
0 & 0 & \frac{12E_iI_{y,i}}{l_i^3(1+\Phi_{z,i})} & & & & & & & & & \\
0 & 0 & 0 & \frac{G_iJ_i}{l_i} & & & & & \text{Symetric} & & & \\
0 & 0 & \frac{-6E_iI_{y,i}}{l_i^2(1+\Phi_{z,i})} & 0 & \frac{(4+\Phi_{z,i})E_iI_{y,i}}{l_i(1+\Phi_{z,i})} & & & & & & & \\
0 & \frac{6E_iI_{z,i}}{l_i^2(1+\Phi_{y,i})} & 0 & 0 & 0 & \frac{(4+\Phi_{y,i})E_iI_{z,i}}{l_i(1+\Phi_{y,i})} & & & & & & \\
\frac{-E_iA_i}{l_i} & 0 & 0 & 0 & 0 & 0 & \frac{A_iE_i}{l_i} & & & & & \\
0 & \frac{-12E_iI_{z,i}}{l_i^3(1+\Phi_{y,i})} & 0 & 0 & 0 & \frac{-6E_iI_{z,i}}{l_i^2(1+\Phi_{y,i})} & 0 & \frac{12E_iI_{z,i}}{l_i^3(1+\Phi_{y,i})} & & & & \\
0 & 0 & \frac{-12E_iI_{y,i}}{l_i^3(1+\Phi_{z,i})} & 0 & \frac{6E_iI_{y,i}}{l_i^2(1+\Phi_{z,i})} & 0 & 0 & 0 & \frac{12E_iI_{y,i}}{l_i^3(1+\Phi_{z,i})} & & & \\
0 & 0 & 0 & \frac{-G_iJ_i}{l_i} & 0 & 0 & 0 & 0 & 0 & \frac{G_iJ_i}{l_i} & & \\
0 & 0 & \frac{-6E_iI_{y,i}}{l_i^2(1+\Phi_{z,i})} & 0 & \frac{(2-\Phi_{z,i})E_iI_{y,i}}{l_i(1+\Phi_{z,i})} & 0 & 0 & 0 & \frac{6E_iI_{y,i}}{l_i^2(1+\Phi_{z,i})} & 0 & \frac{(4+\Phi_{z,i})E_iI_{y,i}}{l_i(1+\Phi_{z,i})} & \\
0 & \frac{6E_iI_{z,i}}{l_i^2(1+\Phi_{y,i})} & 0 & 0 & 0 & \frac{(2-\Phi_{y,i})E_iI_{z,i}}{l_i(1+\Phi_{y,i})} & 0 & \frac{-6E_iI_{z,i}}{l_i^2(1+\Phi_{y,i})} & 0 & 0 & 0 & \frac{(4+\Phi_{y,i})E_iI_{z,i}}{l_i(1+\Phi_{y,i})}
\end{pmatrix} \tag{6.4}$$

$$M_{local,i} = \rho_i A_i l_i \begin{pmatrix}
\frac{1}{3} & & & & & & & & & & & \\
0 & \frac{13}{35}+\frac{6I_{z,i}}{5A_i l_i^2} & & & & & & & & & & \\
0 & 0 & \frac{13}{35}+\frac{6I_{y,i}}{5A_i l_i^2} & & & & & & & & & \text{Symetric} \\
0 & 0 & 0 & \frac{J_i}{3A_i} & & & & & & & & \\
0 & 0 & \frac{-11l}{210}-\frac{I_{y,i}}{10\cdot A_i l_i} & 0 & \frac{l_i^2}{105}+\frac{2I_{y,i}}{15A_i} & & & & & & & \\
0 & \frac{11l}{210}+\frac{I_{z,i}}{10A_i l_i} & 0 & 0 & 0 & \frac{l_i^2}{105}+\frac{2I_{z,i}}{15A_i} & & & & & & \\
\frac{1}{6} & 0 & 0 & 0 & 0 & 0 & \frac{1}{3} & & & & & \\
0 & \frac{9}{70}-\frac{6I_{z,i}}{5A_i l_i^2} & 0 & 0 & 0 & \frac{13l_i}{420}-\frac{I_{z,i}}{10A_i l_i} & 0 & \frac{13}{35}+\frac{6I_{z,i}}{5A_i l_i^2} & & & & \\
0 & 0 & \frac{9}{70}-\frac{6I_{y,i}}{5A_i l_i^2} & 0 & \frac{-13l_i}{420}+\frac{I_{y,i}}{10A_i l_i} & 0 & 0 & 0 & \frac{13}{35}+\frac{6I_{y,i}}{5A_i l_i^2} & & & \\
0 & 0 & 0 & \frac{J_i}{6A_i} & 0 & 0 & 0 & 0 & 0 & \frac{J_i}{3A_i} & & \\
0 & 0 & \frac{13l_i}{420}-\frac{I_{y,i}}{10A_i l_i} & 0 & \frac{-l_i^2}{140}-\frac{2I_{y,i}}{30A_i} & 0 & 0 & 0 & \frac{11l_i}{210}+\frac{I_{y,i}}{10A_i l_i} & 0 & \frac{l_i^2}{105}+\frac{2I_{y,i}}{15A_i} & \\
0 & \frac{-13l_i}{420}+\frac{I_{z,i}}{10A_i l_i} & 0 & 0 & 0 & \frac{-l_i^2}{140}-\frac{2I_{z,i}}{30A_i} & 0 & \frac{-11\cdot l_i}{210}-\frac{I_{z,i}}{10A_i l_i} & 0 & 0 & 0 & \frac{l_i^2}{105}+\frac{2I_{z,i}}{15A_i}
\end{pmatrix} \quad (6.5)$$

6.4. matrix_assemble.m

Stiffness and mass matrices are calculated for each element in a local frame of reference. Before computing the global matrices of the structure, all local matrices must be transferred to a global frame of reference. This is the purpose of the function matrix_assemble.m. The inputs of this section are the lists of nodes and elements defined in Section 5.8. During the process, the script activates the function Element_Matrices.m, detailed in the previous section.

The local element matrices are transferred from a local frame of reference to the global frame of reference. The x axis of the global frame of reference is defined as parallel to the first face of the structure. The z axis is the vertical direction from the seabed to the mean sea level. The y direction is then defined in such a way the global frame of reference is orthonormal.

The steps to compute the transfer matrix are explained in this section. The following demonstration is made for the element i. It has to be done for each element individually. Consequently, a transformation matrix must be built for each member. This matrix consists of the coordinates of the set of vectors representing the local basis expressed in the coordinates system of the global basis. These three vectors corresponding to the element i are noted $e_{i,1}$, $e_{i,2}$ and $e_{i,3}$. The first step of the transformation is to determine the coordinates of this set of vector.

As defined in the local matrix, the element axis is collinear to the x-axis. The coordinates of the nodes of the element i are noted [$x_{i,1}$, $y_{i,1}$, $z_{i,1}$] and [$x_{i,2}$, $y_{i,2}$, $z_{i,2}$]. So, the first vector of the basis is:

$$e_{i,1} = \frac{\begin{pmatrix} x_{i,1} - x_{i,2} \\ y_{i,1} - y_{i,2} \\ z_{i,1} - z_{i,2} \end{pmatrix}}{\left\| \begin{matrix} x_{i,1} - x_{i,2} \\ y_{i,1} - y_{i,2} \\ z_{i,1} - z_{i,2} \end{matrix} \right\|} \tag{6.6}$$

Where ‖ ‖ represents the norm of the vector. $e_{i,1}$ is normalized, since the transfer matrix has to conserve the norm of the element matrices.

By definition, the second vector $e_{i,2}$ has to be orthogonal to the first vector $e_{i,1}$. Therefore, an arbitrary vector N is introduced. Its coordinates are [0 , 0 , 1] (or [1, 0 , 0] if the element is vertical). This won't affect the result since the beam is a tubular element: the vector orthogonal to the x-axis can be in every direction, as long as it forms an orthonormal coordinate system. The second vector of the basis is:

$$e_{i,2} = \frac{e_{i,1} \wedge N}{\|e_{i,1} \wedge N\|} \tag{6.7}$$

Where ∧ corresponds to the cross product operation. $e_{i,1}$ and $e_{i,2}$ are then orthogonal by construction. In order to define the third vector, the cross product of $e_{i,1}$ and $e_{i,2}$ is calculated:

$$e_{i,3} = \frac{e_{i,1} \wedge e_{i,2}}{\|e_{i,1} \wedge e_{i,2}\|} \tag{6.8}$$

These three vectors represent the local frame of reference. The transformation matrix is computed in Equation 6.9.

$$t_i = \begin{pmatrix} e_{x,i,1} & e_{y,i,1} & e_{z,i,1} \\ e_{x,i,2} & e_{y,i,2} & e_{z,i,2} \\ e_{x,i,3} & e_{y,i,3} & e_{z,i,3} \end{pmatrix} \tag{6.9}$$

In order to correspond to the dimension of the element matrix, the matrix t_i is compiled into a 12 by 12 matrix. The resulting transformation matrix is detailed on Equation 6.10.

$$T_i = \begin{pmatrix} t_i & & & \\ & t_i & & \\ & & t_i & \\ & & & t_i \end{pmatrix} \tag{6.10}$$

The element matrices can now be expressed in the global frame of reference:

$$\begin{aligned} K_{global,i} &= T_i^{-1} \cdot K_{local,i} \cdot T_i \\ M_{global,i} &= T_i^{-1} \cdot M_{local,i} \cdot T_i \end{aligned} \tag{6.11}$$

The matrices $K_{global,i}$ and $M_{global,i}$ of all the elements are expressed in the same frame of reference. They can then be assembled into two total matrices: K_{total} and M_{total}. Yet, these two matrices are not those used for the modal analysis. To them must be added the effect of the marine growth (marine_growth.m), the flooded member (flooded_member.m) and the top mass. Then, the boundaries conditions associated to the soil stiffness are considered. This is detailed in Chapter 7.

6.5. drag_inertia_matrices.m

The function drag_inertia_matrices.m is implemented into the program to model the interactions between the structure and the environment. With this script, two coefficients are calculated: the added mass coefficient C_a and the drag coefficient C_d, which correspond respectively to the added mass and the hydrodynamic damping. Each one is associated to a unique element.
C_a and C_d correspond to the coefficients present in the Morrison equation:

$$F(t) = \rho_{fluid}(1 + C_a)V(\dot{u}_{fluid} - \ddot{x}) + \frac{1}{2}\rho C_D A(u_{fluid} - \dot{x})|u_{fluid} - \dot{x}| \tag{6.12}$$

Where ρ_{fluid} is the fluid density, C_a the added mass coefficient, V the volume of the element, C_D the drag coefficient, A the cross section area perpendicular to the direction of the flow, u_{fluid} the fluid velocity and x the element displacement.
The added mass matrix and the hydrodynamic damping matrix are calculated based on Equation 6.13 and Equation 6.14 representing respectively the inertia force and the drag force.

$$f_i(t) = \rho_{fluid}(1 + C_a)V(\dot{u}_{fluid} - \ddot{x}) \tag{6.13}$$

$$f_d(t) = \frac{1}{2}\rho_{fluid} C_D A(u_{fluid} - \dot{x})|u_{fluid} - \dot{x}| \tag{6.14}$$

Because of the term $|u_{fluid} - \dot{x}|$ Equation 6.14 is re written as:

$$f_d(t) = \begin{cases} \frac{1}{2}\rho_{fluid} C_D A(u_{fluid} - \dot{x})^2 & \text{for } u_{fluid} \leq \dot{x} \\ \frac{1}{2}\rho_{fluid} C_D A(u_{fluid} - \dot{x})^2 & \text{for } u_{fluid} > \dot{x} \end{cases} \tag{6.15}$$

The drag force equation is still non linear. By using the Taylor expansion, the linear form is obtained:

$$f_d(t) = \begin{cases} \frac{1}{2}\rho_{fluid} C_D A u_{fluid}^2 - \rho_{fluid} C_D A u_{fluid}\dot{x} + o(\dot{x}^2) & \text{for } u_{fluid} \leq \dot{x} \\ \frac{1}{2}\rho_{fluid} C_D A u_{fluid}^2 + \rho_{fluid} C_D A u_{fluid}\dot{x} + o(\dot{x}^2) & \text{for } u_{fluid} > \dot{x} \end{cases} \tag{6.16}$$

The first step of the drag_inertia_matrices.m function is to calculate the drag and inertia coefficients. The drag coefficient C_d is estimated with the equations established in the *DNV GL-RP-C205* [6]. The following demonstration is made for the element i. It will be repeated for each member of the structure.
First, the ratio between the roughness and the element's diameter is calculated.

$$\Delta_i = \frac{k_i}{D_i} \tag{6.17}$$

Where k_i is the roughness of the element i and D_i the average diameter.
From Δ_i, the relation between the drag coefficient and the roughness is determined:

$$C_{ds,i} = \begin{cases} 0,65 & \text{for } \Delta_i < 10^{-4} \\ (29 + 4 \cdot log(\Delta_i))/20 & \text{for } 10^{-4} < \Delta_i < 10^{-2} \\ 1,05 & \text{for } 10^{-2} < \Delta_i \end{cases} \tag{6.18}$$

Then, the wake amplification factor is calculated:

$$\psi(Kc_i) = \begin{cases} C_{\pi,i} + 0,10 \cdot (Kc_i - 12) & \text{for } 2 < Kc_i < 12 \\ C_{\pi,i} - 1 & \text{for } 0,75 < Kc_i < 2 \\ C_{\pi,i} - 1 - 2 \cdot (Kc_i - 0,75) & \text{for } Kc_i < 0,75 \end{cases} \tag{6.19}$$

Where Kc_i is the Keulen-Carpenter number of the element i and $C_{\pi,i}$ is:

$$C_{\pi,i} = 1,5 - 0,024 \cdot (\frac{12}{C_{ds,i}} - 10) \tag{6.20}$$

Finally, the drag coefficient can be calculated with the following formula:

$$C_{d,i} = C_{ds,i} \cdot \psi(Kc_i) \tag{6.21}$$

The drag coefficient $C_{a,i}$ corresponding to the element i is calculated based on the method given in the *DNV GL-RP-C205* [6]. $C_{a,i}$ depends on the Keulen-Carpenter number and the drag coefficient number of the element:

$$C_{a,i} = \begin{cases} 1 & \text{for } Kc_i < 3 \\ max \begin{cases} (1 - 0,044(Kc_i - 3) \\ 0,6 - (C_{d,i} - 0,65)) \end{cases} & \text{for } Kc_i \geqslant 3 \end{cases} \tag{6.22}$$

Once the coefficients $C_{a,i}$ and $C_{d,i}$ have been calculated for each element of the model, the added mass matrix and the hydrodynamic damping matrix are computed based on Equation 6.13 and Equation 6.16. These two matrices are the outputs of the function drag_inertia_matrices.m.

7

Pile-soil interaction

Once the nodes, the elements, the mass and the stiffness characterizing the model have been calculated, the impact of the soil-pile interaction is considered. The foundations of the structure are defined as vertical piles located at the bottom of each leg. The pile are modelled as beam, as explain in Section 6.3. This chapter detailed the part of the program simulating the soil-piles interaction, as shown on Figure 7.1. The idea of this part is to calculate the piles' static responses corresponding to a load applied at the top of the foundations. This displacements are computed with the helps of the p-y and t-z curves. Once the displacements of the top of the pile are known, the equivalent soil stiffness is calculated. To simulate the static response, the following functions are used:
- soil_boundary_condition.m
- Element_Matrices.m
- matrix_assemble.m
- p_y_t_z_curves.m

The functions Element_Matrices.m and matrix_assemble.m have been detailed in Section 6.3 and Section 6.4.

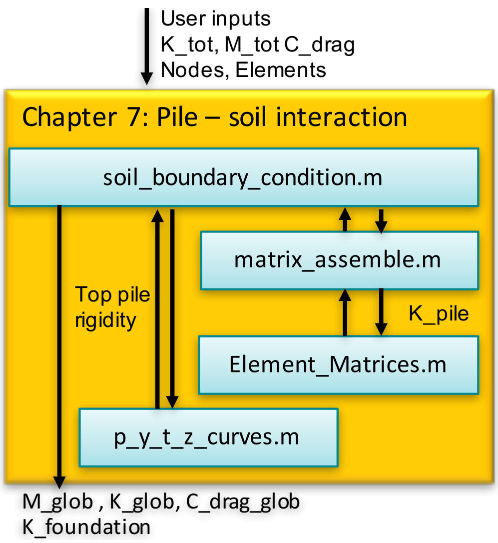

Figure 7.1: Geometry definition section

In the model, the user can choose between several representations of the soil-piles interaction with the input *stiffness_type*. The interaction can be defined as rigid, with all the degrees of freedom constrained, or it can be modelled as three or four vertical piles interacting with the soil. In order to reduce the computational time, the top piles displacements are only calculated for one pile and then apply to the other foundations.
The outputs of the section are the final version of the global mass, stiffness and hydrodynamic damping

matrices. In reality, only the values of the global stiffness matrix are changed with the addition of the soil equivalent stiffness, but in the scenario of a rigid foundation, the dimensions of all the global matrices are modified.

7.1. soil_boundary_condition.m

The function soil_boundary_condition.m is divided in two parts. The first one computes the p-y and t-z curves. Once these values are known, the script p_y_t_z_curves.m is activated and the pile displacements are calculated. The second part of the function updates the global mass, stiffness and hydrodynamic damping matrices. Though, if the user choose stiffness_type = 0 , the rigid foundation option is activated and the first part of soil_boundary_condition.m is skipped.

7.1.1. Rigid foundations

"Rigid foundations" means constraining the 6 degrees of freedom (3 translations and 3 rotations) of the nodes located at the seabed. In other words, the nodes in contact with the seabed won't be able to rotate or translate. These restrictions are achieved by removing the rows and the columns corresponding to these displacements in the mass and stiffness matrices of the structure. Once these degrees of freedom are removed, the eigenvalues can be calculated. This option is selected if the user enter *stiffness_type* = 0 in the section 5.1 of START_OwjEma.m. Figure 7.2 represents the effect of the rigid foundations option on the model.

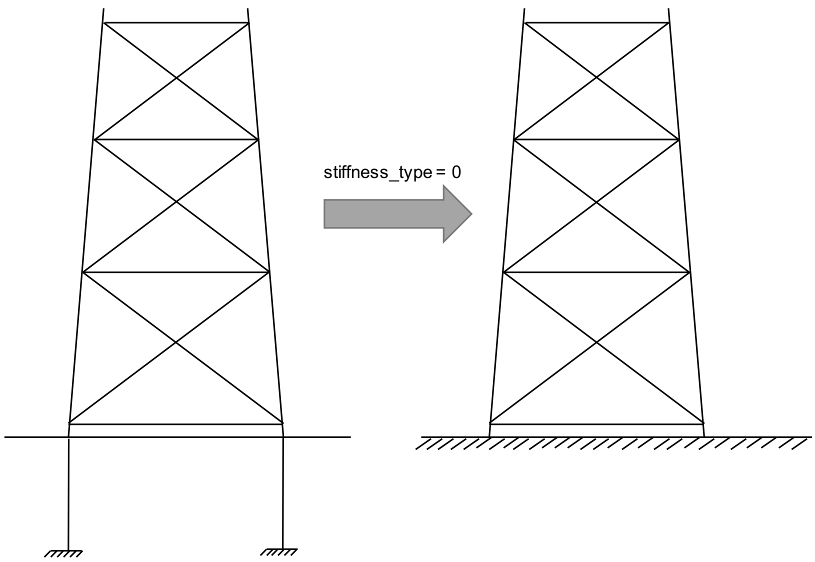

Figure 7.2: Rigid foundation model

This method is the simplest and fastest way to represent the soil-piles interaction. Nevertheless, it is inaccurate as it doesn't account for the soil properties. Postulating the soil is infinitely rigid is a strong assumption as in reality, it never is. Therefore, a more accurate model should be developed. This is discussed in Section 7.1.2.

7.1.2. Stiff foundation

If the user enters *stiffness_type* = 1 or *stiffness_type* = 2 in START_OwjEma.m, the interactions between the soil and the foundations are modelled with horizontal and vertical springs, as shown on Figure 7.3a. It can be noted that, according to the way of representing the soil-piles interaction, the springs are considered as linear, non-linear, coupled or uncoupled. It this model, the springs are represented as linear and uncoupled if *stiffness_type* = 1 and non-linear and uncoupled if *stiffness_type* = 2.

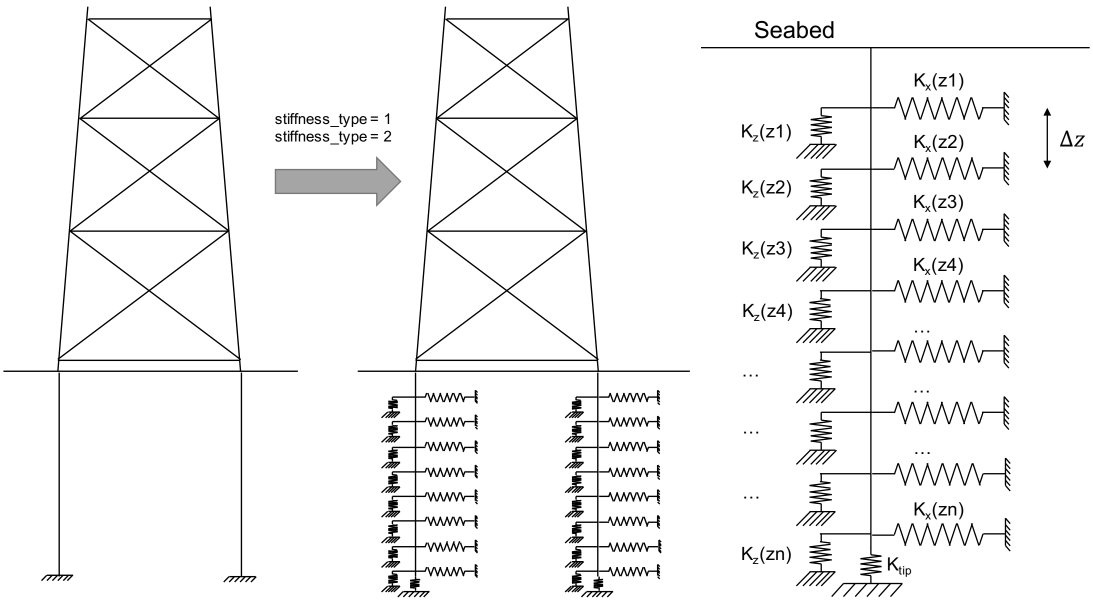

(a) Effect of stiffness_type (b) Pile - Soil interaction model

Figure 7.3: Stiff foundation model

The piles are modelled as a vertical beams with a constant cross section, with the functions Element_Matrices.m and matrix_assemble.m, detailed in Section 6.3 and Section 6.4. However, the function soil_boundary_condition.m calculates the behaviour of only one pile and reproduces the results for the other foundations. The pile is represented by a diameter, a length, a wall thickness, a Young modulus, a Poisson coefficient and a density. Based on these values, the pile stiffness matrix is calculated. It represents the internal stiffness of the pile.
The springs attached to the pile represent the soil resistance. To obtain an accurate result, the pile is divided into several elements with a length of Δz. To each node, three springs are associated. One in the x-direction, one in the y-direction and one in the z-direction. Then, the p-y curves (x and the y directions) and the t-z curve (z direction) are calculated. These curves represent the soil resistance according to the node displacement. At the tip of the pile, a spring modelling the tip resistance is added. The visualization of this model is presented on Figure 7.3b.
As specified previously, the springs stiffness are calculated with the p-y and the t-z curves. These curves depend on the type of soil (sand or clay), the internal friction angle (for the sand), the soil density, the soil layer thickness, the undrained shear strength (for the clay), the vertical strain (for the clay) and the soil Poisson coefficient. These values are entered by the user in the script START_OwjEma.m.
The idea behind this representation is to determine the equivalent stiffness at the top of the pile and implement it in the global stiffness matrix of the structure. Once the p-y and the t-z curves are calculated, the equivalent stiffness at the seabed is determined. To obtain this result, the stiffness of each spring corresponding to a static load, applied at the top of the pile, is calculated. This can be done in several ways, which is detailed in Section 7.1.6. After this operation, the displacement of the top of the pile is calculated and, since the static load is known, the equivalent stiffness is determined. This equivalent stiffness is implemented into the global stiffness matrix. It is also returned to the user as the output *Bladed_stiffness* (detailed in Section 4.7).

7.1.3. P - y curve model

A possibility to represent the non-linearity of the horizontal soil stiffness is to use p-y curves. These curves calculate the soil resistance according to the deflection of the pile. An example is shown on Figure 7.4.

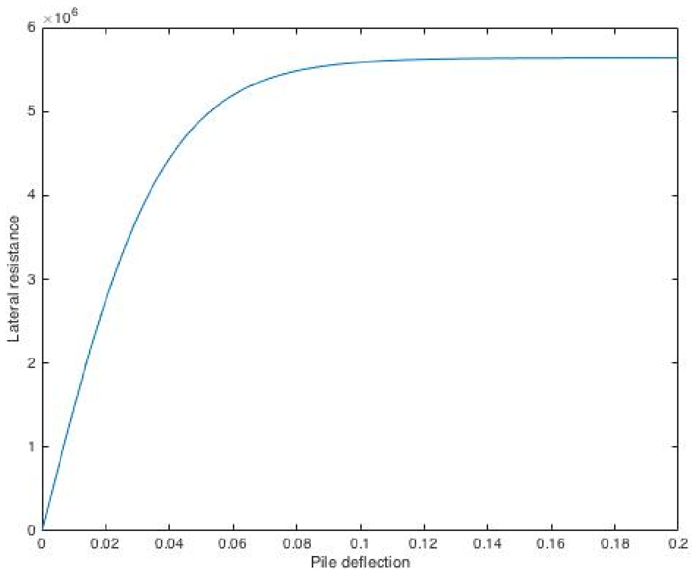

Figure 7.4: Exemple of a p - y curve

The stiffness of each horizontal spring is determined by calculating the p-y curves at the corresponding depth. Yet, according to the *DNV - J101* [10], this method is correct only for the lateral pile capacity at the ULS. It should be used with caution when calculating the equivalent spring stiffness model, especially regarding the initial slope of the p-y curve.
The governing equation of the p-y curve is:

$$EI \cdot \frac{d^4y}{dx^4} + Q_A \cdot \frac{d^2y}{dx^2} - p(y) + q = 0 \tag{7.1}$$

Where:
$EI \cdot \dfrac{d^4y}{dx^3} + Q_A \cdot \dfrac{dy}{dx} = Q_L$
$EI \cdot \dfrac{d^2y}{dx^2} = M$

Q_A: the axial force
Q_L: the lateral force
q: the distributed load along the pile
M: the bending moment

The *DNV GL-ST-0126* [7] explains how to compute the p-y curves for sand and clay when the loads are static:
For the clay:

$$p = \begin{cases} \frac{p_u}{2} \cdot (\frac{y}{y_c})^{\frac{1}{3}} & \text{for } y \leq y_c \\ p_u & \text{for } y > y_c \end{cases} \tag{7.2}$$

Where:

$y_c = 2{,}5 \cdot \varepsilon_c \cdot D_{pile}$

p_u is the static ultimate resistance. Its value depends on the depth:

$$p_u = \begin{cases} (3 \cdot s_u + \gamma \cdot z) \cdot D_{pile} + J \cdot s_u \cdot z & \text{for } z \leqslant z_r \\ 9 \cdot s_u \cdot D_{pile} & \text{for } z > z_r \end{cases} \tag{7.3}$$

Where $z_r = \dfrac{9 \cdot s_u \cdot D_{pile} - 3 \cdot D_{pile} \cdot s_u}{\gamma \cdot D_{pile} + J \cdot s_u}$. γ is the soil density, s_u the undrained shear strength and J a dimensionless constant between 0.25 and 0,5.

The p-y curve of the sand is defined by the following equation:

$$p = A_{static} \cdot p_u \cdot \tanh\left(\frac{k_{mod} \cdot z}{A_{static} \cdot p_u} \cdot y\right) \tag{7.4}$$

In the case of sand, the static ultimate resistance is:

$$p_u = \begin{cases} (C_1 \cdot z + C_2 \cdot D_{pile}) \cdot \gamma \cdot z & \text{for } z \leqslant z_r \\ C_3 \cdot D_{pile} \cdot \gamma \cdot z & \text{for } z > z_r \end{cases} \tag{7.5}$$

Where k_{mod} is the initial modulus of subgrade reaction, A_{static}=(3-0,8$\cdot\dfrac{z}{D_{pile}}$)$\geqslant$0,9 a factor for static loading, and C_1, C_2 and C_3 three coefficients depending on the angle of friction. The value of each can be found on Figure 7.5 [7]. The initial modulus of subgrade k defines the initial slope of the curve. It is defined according to the angle of internal friction. The relation between these two parameters is shown on Figure 7.6 [10].

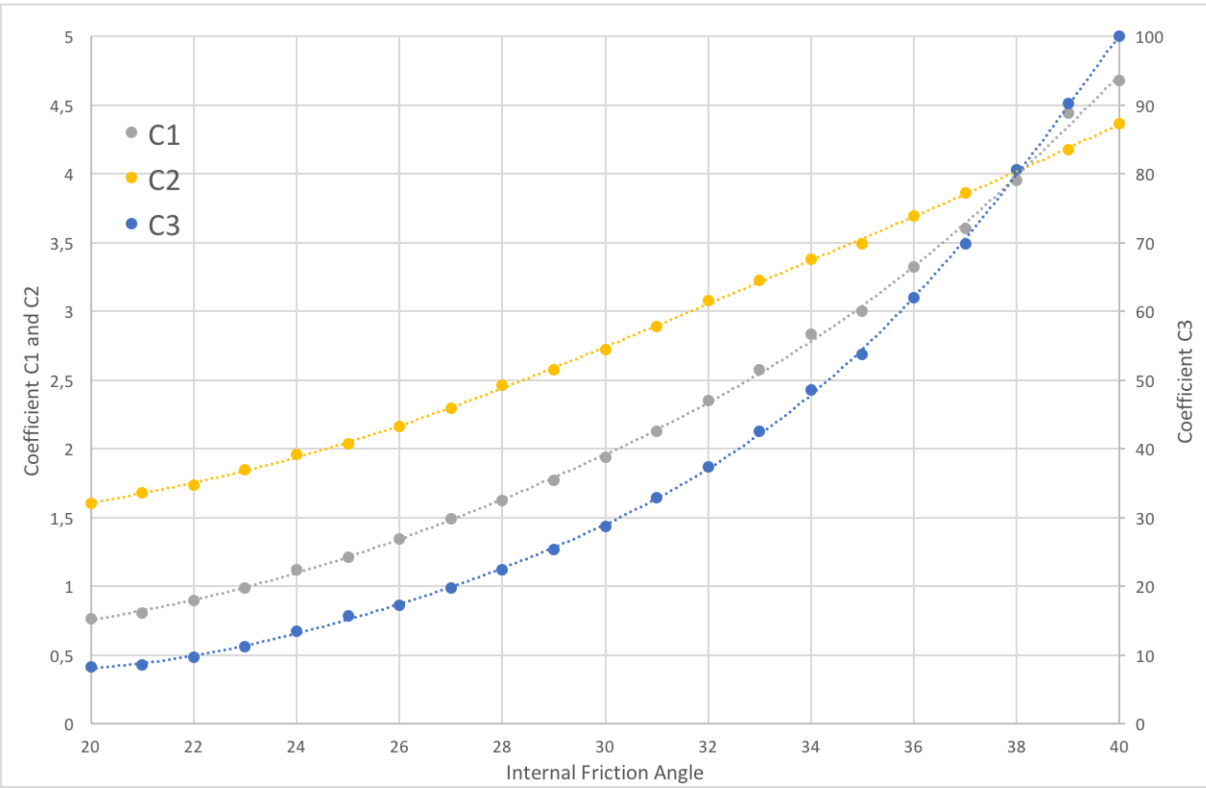

Figure 7.5: Coefficient variation according the internal friction angle - *DNVGL-ST-0126*

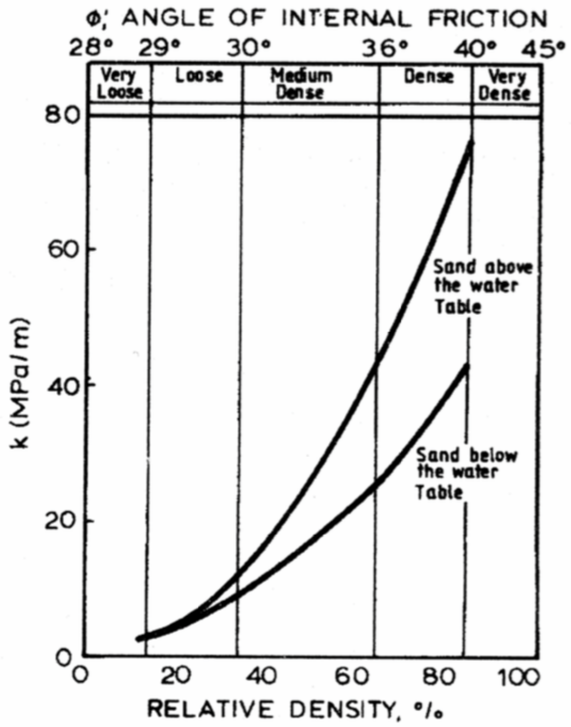

Figure 7.6: Modulus of subgrade reaction as function of friction angle - *DNVGL-ST-0126*

Still, this demonstration was made for a homogeneous soil. If it is composed of several layer of sand and clay, the impact of the upper layers on the others should be taken into account and added to the overburden pressure p_u.

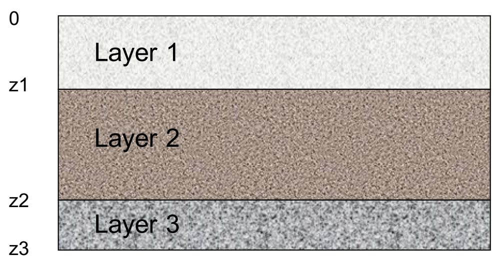

Figure 7.7: Example of a layered soil

The following explanation will be based on the layers shown on Figure 7.7. It is based on the computation given by Lymon C. Reese and Willem van Impe [23].
The p-y curves of layer 1 can be calculated normally by using the equations established previously. Yet, this won't be the case for layer 2 and layer 3. The p-y curve of layer 2 are calculated normally except that to the value of z is added an equivalent depth, corresponding to the layer 1 overburden pressure. The depth, noted z_{eq} is determined by using the following equation:

$$\int_0^{z1} p_u(layer1)dz = \int_0^{z_{eq}} p_u(layer2)dz \tag{7.6}$$

The idea is to represent layer 1 and layer 2 as one single layer with the properties of layer 2. The value of z_{eq} is found iteratively. Then it is added to the previous equation by replacing the value z with $z + z_{eq}$.

7.1.4. T - z curve model

The stiffness representing the skin resistance of the pile is calculated by the use of t-z curves. Those are represented by the Equation 7.7 [7].

$$z = t_{skin}\frac{R_{pile}}{G_0}\ln\left(\frac{z_{if} - r_f\dfrac{t}{t_{skin,max}}}{1 - r_f\dfrac{t}{t_{skin,max}}}\right) \tag{7.7}$$

Where:
- t_{skin}: skin resistance - Pascal
- R_{pile} : radius of the pile - meter
- G_0: initial shear modulus of the soil - Pascal
- z_{if}: dimensionless zone of influence
- $t_{skin,max}$: the maximum skin resistance - Pascal
- r_f: curve lifting factor

G_0 depends on the soil parameter. It can be calculated by using Equation 7.8.

$$G_0 = \begin{cases} 600s_u - 170s_u\sqrt{OCR-1} & \text{for clay} \\ m\dfrac{\sqrt{\sigma_a\sigma_v}}{2(1+\nu_{soil})} & \text{for sand} \end{cases} \tag{7.8}$$

Where:
- OCR: the over-consolidation ratio. It's the highest stress experienced divided by the current stress
- m = 1000tan(ϕ)
- ϕ: the internal friction angle of the soil layer
- σ_a = 100 kPa : the reference pressure
- $\sigma_v = H_{soil}\cdot\gamma_{soil}$: the vertical effective stress - Pascal
- γ_{soil}: the soil density
- s_u: the untrained shear strength

t_{max} is depending on the type of the soil (clay or sand). It can be determined by using Equation 7.9 [7]:

$$t_{skin,max} = \begin{cases} \alpha s_u & \text{for clay} \\ p_u\tan(\phi) \le f_{lim} & \text{for sand} \end{cases} \tag{7.9}$$

Where ϕ is the internal friction angle and α is dependant on s_u and p_u:

$$\alpha = \begin{cases} \dfrac{1}{2\sqrt{s_u/p_u}} & \text{for}\dfrac{s_u}{p_u} \le 1 \\ \dfrac{1}{2(s_u/p_u)^{1/4}} & \text{for}\dfrac{s_u}{p_u} > 1 \end{cases} \tag{7.10}$$

7.1.5. Tip resistance

The pile is modelled with a tip resistance. This is dependant mostly on the type of soil but also on the pile tip area. According to the *DNV GL-ST-0126*, its value is:

$$q_{tip} = \begin{cases} 9s_u & \text{for clay} \\ N_q p_u \le q_{lim} & \text{for sand} \end{cases} \tag{7.11}$$

Where the value of N_q and q_{lim} are dependant on the internal angle of friction and can be found in Table 7.1 [7].

Internal Friction Angle [deg]	f_{lim} [kPa]	N_q	q_{lim} [Mpa]
15	48	8	1,9
20	67	12	2,9
25	81	20	4,8
30	96	40	9,6
35	115	50	12,0

Table 7.1: Tip resistance parameters for a sand layer

By multiplying this resistance by the area of the pile tip, the force in the upward vertical direction can be determined.

7.1.6. Stiffness interpretation

Different interpretations are possible for the p-y curves. Two options are considered in this report: the linear stiffness and the tangential stiffness. Both of them are based on the slope of the p-y curves. The linear stiffness represents the initial slope, while the tangential stiffness the slope at any point of the curve. These definitions are shown on Figure 7.8.

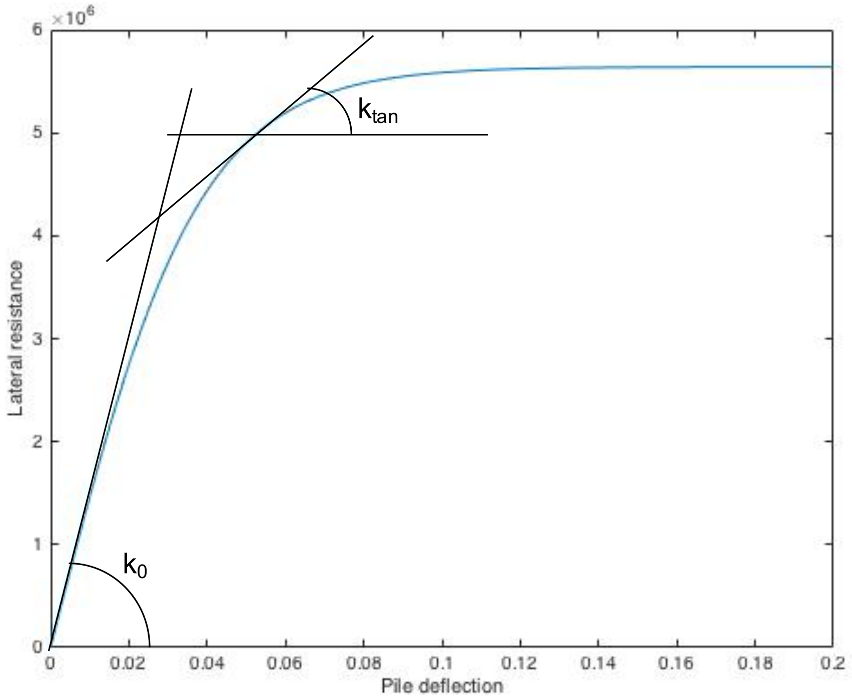

Figure 7.8: Linear and tangential stiffness interpretation

Based on Equation 7.2 and Equation 7.4, the linear stiffness equation is indicated in Table 7.2. However, the linear stiffness doesn't take into account the deflection of the pile. The tangential stiffness returns a more accurate soil stiffness model, at the cost of a higher computational effort.

Soil type	Linear Stiffness	Tangential stiffness
Sand	$k_{mod} \cdot z$	$k_{mod} \cdot z \cdot (1 - \tanh(\frac{k_{mod} \cdot z}{A \cdot p_u} \cdot y))$
Clay	∞	$\frac{p_u}{6 \cdot y_c} \cdot (\frac{y}{y_c})^{-2/3}$

Table 7.2: Soil stiffness based on the p-y curve

It seems that the linear stiffness is infinite, which corresponds to an infinite rigid soil layer. Furthermore, this leads to a numerical problem in the Matlab function. Therefore, the initial slope can be calculate using Equation 7.12 [7].

$$k_{ini} = \xi \frac{p_u}{D_{pile}(\varepsilon_c)^{0.25}} \tag{7.12}$$

Where ξ= 10 for consolidate clay and ξ= 30 for over-consolidated clay.

7.2. p_y_t_z_curves.m

The soil_boundary_condition.m function calculates all the parameters of the p-y and t-z curves. The function p_y_t_z_curves.m uses all of these results to calculate the static response to a load applied on the top of the foundation. This load is defined as a combination of three forces in the three directions : x, y z, respectively noted F_x ,F_y and F_z . The values of F_x and F_y are entered by the user in the script START_OwjEma.m. The load F_z corresponds to the structure weight plus the buoyancy (Section 6.1) and the marine growth weight (Section 6.2).
Since the p-y and the t-z curves are non linear, the static displacement is found iteratively. Consequently, the computation is much faster if stiffness_type = 1, which corresponds to a linear interpretation of the p-y curve (Section 7.1.6). But in this case the result is less accurate than for stiffness_type = 2.
The output of this function is the static displacement of one pile. By dividing the static loads by the displacement of the top of the pile, the equivalent stiffness is obtained. However, as it is specified in the *DNV-J101* [10], this method is made for the ULS. As a result, the equivalent stiffness might be over-estimated by the model.

8
Modal analysis

The last step of the program is the modal analysis. This consist in calculating the modes and the eigenvalues. A representation of this part is shown on Figure 8.1. Only one function is used, the eigenvalue_calculator.m function.

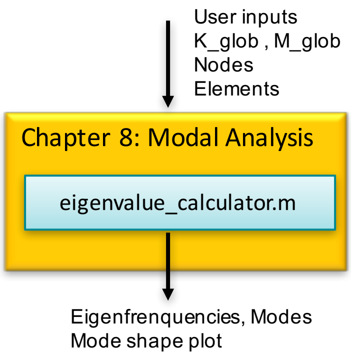

Figure 8.1: Modal analysis section

The outputs of this section (the eigenfrequencies, the modes and the modes shape plots) are part of the outputs returned to the user.

8.1. eigenvalue_calculator.m

The eigenfrequencies of the system are calculated with the global mass and stiffness matrices determined in the previous chapters. By definition, the eigenfrequencies are the positive roots of the following equation:

$$\det(-\omega^2 \cdot (M_{glob} + M_{added}) + K_{glob}) = 0 \tag{8.1}$$

To each eigenfrequency calculated, a mode shape is associated. It represents the deformation of the structure when resonance occurs. This mode shape is represented by a vector where each line represents the spatial variation of a degree of freedom. These displacements are not absolute, they are relative to each other. Consequently, the modes return the shape of the deformation and not the amplitude of it. The amplitude can be calculated but must be associated to an external force.
In eigenvalue_calculator.m, the modes and the eigenfrequencies are calculated with the Matlab function *eig* where [V,D] = eig (K_{glob} , M_{glob}) corresponds to the following equation:

$$K_{glob} V_\omega = M_{glob} V_\omega D_\omega \tag{8.2}$$

Where V_ω is the eigenmatrix and D_ω the diagonal matrix corresponding to the eigenfrequencies.
Deformation can occur in the x-direction or the y-direction. If the structure is perfectly symmetrical, each

mode shape and eigenfrequency representing a deformation in the x-direction will have a "double" representing the same deformation but in the y-direction. However, the eccentricity caused by the rotor will "break" this symmetry and cause a deformation in the fore-aft direction different than in the side-to-side direction.

8.2. Modal Analysis Outputs

The outputs of this section are the matrix of all the modes (the eigenmatrix) and the vector corresponding to the natural frequencies. The results are presented in a table where each line correspond to a mode, the associated natural frequency, the associated modal mass and the associated modal stiffness. An example of this output is shown on Table 8.1. It can be noticed that all the modal mass are equal to one; it's because the modes are mass normalized.

Modes	Eigenfrequencies [Hz]	Modal Mass [Kg]	Modal Stiffness [Nm^2]
1	0,300	1,000	3,565
2	0,302	1,000	3,602
:	:	:	:
8	4,946	1,000	965,952

Table 8.1: Example eigenfrequencies output

The modes shape can be plotted by adding the value of the deformation in the x, y and z directions to the associated nodes coordinates. The result is shown on Figure 8.2. The function eigenvalue_calculator.m plots only the modes specified by the user in the input *Mode_plot*. If the user enters *Mode_plot* = [1 5 8 13], the program returns the plots of the modes 1, 5 8 and 13. If the user enters a mode number higher than the number of degree freedom, the program stops and returns an error message asking to reduce the values in *Mode_plot*. If *Mode_plot* is empty, no mode are plotted.

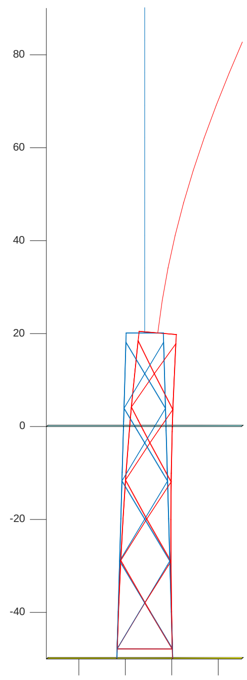

(a) First mode shape

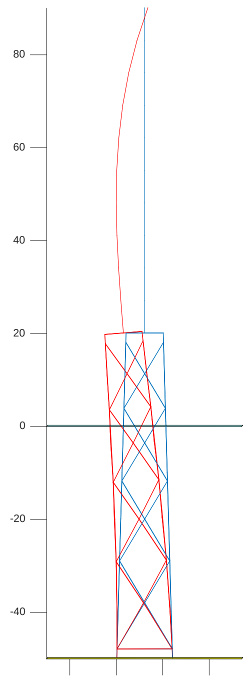

(b) Second mode shape

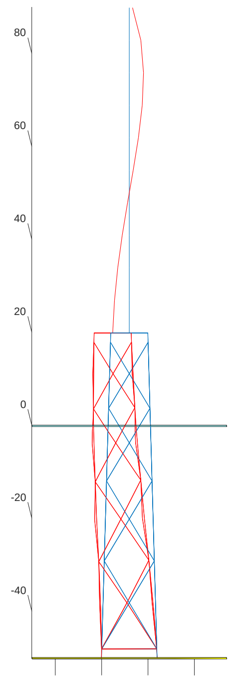

(c) Third mode shape

Figure 8.2: Example of outputs of the eigenvalue calculator

9
Dynamic response analysis

This section of the program is not part of the initial objective: the modal analysis. However, the user may be interested in simulating the dynamic response to a harmonic load on the structure. This is the purpose of this section, represented by Figure 9.1.

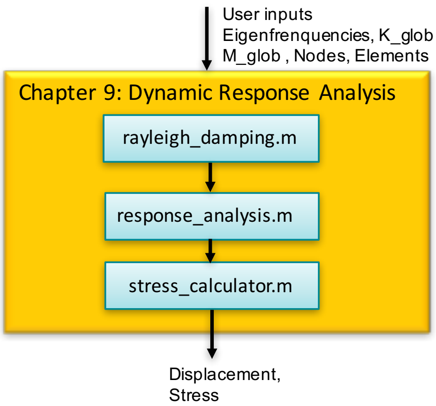

Figure 9.1: Dynamic response analysis section

This part is composed of three functions:
- rayleigh_damping.m
- response_analysis.m
- stress_calculator.m

The idea is to add a material damping to the structure with the function rayleigh_damping.m. This create a new damping matrix, based on the eigenfrequencies obtained in Section 8.1. Once this damping matrix is calculated, a harmonic load is applied on the top node, simulating the wind force on the rotor. The dynamic response to this load is calculated with the function response_analysis.m. Finally, if the user specifies it, the stress in the nodes is calculated with the function stress_calculator.m. The outputs of this section are plots of the displacements, velocities and accelerations of the selected nodes and the stress applied on the nodes.

The damping matrix is essential to understand and estimate the dynamic behaviour of the structure. This damping can take various forms, such as material, viscous or hydrodynamic damping. In this model the hydrodynamic damping has already been introduced in Section 6.5. The material damping can be modelled with a Kelvin-Voigt damping or with a Rayleigh damping.

9.1. Kelvin-Voigt damping

The Kelvin-Voigt damping is a way of representing a viscoelastic material. The classic representation of it is a spring and a damper assembled in parallel. The model is presented on Figure 9.2. This damping definition is not implemented yet into the model, this section gives an indication on how it can be added to the program.

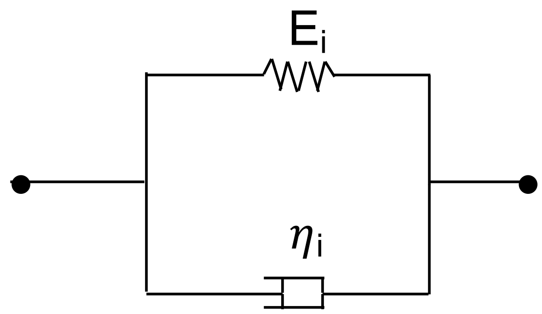

Figure 9.2: Kelvin-Voigt model

According to L. Gaul (1999) [16],and to R.F.Kristensen, K.L.Nielsen and L.P.Mikkelsen (2008) [21], the Kelvin-Voigt model applied to the element i can be expressed by the following equation :

$$M_i \ddot{X}_i + \frac{\eta_{damp,i}}{E_i} K_i \dot{X}_i + K_i X_i = F_i(t) \tag{9.1}$$

The demonstration of Equation 9.1 is made for the element i. The calculation is the same for all the other structure's members.
In this figure, E_i represents the Young's modulus and $\eta_{damp,i}$ the viscous coefficient of element i. Since the model is built in parallel, the strain is the same for the damper and the spring. In addition, the total stress is equal to the sum of the spring stress and the damper stress. Consequently, the following equation is obtained:

$$\sigma_i(t) = E_i \varepsilon_i(t) + \eta_{damp,i} \frac{d\varepsilon_i(t)}{dt} \tag{9.2}$$

The Kelvin-Voigt model can also be expressed with a complex dynamic modulus:

$$E_i^*(\omega) = E_i + i\omega\eta_{damp,i} \tag{9.3}$$

Since the mass and the stiffness matrices are known, it can be deduced:

$$M_i \ddot{X}_i + K_i X_i = F_i(t) \tag{9.4}$$

Where X_i represents the vector of the displacements of element i. In the frequency domain, the equation is:

$$-\omega^2 M_i \tilde{X}_i + K_i \tilde{X}_i = \tilde{F}_i \tag{9.5}$$

Equation 9.3 is then substituted in Equation 6.4.

$$-\omega^2 M_i \tilde{X}_i + i\omega \frac{\eta_{damp,i}}{E_i} K_i \tilde{X}_i + K_i \tilde{X}_i = \tilde{F}_i \tag{9.6}$$

By transferring Equation 9.6 into the time domain, it is finally obtained:

$$M_i \ddot{X}_i + \frac{\eta_{damp,i}}{E_i} K_i \dot{X}_i + K_i X_i = F_i(t) \tag{9.7}$$

The Kelvin-Voigt damping matrix is then expressed as:

$$C_{KV,i} = \frac{\eta_{damp,i}}{E_i} K_i \tag{9.8}$$

With this method, the damping matrix of each element is determined, then assembled into a global damping matrix.

9.2. rayleigh_damping.m

The Rayleigh damping introduces the material damping. The idea of such damping is to represent the internal damping of the structure, in other words the energy dissipation of the system. This method leads to a proportional damping which is expressed on Equation 9.9.

$$C_{Rayleigh} = \alpha_{Rayleigh} M + \beta_{Rayleigh} K \tag{9.9}$$

where $\alpha_{Rayleigh}$ and $\beta_{Rayleigh}$ are respectively the mass and the stiffness damping coefficient. A method to determine these coefficients is detailed by Indrajit Chowdhury and Shambhu P. Dasgupta (2003) [14]. The purpose of this method is to estimate the value of these coefficients. It is known that the behaviour of the system is characterized by Equation 9.10

$$M\ddot{X} + C_{Rayleigh}\dot{X} + KX = F(t) \tag{9.10}$$

Equation 9.10 is pre-multiplied by V_ω^t and multiplied by V_ω, which is the eigenmatrix.

$$V_\omega^t M V_\omega \ddot{X} + V_\omega^t C_{Rayleigh} V_\omega \dot{X} + V_\omega^t K V_\omega X = V_\omega^t F(t) \tag{9.11}$$

Equation 9.11 can be also written with the modal matrices notation such as:
- $M^* = V_\omega^t M V_\omega$
- $C^*_{Rayleigh} = V_\omega^t C_{Rayleigh} V_\omega$
- $K^* = V_\omega^t K V_\omega$

Thus, Equation 9.11 becomes:

$$M^* \ddot{X} + C^*_{Rayleigh}\dot{X} + K^* X = V_{omega}^t F(t) \tag{9.12}$$

By pre-multiplying the previous equation by M^{*-1}, the following equation is obtained:

$$I\ddot{X} + M^{*-1} C^*_{Rayleigh}\dot{X} + M^{*-1}K^* X = M^{*-1}\phi^t F(t) \tag{9.13}$$

By construction, the modal matrices are diagonal. As a result, for each mode, an equation is derived and is expressed in the following form:

$$\ddot{x_{ii}} + \frac{c^*_{ii}}{m^*_{ii}} \cdot \dot{x_{ii}} + \omega_i^2 \cdot x_{ii} = \frac{f(t)^*_i}{m^*_{ii}} \tag{9.14}$$

The modal damping ratios are introduced. They are expressed in the form:

$$\xi_i = \frac{c^*_{ii}}{c^{cr}_{ii}} = \frac{c^*_{ii}}{2\sqrt{m^*_{ii}k^*_{ii}}} = \frac{c^*_{ii}}{2m^*_{ii}\omega_i} \tag{9.15}$$

By substituting this into Equation 9.14, it is obtained:

$$\ddot{x_{ii}} + 2\xi_i\omega_i\dot{x_{ii}} + \omega_i^2 x_{ii} = \frac{f(t)^*_i}{m^*_{ii}} \tag{9.16}$$

Equation 9.9 is substituted into Equation 9.11.

$$V_\omega^t M V_\omega \ddot{X} + \alpha V_\omega^t M V_\omega \dot{X} + \beta V_\omega^t K V_\omega \dot{X} + V_\omega^t K V_\omega X = V_\omega^t F(t) \tag{9.17}$$

$$M^* \ddot{X} + \alpha_{Rayleigh} M^* \dot{X} + \beta_{Rayleigh} K^* \dot{X} + K^* X = V_\omega^t \cdot F(t) \tag{9.18}$$

By following the same steps detailed in Equation 9.13 and Equation 9.14, the following result is obtained :

$$c^*_{ii} = \alpha m^*_{ii} + \beta k^*_{ii} \tag{9.19}$$

$$\xi_{mod,i} = \frac{\alpha_{Rayleigh} m^*_{ii} + \beta_{Rayleigh} k^*_{ii}}{c^{cr}_{ii}} = \frac{\alpha_{Rayleigh}}{2\omega_i} + \frac{\beta_{Rayleigh}\omega_i}{2} \tag{9.20}$$

To solve this system of equation, two values of ξ_{mod} are needed. The modal damping is not known. However, in the industry, some values are assumed for the first three modes. According to Golafshani, Ali Akbar and Gholizad, Amin (2009) [18], the damping ratio for the first three modes are assumed to be $\xi_{1mod,} = 0.05$, $\xi_{mod,2} = 0.03$ and $\xi_{mod,3} = 0.02$. This assumption is also made by Madjid Karimirad (2014)[20] with $\xi_{mod,1} = 0.05$.

The output of this section is the damping matrix $C_{rayleigh}$, which is used to estimate the dynamic response of the model.

9.3. response_analysis.m

If the selected modal_displacement_analysis = 'Y', the program activates the function response_analysis.m. The role of this function is to calculate the dynamic response to a harmonic load applied on the top node. Such operation requires the global mass matrix, the global stiffness matrix and the damping matrices. Once the modes and the eigenfrequencies are determined, the modal matrices are calculated :

$$M^* = V_\omega^t M V_\omega \tag{9.21}$$

$$C^* = V_\omega^t C V_\omega \tag{9.22}$$

$$K^* = V_\omega^t K V_\omega \tag{9.23}$$

These matrices are diagonal and their coefficients can be written as m^*_{ii}, c^*_{ii} and k^*_{ii}. From c^*_{ii} the damping ratio of each mode can be calculated:

$$\xi_i = \frac{c^*_{ii}}{2m^*_{ii}\omega_i} \tag{9.24}$$

The next step is to calculate the modal displacement with Equation 9.25.

$$u_{mod,i}(t) = A_i \exp(-\xi_i\omega_i t)\sin(\omega_i t\sqrt{1-\xi_i^2}+\varphi_i)+\frac{1}{m^*_{ii}\omega_i\sqrt{1-\xi_i^2}}\int_0^t F_i^*(\tau)\sin(\omega_i\sqrt{1-\xi_i^2}(t-\tau))\exp(-\xi_i\omega_i(t-\tau))d\tau \tag{9.25}$$

Where A_i and φ_i are determined according to the initial conditions. Nevertheless, we are interested in the steady-state response to the force. In consequence, the modal displacement can be written as:

$$u_{mod,i}(t) = \frac{1}{m^*_{ii}\omega_i\sqrt{1-\xi_i^2}}\int_0^t F_i^*(\tau)\sin(\omega_i\sqrt{1-\xi_i^2}(t-\tau))\exp(-\xi_i\omega_i(t-\tau))d\tau \tag{9.26}$$

Where $F_i^*(t) = \underline{\hat{x}}_i^T \cdot f(t)$, $\underline{\hat{x}}_i$ the eigenvector i and f(t) the external exciting force.
From Equation 9.26, the general displacement can be computed:

$$x(t) = V_\omega u(t) \tag{9.27}$$

Based on the user inputs, the program returns the displacement, velocity, acceleration and the force and moment applied on the selected nodes. The outputs are selected with the following inputs:

- *Node_plot* = [55 29] if the user wants to do the calculations for the nodes 55 and 29
- *Dir_plot* = ['x' 'y' 'z'] if the user wants to do the calculations in the x, y and a directions
- *Displacement_plot* = 'Y' if the user wants to plot the nodes displacements
- *Force_plot* = 'Y' if the user wants to plot the force applied on the selected nodes
- *Moment_plot* = 'Y' if the user wants to plot the moment applied on the selected nodes
- *Stress_plot* = 'Y' if the user wants to plot the stress applied on the selected nodes

The user has also the possibility to select the time of the simulation (in second) with the input *time_simulation*.

9.4. stress_calculator.m

From Section 9.3, the general displacements are known. So, the velocity and the acceleration vectors can be computed. Once $\ddot{X}$,$\dot{X}$ and X are determined, the loads applied on the nodes are calculated:

$$M\cdot\ddot{X}+C\cdot\dot{X}+K\cdot X = F(t) \tag{9.28}$$

From this equation, the axial loads in each member can be calculated, as well as the moments around the local y and z axis. The stress applied on one specific node in one specific element is:

$$\sigma = \frac{F_x}{A}+\frac{M_y}{V}+\frac{M_z}{V} \tag{9.29}$$

9.5. Dynamic response analysis

The outputs of this section are the plots of the displacement, velocity, acceleration, force, moment and stress. These depend on the inputs, detailed in Section 9.3. Examples of these plots are presented on Figure 9.3 , Figure 9.4, Figure 9.5 and Figure 9.6. These plots correspond to the response of the top node (node 55) to a force in the x direction with an amplitude of 100 kN and a frequency of 0.3093 Hz, which correspond to the first natural frequency in this example.

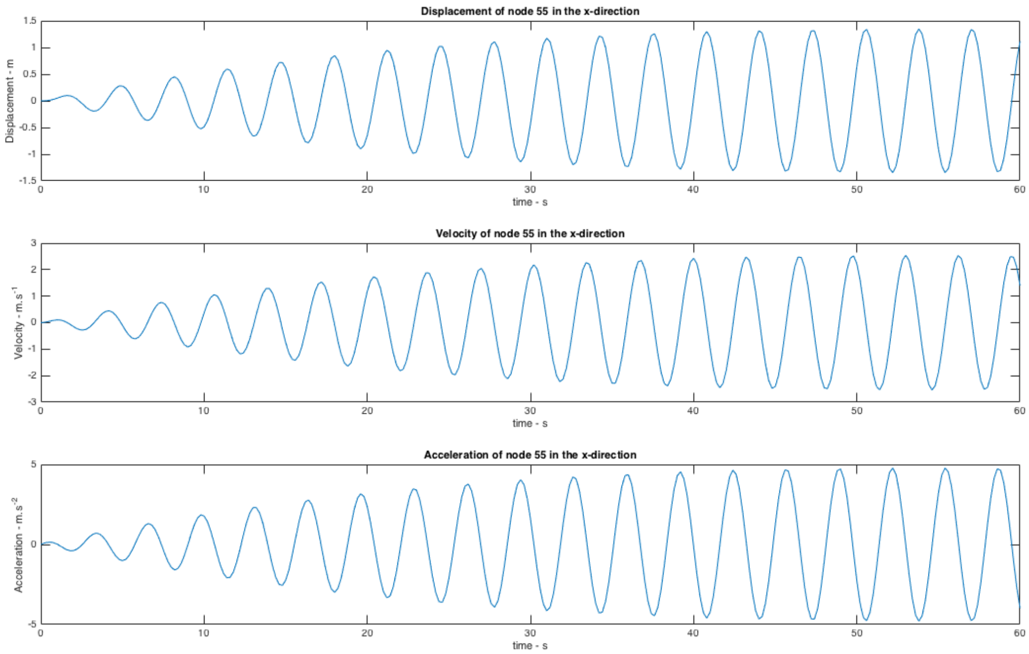

Figure 9.3: Example of dynamic response

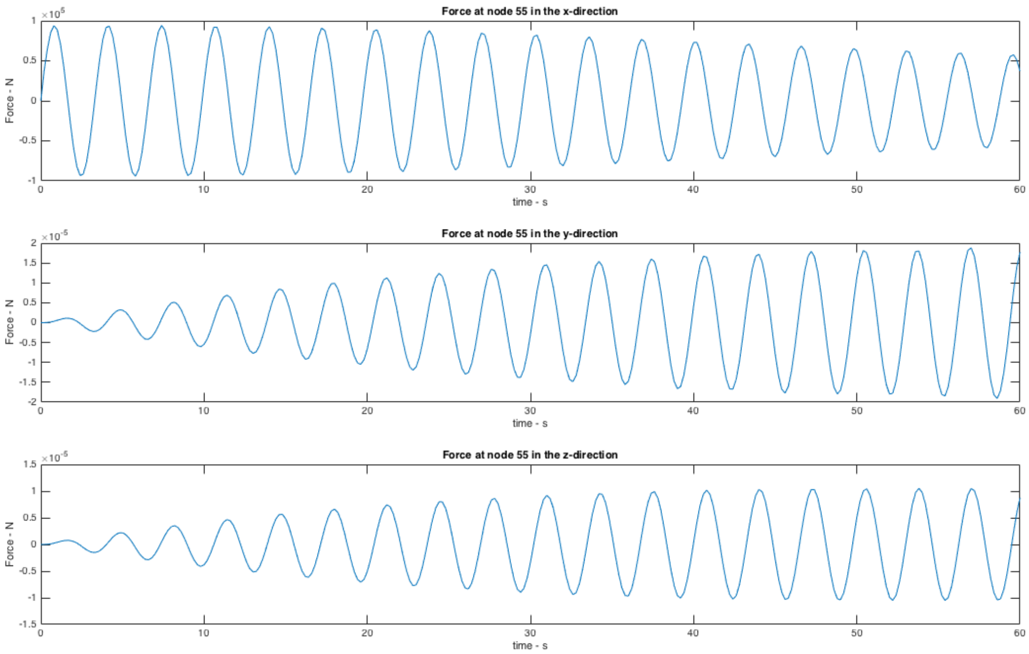

Figure 9.4: Example of force at a node

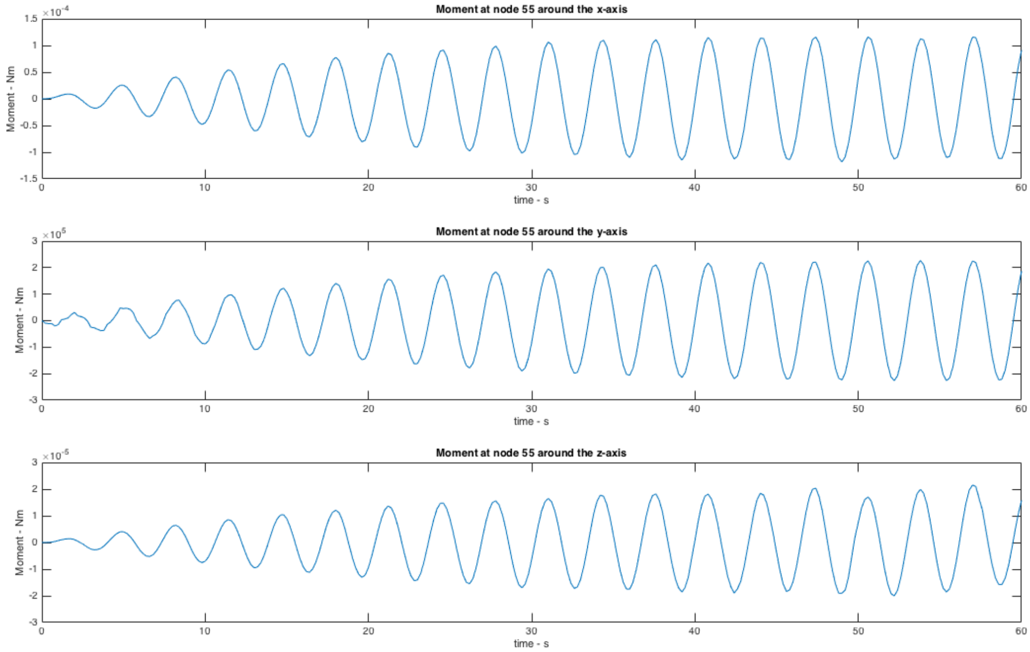

Figure 9.5: Example of moment at a node

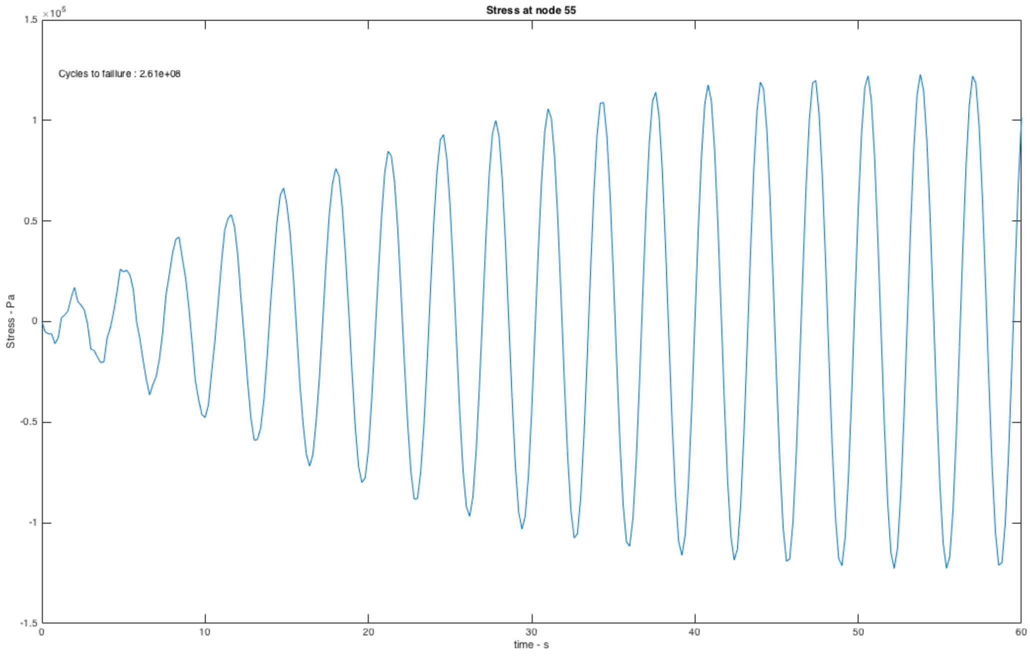

Figure 9.6: Example of stress at a node

III

Finite Element Model Checks

10

Test of a simplified structure

The program OwjEma was built to estimate the modes shape and eigenvalues of an offshore wind support structure. Yet, before using the model, it must be tested to ensure that the program's outputs are correct. The first step in model verification is to define a simple structure. This check was done during the construction of OwjEma, to ensure that the coding was correct before proceeding to the next step. The structure used is a clamped beam with a constant cross section. Several checks are performed with this beam, as detailed in the figure 10.1.

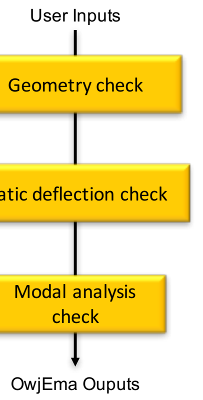

Figure 10.1: Verification steps of OwjEma

The three steps, geometry checks, static deflection checks and modal analysis, correspond respectively to the verification of the inputs, the stiffness matrix and the mass matrix. If the two global matrices characterizing the model are correct, the results of the modal analysis can be trusted.
In this chapter, the results of OwjEma are compared to the analytical results, provided by the equations related to a clamped beam.

10.1. Structure definition

The first check of the OwjEma program is to model a clamped beam. Such a structure can be modelled easily. Its mass matrix and stiffness matrix are calculated via the functions Element_Matrices.m and matrix_assembly.m. The clamped beam model is shown in Figure 10.2.

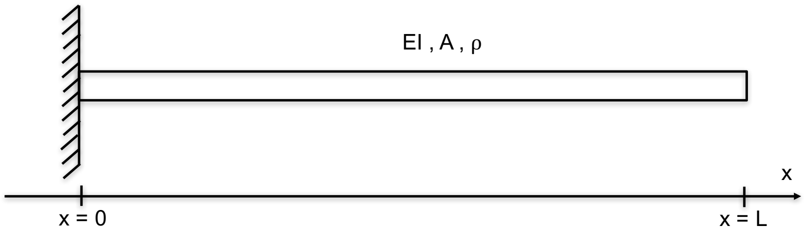

Figure 10.2: Model of a clamped beam

In this section, the values characterizing the model are:
- E = 210E9 Pa
- ρ = 8500 kg·m^{-3}
- L = 70 m
- D = 2 m
- t = 0,02 m

The beam is discretized with 20 nodes. The result is shown on Figure 10.3. Visually, it can be confirmed that the construction of the geometry is correct. But, this graph does not show the aspect of the volume of the structure.

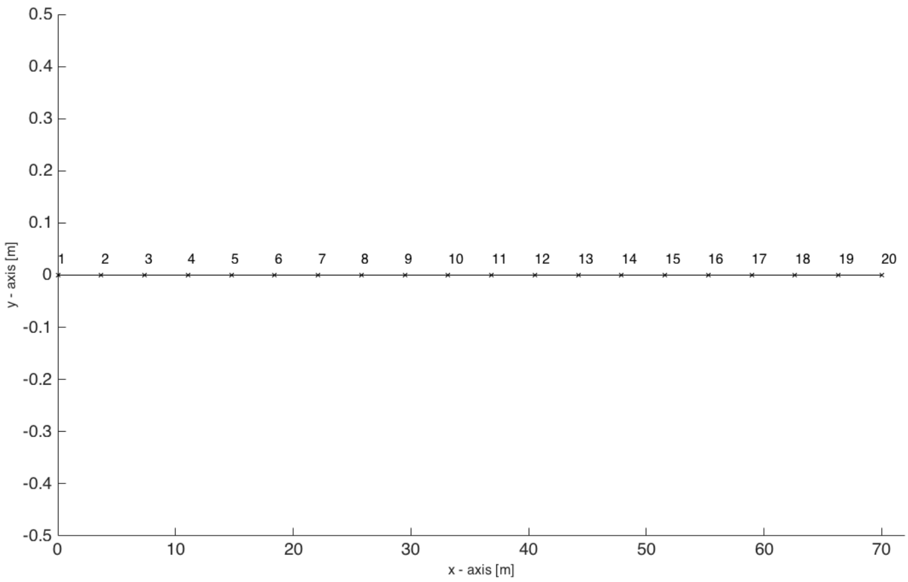

Figure 10.3: Clamped beam model in OwjEma

To ensure the model has correctly defined the beam geometry, the mass of all the elements of the model is calculated and compared to the theoretical mass. The results are presented on Table 10.1.

Theoretical mass [kg]	OwjEma mass [kg]
74022,20	74022,20

Table 10.1: Mass comparison for a clamped beam

The results are exactly the same in both case, which can confirm the geometry definition is correct for a simple structure.

10.2. Static check

To check whether the stiffness matrix is correct or not, a force is applied at the tip of the beam, as presented on Figure 10.4.

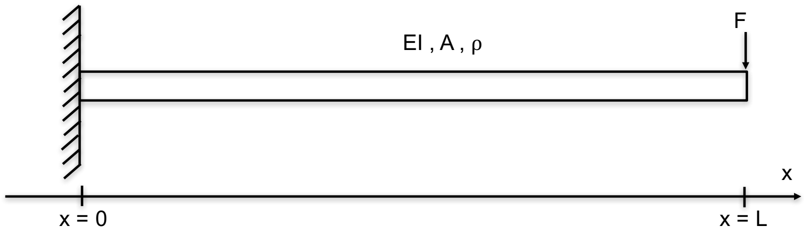

Figure 10.4: Static force at the tip of a clamped beam

If the static force F is represented as a vector, the associated displacement can be calculated with the following Equation:

$$q_{numerical} = K_{glob}^{-1} F \tag{10.1}$$

Analytically, the tip displacement can also be calculated. It is know that the moment of the beam is:

$$M = -EI\frac{dy^2}{d^2x} \tag{10.2}$$

Since a force F is applied in the y direction at the location x = L, the moment M is:

$$M(x) = F(x-L) \tag{10.3}$$

By substituting Equation 10.3 into Equation 10.2, it is obtained:

$$\frac{dy^2}{d^2x} = \frac{F(x-L)}{-EI} \tag{10.4}$$

Equation 10.4 is integrated twice. So, the static displacement is:

$$y(x) = \frac{Fx^3}{6EI} + C_1 x + C_2 \tag{10.5}$$

The constants C_1 and C_2 are determined with the boundaries conditions. Since y(0) = 0 and $\frac{dy}{dx}$ = 0, it is obtained C_1 = $\frac{1}{2}$ FL^2x and C_2 =0. Then, if the static displacement at x = L is noted $q_{analytical}$, it is obtained:

$$q_{analytical} = \frac{FL^2}{3EI} \tag{10.6}$$

The value of $q_{analytical}$ and $q_{numerical}$ are calculated and compared for a force F varying from 1 N to 100 kN. The results are shown on Figure 10.5.

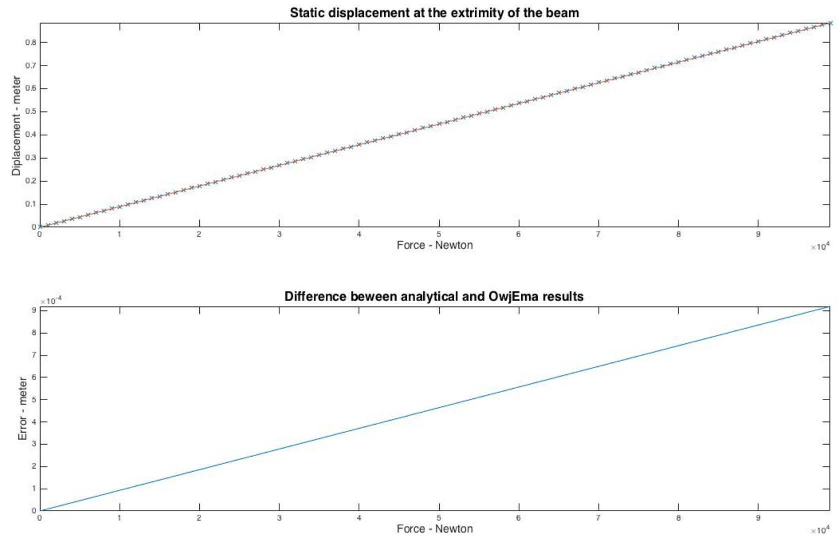

Figure 10.5: Static displacement of the tip of the clamped beam

It can be noticed that even for a force of 100 kN, the difference between the analytical result and the OwjEma result is only of 9,1957E-4 m, which can be neglected. The static displacements of the complete beam is also calculated numerically and analytically. The results are presented on Figure 10.6.

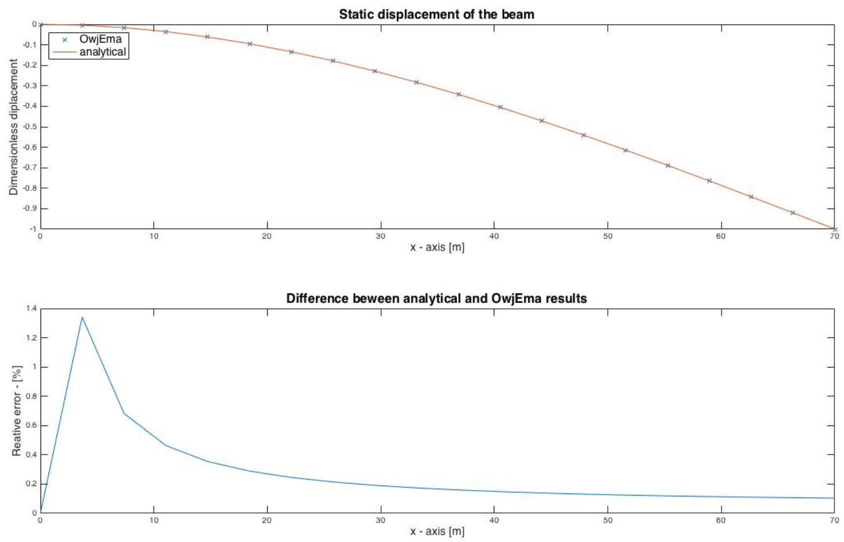

Figure 10.6: Static displacement of the clamped beam

The results are similar in both cases with a maximum relative error of 1,4%. As a result, the stiffness calculated with OwjEma for a clamped beam can be validated. However this is a validation only for a simple model. The model should also be checked for more complex structure which will be performed in the next chapter.

10.3. Modal analysis check

Once the stiffness matrix is validated for the clamped beam model, the mass matrix is checked. This is done by calculating the modes and the natural frequencies of the beam with the global matrices K_{glob} and M_{glob}. The natural frequencies of a clamped beam can be calculated by hand according to the Equations 10.7, 10.8 and 10.9.

$$\omega_1 = 1.875^2\sqrt{\frac{EI}{\rho AL^4}} \tag{10.7}$$

$$\omega_2 = 4.694^2\sqrt{\frac{EI}{\rho AL^4}} \tag{10.8}$$

$$\omega_3 = 7.855^2\sqrt{\frac{EI}{\rho AL^4}} \tag{10.9}$$

Based on the the values of E, I ρ, A and L, the natural frequencies of the beam are :
- $\omega_{1,analytical}$ = 2,4969 rad·s^{-1}
- $\omega_{2,analytical}$ = 15,6477 rad·s^{-1}
- $\omega_{3,analytical}$ = 43,8139 rad·s^{-1}

The modes and the eigenfrequencies are also calculated with the Matlab function *eig* and the global matrices K_{glob} and M_{glob}. The natural frequencies are:
- $\omega_{1,numerical}$ = 2,4943 rad·s^{-1}
- $\omega_{2,numerical}$ = 15,5354 rad·s^{-1}
- $\omega_{3,numerical}$ = 43,0736 rad·s^{-1}

The relative error for ω_1, ω_2 and ω_3 are respectively of 0,10 %, 0,72 % and 1,72 %.
The modes shape corresponding to these three natural frequencies and calculated with OwjEma are presented on Figure 10.7. These modes correspond to the first, second and third mode shape of a clamped beam.

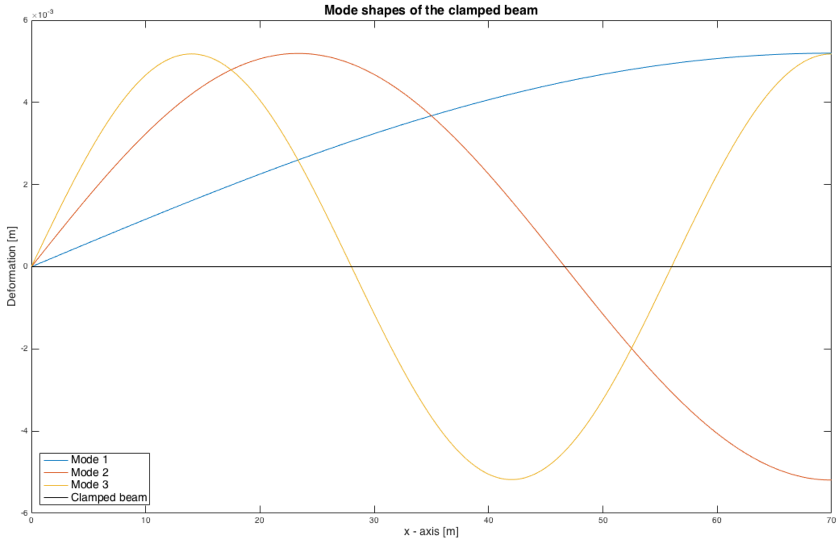

Figure 10.7: Calculated mode shape of the clamped beam

Since the modes shape calculated correspond to the expected modes shape and since the analytical and numerical natural frequencies are similar, the mass matrix is validated for a clamped beam.

11

Bladed comparison checks

In Chapter 10, it has been verified that the model was able reproduce the modal behaviour of a simple beam. However, in order to validate OwjEma, verifications must be performed for a more complex structure. For this check, the OwjEma results are compared to the result of the Bladed software, described in Section 2.1. Since the method for calculating eigenfrequencies and mode shapes in Bladed and OwjEma are not the same (as detailed in Section 11.4), additional steps must be performed in the check. The OwjEma code is adapted to return the same output as Bladed.

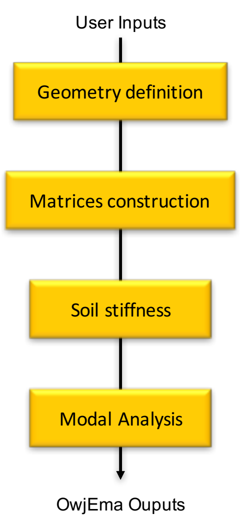

Figure 11.1: Verification steps of OwjEma

As shown in Figure 11.1 and as explained in the previous chapters, the algorithm is composed of different steps: the definition of the geometry, the construction of the matrices, the definition of the soil stiffness and the modal analysis. The part concerning the plotting of the structure is not considered in this chapter because it can be assimilated to the geometry definition. All parts of OwjEma are checked with the Bladed outputs.

11.1. Scenario definition

In Section 10.1, the stiffness matrix and the mass matrix constructed by OwjEma for a simple model have been validated. Nevertheless, the matrices must be verified for a complex structure. Since the analytical solution can not be calculated for a multi-member structure, OwjEma outputs are compared to Bladed outputs. In the model, several parameters are implemented and must be checked. As a result, several scenarios have been established to isolate the influence of these parameters and to verify if they have been correctly implemented. The different scenarios are presented on Table 11.1.

	Scenario 1	Scenario 2	Scenario 3	Scenario 4	Scenario 5	Scenario 6
NL	4	3	4	4	4	4
Fl_{leg}	N	N	N	N	Y	N
Fl_{brace}	N	N	N	N	Y	N
Nb	4	4	4	4	4	4
Brace pattern	X	X	Z	X	X	X
marine growth [m]	0	0	0	0	0	0,1
E_{TP} [Pa]	2.10e13	2.10e13	2.10e13	2.10e11	2.10e13	2.10e13

Table 11.1: Scenario definition

All the scenarios are based on the inputs listed in Table 11.2.

rho_s [kg·m^{-3}]	**E_s [Pa]**	**nu_s**	**rho_TP [kg·m^{-3}]**	**nu_TP**
8500	2,10E11	0,3	8500	0,3P
Jh [m]	**L_bottom [m]**	**L_top [m]**	**h0 [m]**	**TPL [m]**
70	12	8	2	2
h_tp [m]	**Dl_bottom [m]**	**Dl_top [m]**	**tl_bottom [m]**	**tl_top [m]**
0	1,289	1,123	0,0537	0,0312
BA	**Nb**	**Horizontal_member**	**D_brace [m]**	**t_brace [m]**
Y	4	N	0,732	0,020
ht [m]	**Dt_bottomp [m]**	**Dt_top [m]**	**Tt_bottom [m]**	**Tt_top [m]**
70	5,5	4	0,034	0,020
M_nacelle [ton]	**M_rotor [ton]**	**msl [m]**	**rho_w [kg·m^{-3}]**	**splash_zone [m]**
240	110	50	1025	2

Table 11.2: Base geometry

These scenarios should be tested for a case with rigid foundations and for a case with stiff foundations. The soil parameters used for verification are presented in Table 11.3. The piles of the structure are modelled as a vertical beam with a diameter of 1.22 m, a thickness of 0.01 m and a length of 30 m. The curves p-y and t-z are calculated every 1 meter. The static forces in the x and y directions are both equal to 1 000 000 N.

Layer ID	Layer Type	Layer depth [m]	Density [kg· m $^{-3}$]	Friction angle [deg]	Undrained shear strength [Pa]	Vertical Strain	Poisson coefficient
1	Clay	0	8000	-	25000	0.02	0.3
2	Sand	2	8000	30	-	-	0.3
3	Clay	4	10000	-	100000	0.005	0.3

Table 11.3: Soil stiffness scenario

11.2. Geometry checks

The model has been verified for a simple structure, but this is not enough to validate it. Verifications must be done for a more complex structure. Bladed software is used in this section to compare OwjEma results. The first step is to check the construction of the geometry. A basic check is to compare the Bladed and OwjEma plots for different structures, as shown in Figure 11.2 and Figure 11.3. These figures represent different variations in the design of the structure. It can be noted that the graphics are the same for both programs. Even if this does not validate the model at all, it confirms that Bladed and OwjEma will perform a simulation based on the same structures.

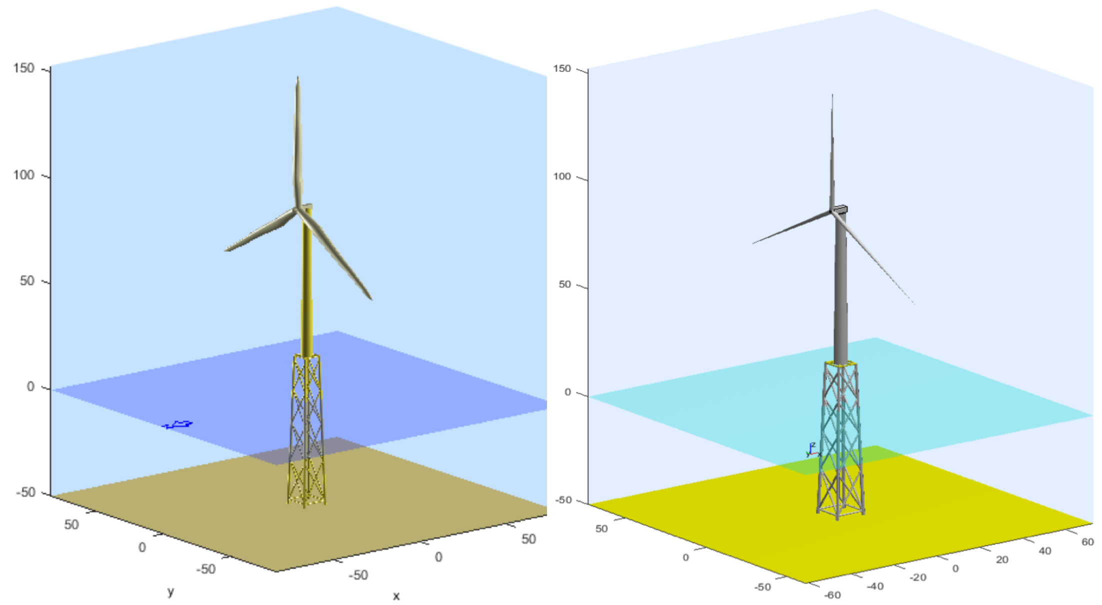

(a) Bladed geometry visualization (b) OwjEma geometry visualization

Figure 11.2: Comparison of the Bladed and OwjEma geometry output for scenario 1

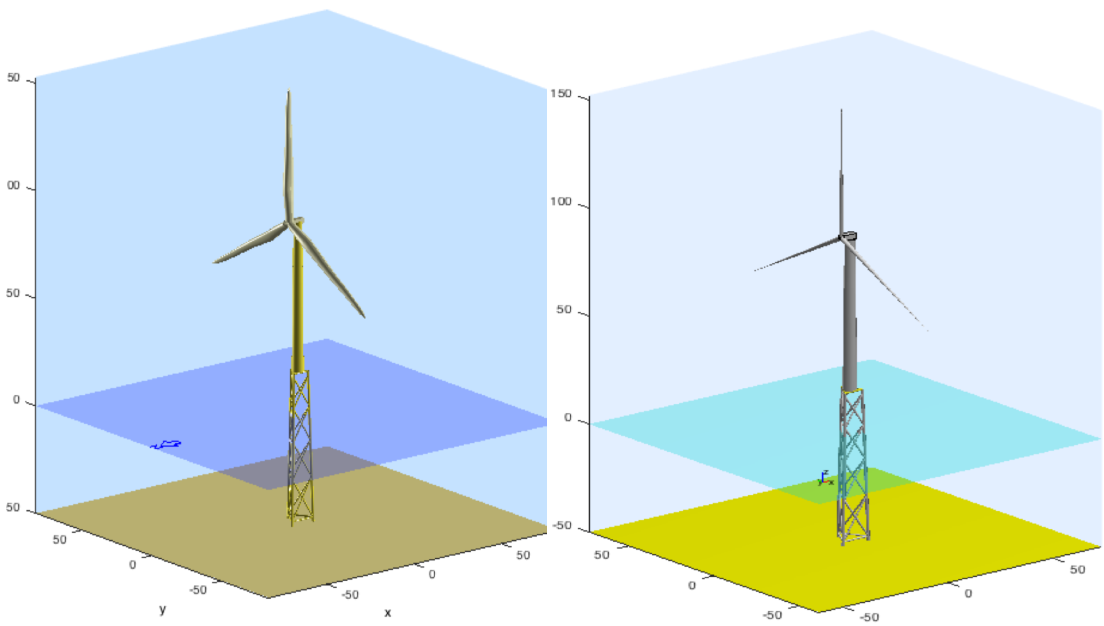

(a) Bladed geometry visualization (b) OwjEma geometry visualization

Figure 11.3: Comparison of the Bladed and OwjEma geometry output for the scenario 2

An output of Bladed is the multi-member structure's mass. This only concerns the elements' mass, without the weight of marine growth and without the water in the members. As a result, the mass of Scenario 1, 2, and 3 models are compared. The results are presented in Table 11.4. Lines 4 and 5 of the table correspond respectively to a different brace pattern and to a different number to the bay. The idea is to compare different configurations of geometry.

Scenario	Bladed model mass [kg]	OwjEma model mass [kg]	Error (%)
1	886361	886221	0,016
2	723894	723773	0,017
3	769292	769152	0,018
Brace pattern K	906040	905901	0,015
3 bay	872466	872303	0,019

Table 11.4: Comparison of the mass model

The mass is similar in both programs, with a small relative error in each scenario. The differences may come from the discontinuity of the model. Still, these results provide a good basis for confirming the geometric definition in OwjEma.

11.3. Static checks

To check the stiffness matrix of the model, a static force is applied at the top of the structure. Then, the static deformations of the model are calculated and compared to the results from Bladed. Yet, it is not possible to directly apply a static charge in Bladed, the deformations are obtained from the loads caused by the wind on the rotor. Ergo, the static loads are a function of the wind speed in Bladed. For a 61m wind turbine, and a wind speed from 3 m$\cdot$ s^{-1} to 25 m$\cdot$ s^{-1}, the loads are calculated. The results are shown on Figure 11.4.

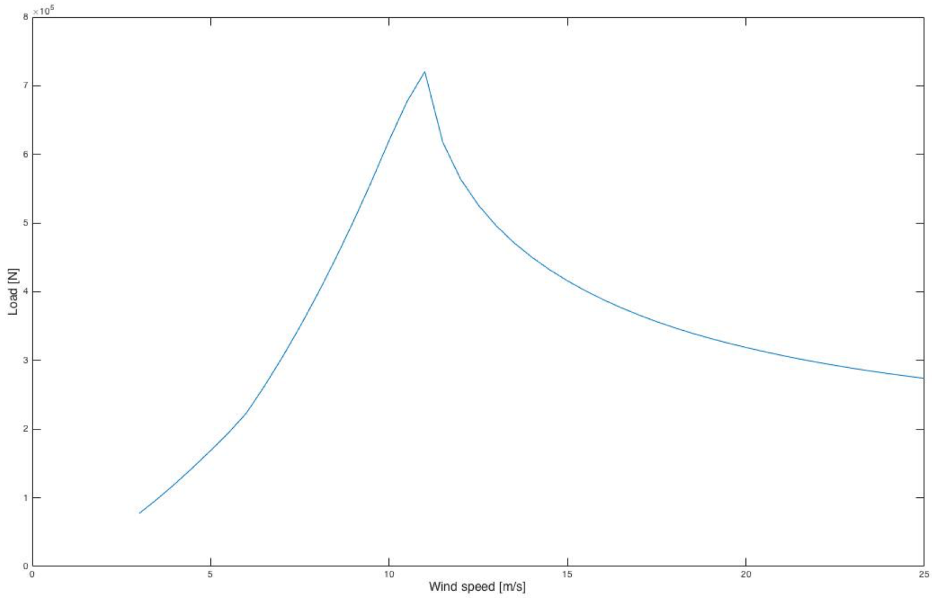

Figure 11.4: Variation of the loads applied on the rotor according to the wind speed

Loads values are extracted from Bladed and implemented in OwjEma. From this, the static displacement of the model is calculated. The results for scenario 1 with rigid foundations are shown on Figure 11.5.

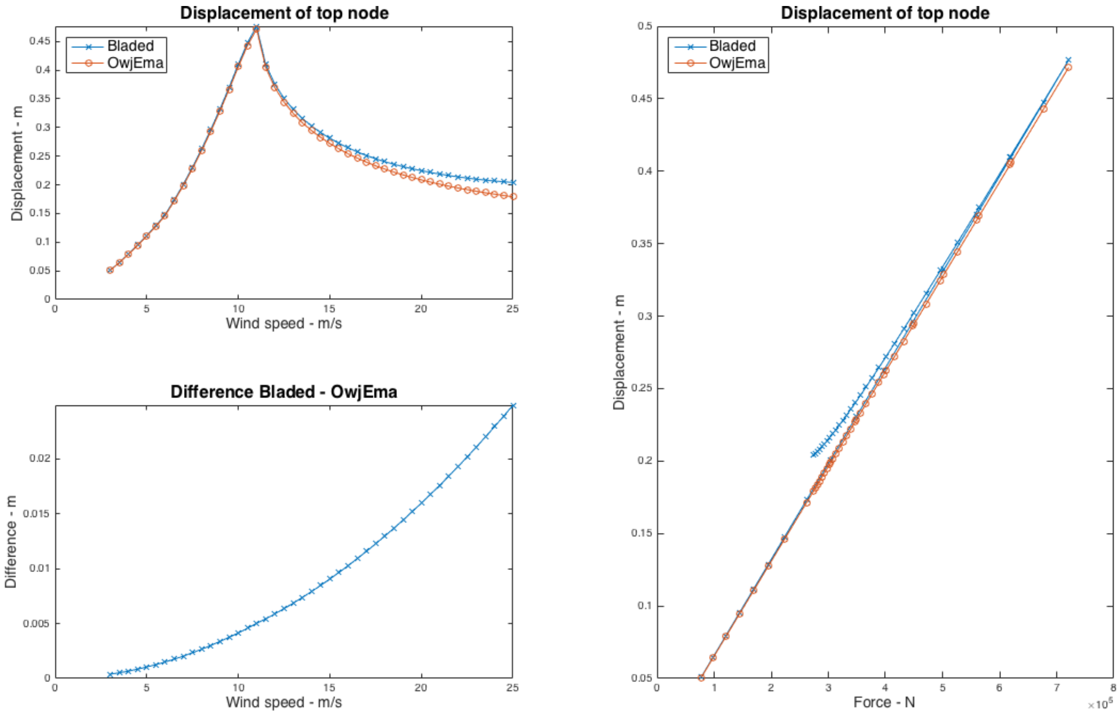

Figure 11.5: Static displacement of top node in scenario 1

The first thing to note about Figure 11.5 is that the deformation is not similar between OwjEma and Bladed after the wind speed of 11 m·s^{-1}. After the peak, the charges decrease, but the structure does not return to its initial position. It can be viewed with the graph on the right of the figure. In OwjEma, the deformations according to the loads are perfectly linear, which is not the case in the Bladed model. This could be explained by the drag force that act on the structure in Bladed and which is not implemented in OwjEma. Apart from the non-linearity of the deformation after the peak, the results from Bladed and from OwjEma are similar. Static deformation is also tested for scenarios 1, 2, 3 and 4 at different nodes of the model. These nodes are presented on Figure 11.6. Scenarios 5 and 6 are not statically tested because the changing parameters (flooded members and marine growth) do not influence the rigidity of the model.

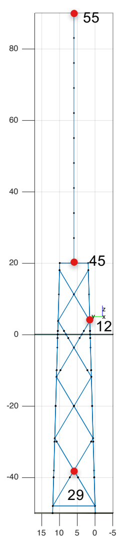

(a) Scenarios 1 and 4

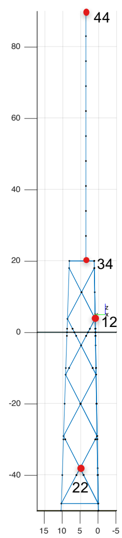

(b) Scenario 2

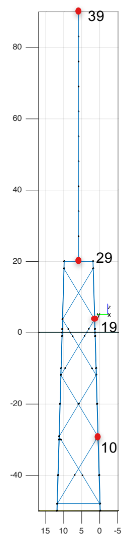

(c) Scenario 3

Figure 11.6: Position of the nodes in scenario 1 to 4

A static load varying from 77346 N to 720673 N (corresponding to a wind speed from 3 m·s^{-1} to 11 m·s^{-1}) is applied at the top node of the structure in the x-direction. The static response obtained with Bladed and OwjEma, for rigid foundations, are presented on Figure 11.7, Figure 11.8, Figure 11.9 and Figure 11.10.

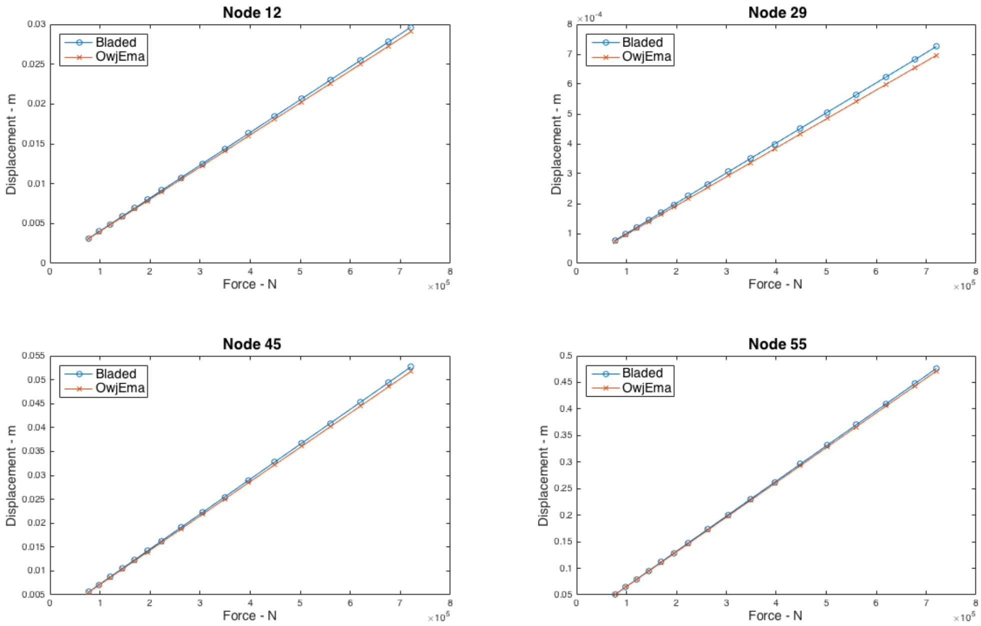

Figure 11.7: Static response scenario 1 with rigid foundation

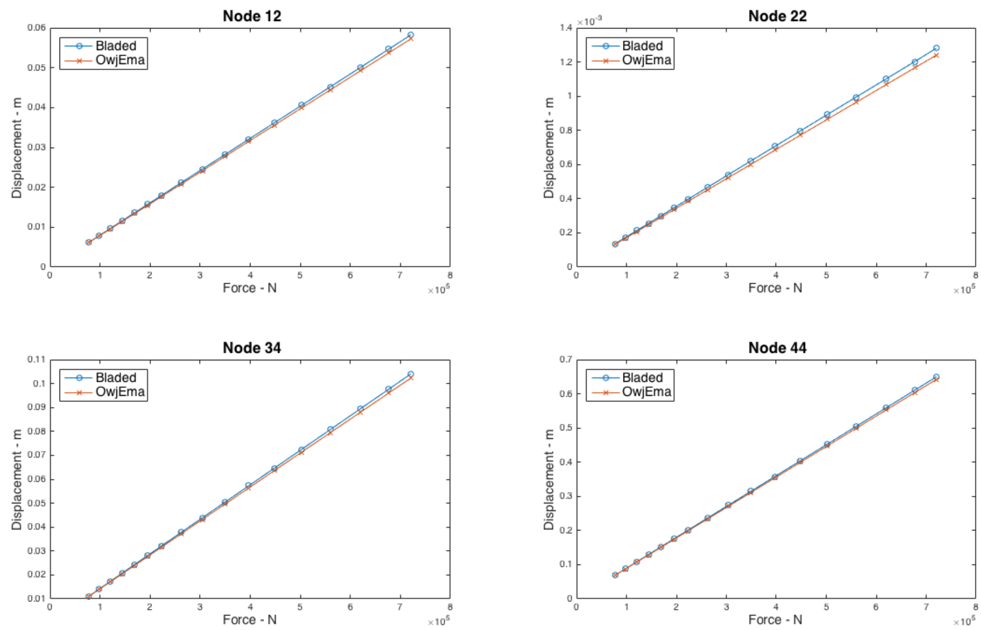

Figure 11.8: Static response scenario 2 with rigid foundation

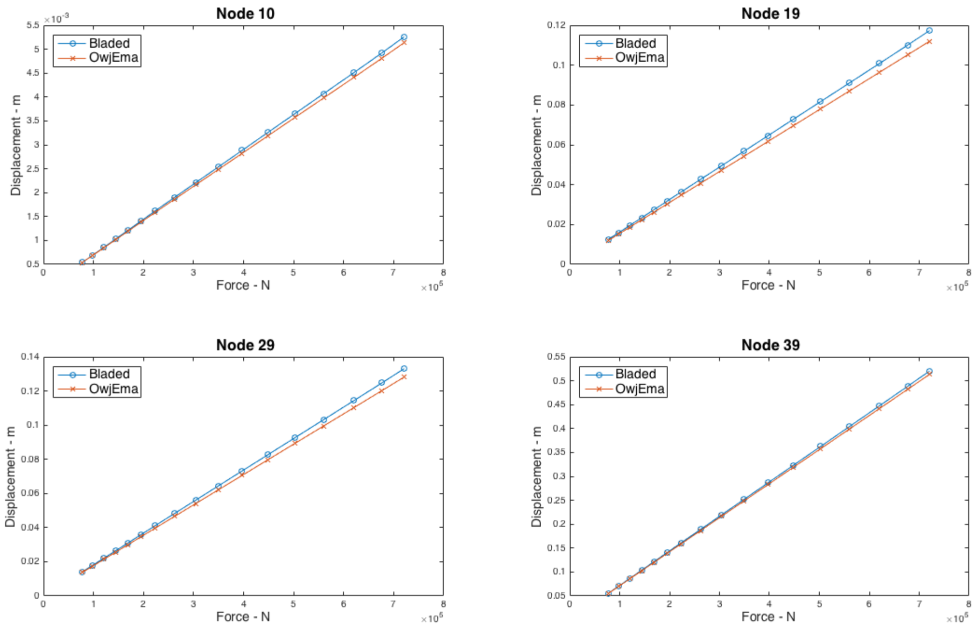

Figure 11.9: Static response scenario 3 with rigid foundation

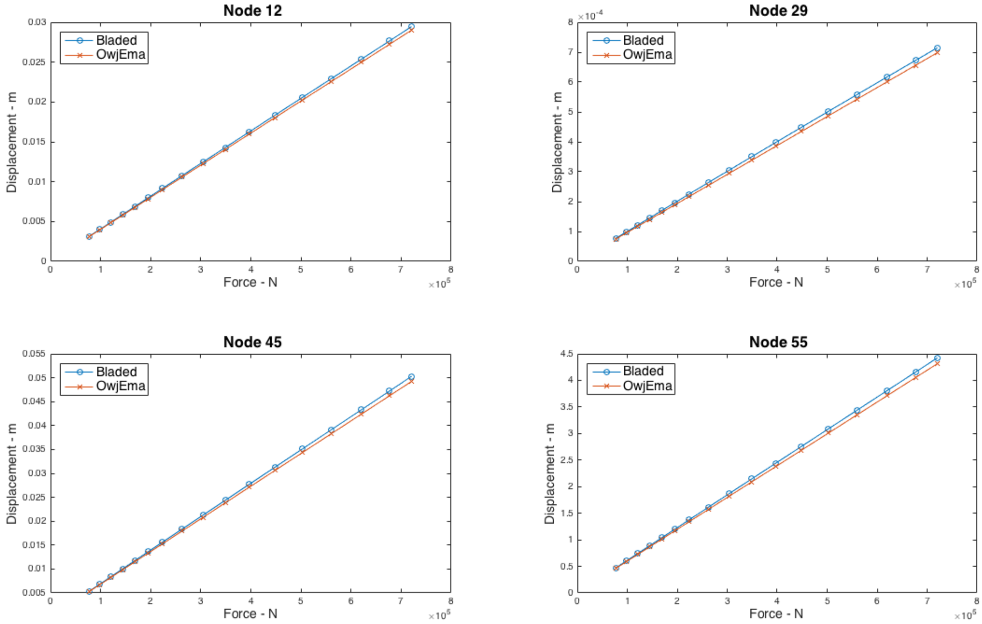

Figure 11.10: Static response scenario 4 with rigid foundation

In all scenarios, static responses are similar to Bladed displacements. It should be noted that these results are for rigid foundations. The same simulations are performed but with the soil properties defined in Table 11.3. The results are presented on Figure 11.11, Figure 11.12, Figure 11.13 and Figure 11.14.

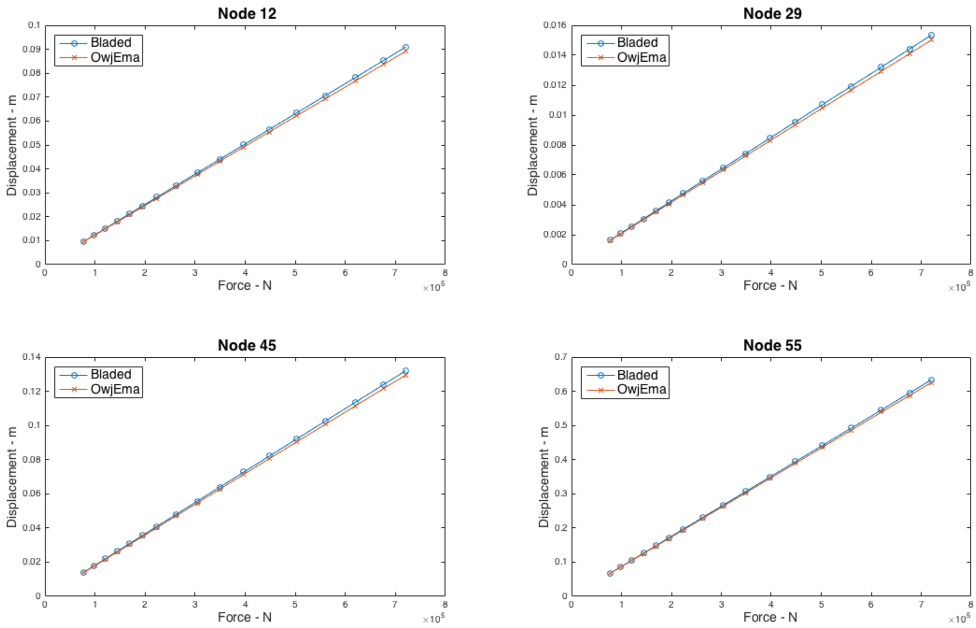

Figure 11.11: Static response scenario 1 with stiff foundation

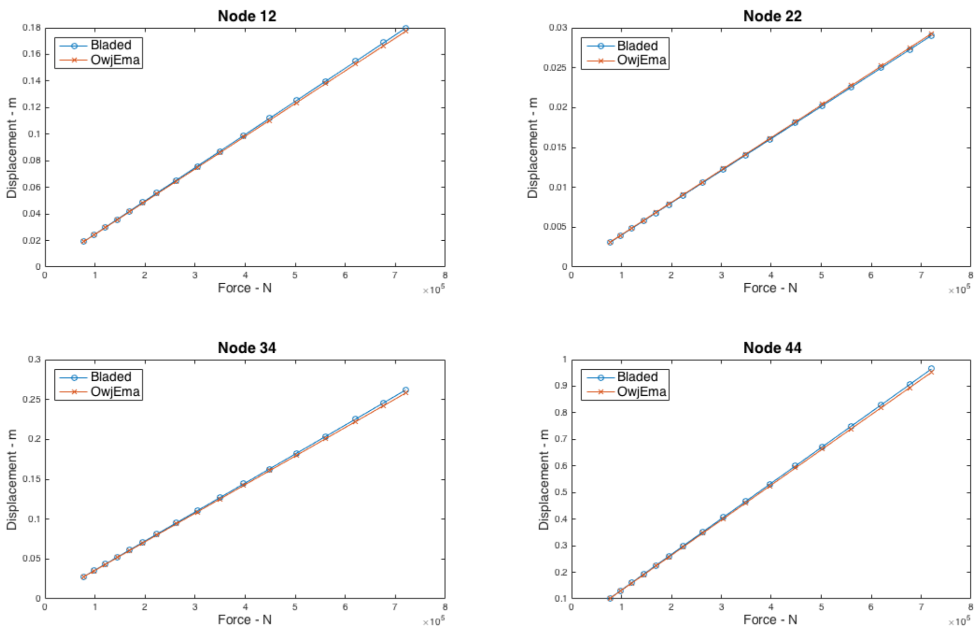

Figure 11.12: Static response scenario 2 with stiff foundation

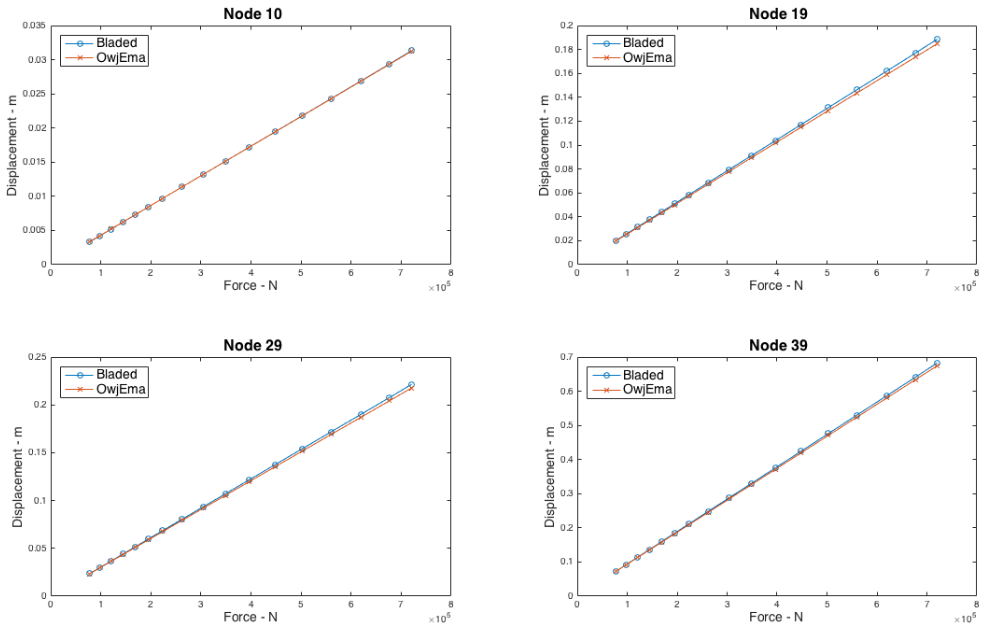

Figure 11.13: Static response scenario 3 with stiff foundation

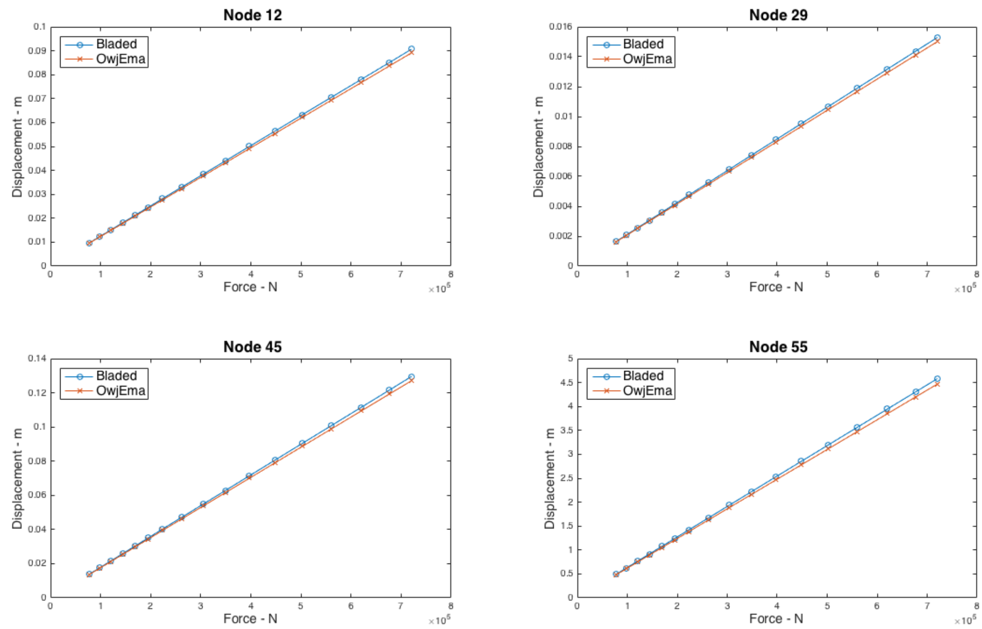

Figure 11.14: Static response scenario 4 with stiff foundation

In each situation, the static responses at the different nodes are the same in Bladed and OwjEma. The conclusion of such results is that the stiffness matrix K $_{glob}$ defined in OwjEma can be trusted.

11.4. Modal analysis check

The last part of the model to be checked is the modal analysis section. Since the stiffness matrix of the model has been verified in the previous section, checking the results of the modal analysis is equivalent to verifying the reliability of the mass matrix. Again, this check is done by comparing Bladed's results to OwjEma's results. However, the modal analysis in Bladed is not the same as the one proposed by OwjEma. In Matlab, the function used for modal analysis is *eig*, which solves the following equation:

$$K_{glob} V_{\omega} = M_{glob} V_{\omega} D_{\omega} \tag{11.1}$$

Where V_{ω} is the eigenmatrix and D_{ω} the diagonal matrix of the eigenvalues.
In Bladed the modes of the structure calculated are not the natural modes of the model. In fact they are split in two parts named attachment modes and normal modes. The attachments modes correspond to the structure static response to a unit load applied on the top node in one of the six direction. The normal modes refer to the modes calculated when the top node is constrained. The calculated modes are coupled by the equation of motion. For this reason, the natural frequencies are subject to change. Nevertheless, the natural frequencies returned by the modal analysis in Bladed correspond to the model linearisation.
To obtain the natural frequencies of the attachment modes, a unit load is applied at the top of the model. Each of the attachment modes corresponds to a different direction :

- Support structure fore-aft translational attachment node: force in the x- direction
- Support structure side-side translational attachment node: force in the y-direction
- Support structure vertical translational attachment node: force in the z-direction
- Support structure fore-aft rotational attachment node: moment around the x-axis
- Support structure side-side rotational attachment node: moment around the y-axis
- Support structure torsional rotational attachment node: moment around the z-axis

The definition of the Bladed modes is presented on Figure 11.15

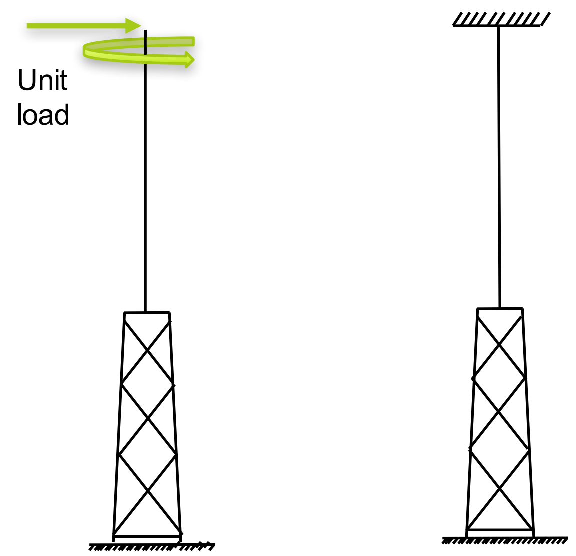

(a) Attachment modes definition

(b) Normal modes definition

Figure 11.15: Bladed modes definition

The attachment modes correspond to the static deformation associated to the unit load. Consequently, the mode shape is defined by:

$$V_{attachement,i} = K_{glob}^{-1} F_i \tag{11.2}$$

Where $V_{attachement,1}$ represents the attachment mode i and F_i the vector corresponding to the unit load. Once $V_{attachement,1}$ is known, the associated frequency is calculated with Equation 11.3.

$$M_{glob} V_{attachement,i} \omega_i^2 = K_{glob} V_{attachement,1} \tag{11.3}$$

It has to be noted that for the rotational attachment modes, the top node is considered as a hinge. The node can only rotate, the translations are constrained.
To verify the mass matrix of the model, a function Bladed_mode.m is created in OwjEma. This function calculates the modes and the natural frequencies the same way Bladed does. If the results are similar, the mass matrix can be validated and the finite element model considered as relevant for modal analysis.
A modal analysis is done for the scenarios 1, 2 , 3 and 4 for rigid foundation. The scenario 5 and 6 are tested in a different section since they represent the effect of an extra mass in the system. The simulations are done in Bladed and OwjEma. The results are presented on Table 11.5, Table 11.6, Table 11.7 and Table 11.8.

Bladed Frequencies [Hz]	OwjEma Frequencies [Hz]	Mode Type	Error (%)
0,304	0,303	Support structure side-side translational attachment node	0,33
0,306	0,305	Support structure fore-aft translational attachment node	0,33
1,307	1,302	Support structure torsional rotational attachment node	0,38
1,698	1,697	Support structure side-side rotational attachment node	0,06
1,990	1,999	Support structure fore-aft rotational attachment node	0,45
2,029	2,035	Support structure normal mode	0,30
2,029	2,035	Support structure normal mode	0,30
4,777	4,826	Support structure normal mode	1,03
4,777	4,826	Support structure normal mode	1,03
4,982	4,991	Support structure normal mode	0,18
5,816	5,820	Support structure vertical translational attachment node	0,07
6,366	6,394	Support structure normal mode	0,44

Table 11.5: Modal analysis result scenario 1 - rigid foundation

Bladed Frequencies [Hz]	OwjEma Frequencies [Hz]	Mode Type	Error (%)
0,258	0,258	Support structure side-side translational attachment node	0
0,258	0,258	Support structure fore-aft translational attachment node	0
0,993	0,989	Support structure torsional rotational attachment node	0,40
1,540	1,538	Support structure side-side rotational attachment node	0,13
1,770	1,775	Support structure fore-aft rotational attachment node	0,28
1,828	1,835	Support structure normal mode	0,38
1,828	1,835	Support structure normal mode	0,38
4,445	4,450	Support structure normal mode	0,11
4,457	4,497	Support structure normal mode	0,90
4,457	4,497	Support structure normal mode	0,90
5,527	5,530	Support structure vertical translational attachment node	0,05
6,845	6,898	Support structure normal mode	0,77

Table 11.6: Modal analysis result scenario 2 - rigid foundation

Bladed Frequencies [Hz]	OwjEma Frequencies [Hz]	Mode Type	Error (%)
0,285	0,285	Support structure side-side translational attachment node	0
0,286	0,286	Support structure fore-aft translational attachment node	0
0,540	0,538	Support structure torsional rotational attachment node	0,37
0,798	0,801	Support structure normal mode	0,38
0,798	0,801	Support structure normal mode	0,38
0,892	0,891	Support structure side-side rotational attachment node	0,11
0,940	0,941	Support structure fore-aft rotational attachment node	0,11
2,115	2,119	Support structure normal mode	0,19
2,430	2,437	Support structure normal mode	0,29
2,539	2,547	Support structure normal mode	0,32
2,539	2,547	Support structure normal mode	0,32
3,965	3,968	Support structure normal mode	0,08

Table 11.7: Modal analysis result scenario 3 - rigid foundation

Bladed Frequencies [Hz]	OwjEma Frequencies [Hz]	Mode Type	Error (%)
0,100	0,100	Support structure side-side translational attachment node	0
0,100	0,100	Support structure fore-aft translational attachment node	0
0,884	0,885	Support structure torsional rotational attachment node	0,11
1,669	1,667	Support structure side-side rotational attachment node	0,12
1,904	1,907	Support structure normal mode	0,16
1,904	1,907	Support structure normal mode	0,16
1,965	1,974	Support structure fore-aft rotational attachment node	0,46
2,106	2,138	Support structure vertical translational attachment node	1,52
4,030	4,077	Support structure normal mode	0,99
4,030	4,077	Support structure normal mode	0,99
4,828	4,840	Support structure normal mode	0,25
5,878	5,900	Support structure normal mode	0,37

Table 11.8: Modal analysis result scenario 4 - rigid foundation

In every cases, the frequencies calculated with Bladed and OwjEma are similar. These calculations have been done for rigid foundations. Stiff foundations shouldn't make the natural frequencies differ since the soil stiffness only impact the stiffness matrix, which has already been verified. However, to be sure of this assumption, the frequencies are also calculated for scenario 1, 2, and 3 with stiff foundations. The results are presented in Table 11.9,Table 11.10 and Table 11.11.

Bladed Frequencies [Hz]	OwjEma Frequencies [Hz]	Mode Type	Error (%)
0,259	0,259	Support structure side-side translational attachment node	0
0,260	0,260	Support structure fore-aft translational attachment node	0
1,268	1,263	Support structure torsional rotational attachment node	0,39
1,371	1,368	Support structure side-side rotational attachment node	0,22
1,405	1,409	Support structure normal mode	0,28
1,405	1,409	Support structure normal mode	0,28
1,534	1,536	Support structure fore-aft rotational attachment node	0,13
3,943	3,951	Support structure normal mode	0,20
4,049	4,079	Support structure normal mode	0,74
4,049	4,079	Support structure normal mode	0,74
4,869	4,871	Support structure vertical translational attachment node	0,04
4,883	4,899	Support structure normal mode	0,33

Table 11.9: Modal analysis result scenario 1 - stiff foundation

Bladed Frequencies [Hz]	OwjEma Frequencies [Hz]	Mode Type	Error (%)
0,207	0,207	Support structure side-side translational attachment node	0
0,208	0,208	Support structure fore-aft translational attachment node	0
0,950	0,947	Support structure torsional rotational attachment node	0,32
1,229	1,226	Support structure side-side rotational attachment node	0,24
1,310	1,315	Support structure normal mode	0,38
1,310	1,315	Support structure normal mode	0,38
1,355	1,355	Support structure fore-aft rotational attachment node	0
3,701	3,724	Support structure normal mode	0,62
3,701	3,724	Support structure normal mode	0,62
3,764	3,769	Support structure normal mode	0,13
4,513	4,515	Support structure vertical translational attachment node	0,04
5,659	5,699	Support structure normal mode	0,71

Table 11.10: Modal analysis result scenario 2 - stiff foundation

Bladed Frequencies [Hz]	OwjEma Frequencies [Hz]	Mode Type	Error (%)
0,243	0,243	Support structure side-side translational attachment node	0
0,244	0,244	Support structure fore-aft translational attachment node	0
0,510	0,509	Support structure torsional rotational attachment node	0,20
0,748	0,751	Support structure normal mode	0,40
0,748	0,751	Support structure normal mode	0,40
0,792	0,791	Support structure side-side rotational attachment node	0,13
0,828	0,829	Support structure fore-aft rotational attachment node	0,12
1,913	1,918	Support structure normal mode	0,26
2,225	2,232	Support structure normal mode	0,31
2,315	2,324	Support structure normal mode	0,39
2,315	2,324	Support structure normal mode	0,39
3,782	3,785	Support structure normal mode	0,08

Table 11.11: Modal analysis result scenario 3 - stiff foundation

Here again, the natural frequencies in Bladed and OwjEma are similar. The last step of the modal analysis verification is to compare the modes shape. The deformations from Bladed and OwjEma are compared on Figure 11.16 for the attachment modes and on Figure 11.17 for the normal mode. On the figures, the plots with the dots came from Bladed, the ones without the dots were from OwjEma. All the modes from Bladed and OwjEma are similar. As a result, it is safe to assumed that the modal analysis of the finite element model is correctly implemented in Matlab. This directly confirms that the mass matrix of the model is correct. Both mass and stiffness matrix describe correctly the system and take into account correctly the soil stiffness.

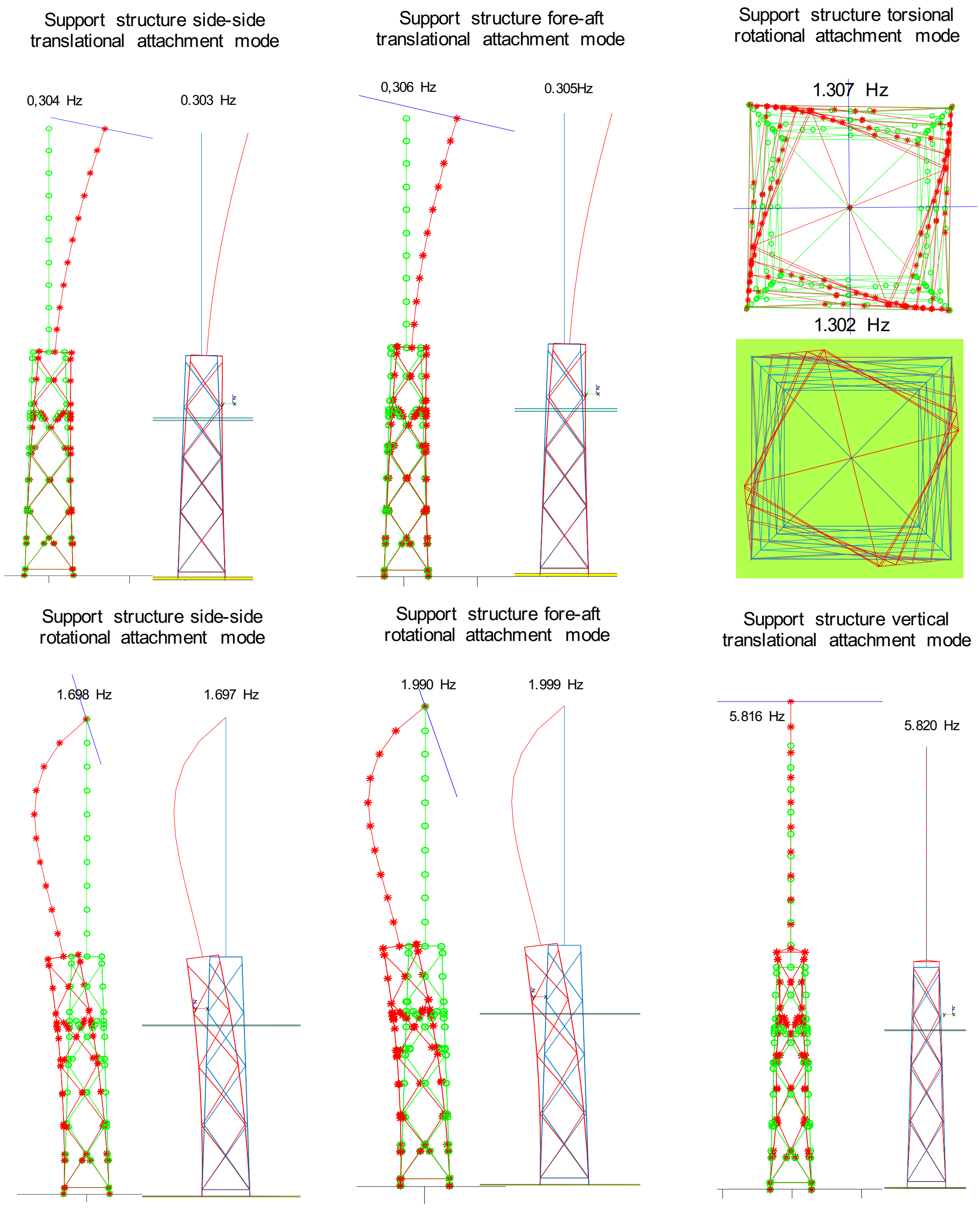

Figure 11.16: Attachment modes - scenario 1

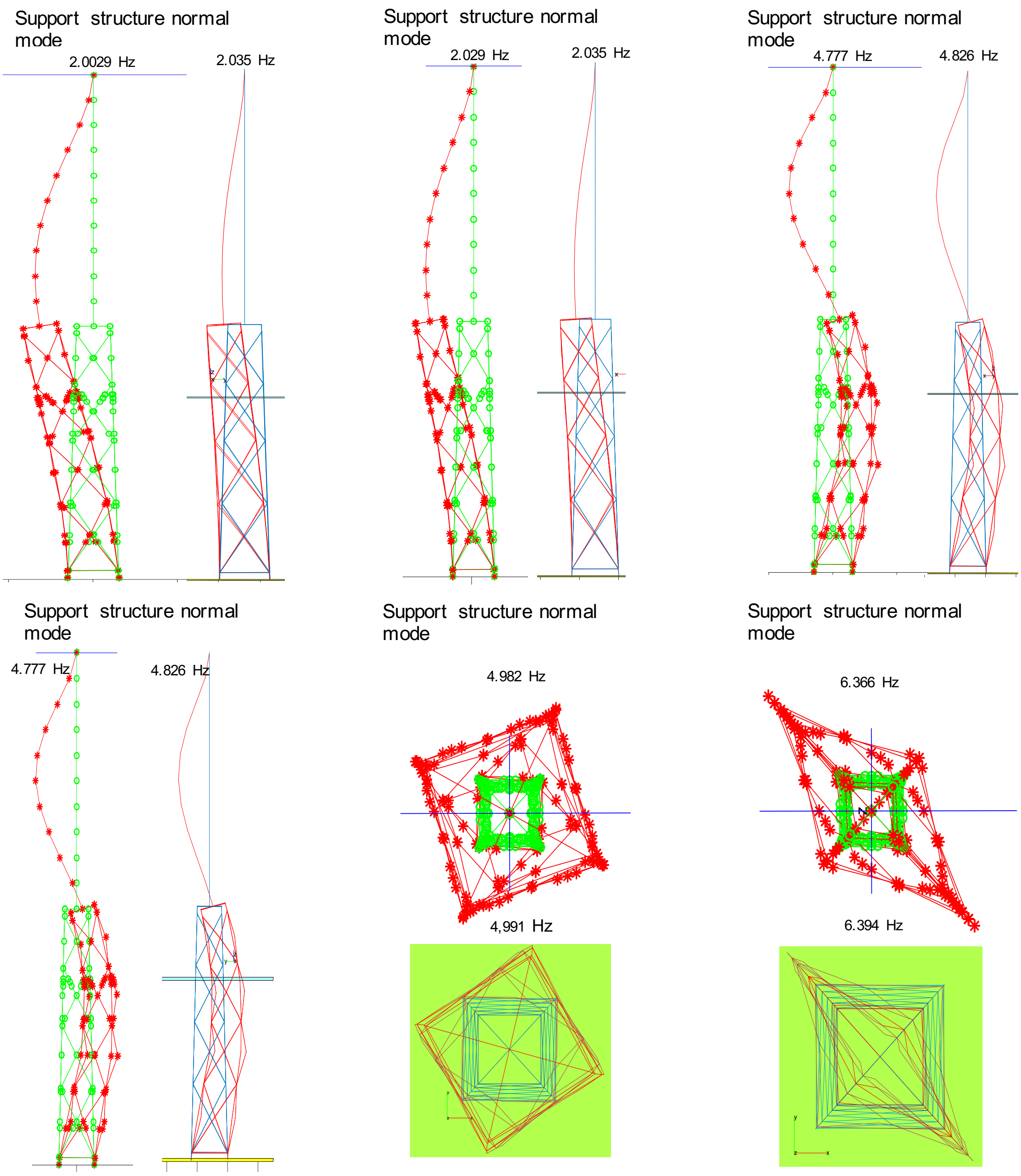

Figure 11.17: Normal modes - scenario 1

11.5. Extra mass check

In the previous section, the model mass and stiffness matrices were checked. However, the verifications carried out do not take into account the mass induced by the marine growth and the flooded members. In Bladed, these two parameters are accounted by specifying the thickness of marine growth around each member, and specifying whether the elements are flooded or not.

Scenario 5 checks the flooded elements option. In this case, both legs and brace members are flooded. Bladed has two parameters for characterizing flooded members, named *sealed* and *flooded*. The sealed parameter sets whether the member is open or not. This influences the buoyancy of the model. If the member is chosen to be sealed, the user can choose whether the item is flooded or not. In that case, the mass of the water and the mass of the member are combined in the mass matrix of the element. In OwjEma, indicating flooded members is equivalent to a sealed and flooded member option in Bladed. Verification of this statement is made with scenario 5 which considers that the legs and brace members are flooded. The modal analysis of such a scenario is carried out in Bladed and OwjEma, considering rigid foundations. The results are presented on Table 11.12.

Bladed Frequencies [Hz]	OwjEma Frequencies [Hz]	Mode Type	Error (%)
0,304	0,304	Support structure side-side translational attachment node	0
0,305	0,306	Support structure fore-aft translational attachment node	0,33
1,299	1,299	Support structure torsional rotational attachment node	0
1,690	1,689	Support structure side-side rotational attachment node	0,06
1,907	1,913	Support structure normal mode	0,31
1,907	1,913	Support structure normal mode	0,31
1,977	1,986	Support structure fore-aft rotational attachment node	0,46
4,094	4,109	Support structure normal mode	0,37
4,132	4,169	Support structure normal mode	0,90
4,132	4,169	Support structure normal mode	0,90
4,826	4,852	Support structure normal mode	0,54
5,644	5,660	Support structure normal mode	0,28

Table 11.12: Modal analysis result scenario 5 - rigid foundation

It can be noticed from the results presented in Table 11.12 that the frequencies calculated in Bladed and OwjEma are similar for scenario 5. The maximum relative error is about 0,90%, which can be considered negligible. It can be concluded that the flooded member effect is correctly implemented in OwjEma.

As for the flooded member option, the marine growth effect is verified with Bladed. According to the Bladed user manual, the marine growth is considered as an extra mass on the members. Ergo, the marine growth mass is combined to the element mass.

For this verification, the marine growth thickness is considered to be 100 mm around each submerged member with a density of 1325 kg$\cdot$m$_{-3}$. The results of the simulation are presented in Table 11.13.

Bladed Frequencies [Hz]	OwjEma Frequencies [Hz]	Mode Type	Error (%)
0,304	0,304	Support structure side-side translational attachment node	0
0,306	0,306	Support structure fore-aft translational attachment node	0
1,305	1,300	Support structure torsional rotational attachment node	0,38
1,693	1,692	Support structure side-side rotational attachment node	0,06
1,942	1,956	Support structure normal mode	0,72
1,942	1,956	Support structure normal mode	0,72
1,981	1,991	Support structure fore-aft rotational attachment node	0,5
4,280	4,364	Support structure normal mode	1,96
4,280	4,364	Support structure normal mode	1,96
4,348	4,409	Support structure normal mode	1,40
5,215	5,322	Support structure normal mode	2,05
5,784	5,791	Support structure vertical translational attachment node	0,12

Table 11.13: Modal analysis result scenario 6 - rigid foundation

The frequencies calculated in Bladed and OwjEma with a marine growth thickness of 100 mm and a density of 1325 kg $\cdot$m$_{-3}$ are similar. For the modes 8, 9 and 10, the relative error is higher than in the scenarios without biofouling. Even if these errors are relatively small (less than 2%), the result should be considered carefully for higher modes.

11.6. Conclusion verifications

In this part, the model has been verified in several ways, from simple checks to more complex verifications. The clamped beam checks in Chapter 10 has shown that the physics implemented in the model was correct for the basic structures.
Chapter 11 showed the model was able to reproduce the Bladed results. Assuming that the Bladed software provides reliable outputs, it can be stated that the OwjEma program returns correct results. Since these outputs are based on the model's mass and stiffness matrices, we can assume that the matrices are correctly defined. In conclusion, even though the modes and eigenfrequencies can not be directly verified with Bladed, their values are assumed to be correct. The modal analysis of OwjEma is validated for an offshore lattice structure.
It has been proven that the model returns a correct result for a modal analysis. Still, it should be kept in mind that the model is constructed according several assumptions, such as the design of the transition piece or the use of the p-y curve to estimate the equivalent stiffness of the soil. These assumptions may influence the results and the user should carefully consider the results based on the data provided to the model.

IV

Sensitivity Study

12

Comparison between a three-legged and four-legged structure

The program OwjEma offers the possibility to compare a three-legged structure with a four-legged structure. Based on this option, a sensitivity study is conducted. The objectives of this Chapter 12 is to understand how the inputs influence the structure's eigenvalues and then estimate which structure's configuration is the more appropriate. For this sensitivity study, a methodology is defined:

- First a reference configuration is considered. The structure is modelled with four legs. Since the sensitivity study is realised for the same location, the environmental inputs are assumed unchangeable. The hub height and the turbine parameters are also non modifiable, since the study is only for the substructure design. The rest of the geometric parameters are subject to change.

- Then, the modes and the eigenfrequencies are calculated. Since this output depends on the type of soil rigidity, the study is done for the three cases stiffness_type = 0, stiffness_type = 1 and stiffness_type = 2. In each case, the value of the first six natural frequencies are presented. Additionally, to each scenario are calculated the structure's mass, the volume of steel, the surface (to estimate the "structure transparency") and the number of nodes and elements. These parameters are used to choose the more appropriate scenario.

- After establishing the reference configuration, a similar three-legged structure is modelled in OwjEma. The structure has the same parameters as the base case except for the number of legs. The natural frequencies are calculated.

- The next step is the modification of the three-legged structure's inputs until reaching a similar first natural frequency as the one from the reference configuration structure. The parameters modified are split in two categories: the ones with a large influence, and the ones with a small impact on the natural frequencies.

- Once the parameters have been modified individually, they are combined to obtain an optimal three-legged design. The mass, the amount of steel, the number of nodes and element and the structure's surface are computed for both configurations and compared. This comparison is used to estimate which concept is the best. The behaviour of the other natural frequencies is also considered.

12.1. Unchangeable parameters

Before modelling the four-legged structure, the environmental parameters are established. In this chapter, all the scenarios are assumed to be at the same location. Consequently, the environmental parameters remain the same in all cases. These inputs are listed in Table 12.1 and Table 12.2. The soil parameters are used when the stiff foundations option is selected. For this study, the soil is composed of three layers, two of clay and one of sand.

Input	**Description**	**Values**	**Unit**
msl	Mean sea level	50	meter
rho_w	Sea water density	1025	$kg.m^{-3}$
splash_zone	Splash zone amplitude	2	meter
u_current	Current velocity	0	$m.s^{-1}$
current_dir	Current direction	0	rad
T	Wave period	100	s
wave_a	wave amplitude	0	meter
wave_dir	Wave direction	0	rad
mg_region	Geographical region (for the marine growth)	N/A	-
mg	Marine growth thickness. If the region is unknown, the average marine growth is entered here. Otherwise it should be entered 'N'	0	meter
rho_mg	Marine growth density	1325	$kg.m^{-3}$

Table 12.1: Base case environmental inputs

Layer ID	Layer type	Layer depth [m]	γ [$kg\cdot m^{-3}$]	ϕ [deg]	s_u [Pa]	ε [-]	ν [-]
1	2	0	8000	0	25000	0,02	0,3
2	1	2	8000	30	0	0	0,3
3	2	4	10000	0	100000	0,005	0,3

Table 12.2: Base case soil parameters inputs

Table 12.1 and Table 12.2 list the inputs which cannot be modified (not without changing the structure's location). The structure needs to be adapted to those parameters. However, it exists another type of inputs non subject to change, the ones representing the turbine.
The turbine is considered as non-modifiable parameter for two reasons. The first reason is that the chosen concept should not influence the production of electricity. Therefore, the wind turbine and the hub height cannot be changed. The second reason is that the purpose of this section is to understand the differences between a three-legged and a four-legged structure. Consequently, to obtain results as accurate as possible, the turbine should not influence the results of the study.
The parameters of the turbine are presented in Table 12.3.

Input	**Description**	**Values**	**Unit**
M_nacelle	Mass of the nacelle	240	tons
M_rotor	Mass of the rotor	110	tons
Rotor_inertia	Rotor moment of inertia	38791490	$kg.m^2$
Yaw_inertia	Yaw moment of inertia	24000000	$kg.m^2$
Hub height	Hub height, from the mean sea level	90	meter

Table 12.3: Rotor inputs

12.2. Reference configuration definition

To conduct this study, a reference configuration is defined. The main characteristic of this base scenario is to be a four-legged structure. The rest of the scenario's inputs are presented in Table 12.4, Table 12.5 and Table 12.6. The first table represents the elements' material properties (density, Young's modulus and Poisson's coefficient), the second one the geometric inputs used to establish the structure's shape. The third table is used only when stiff foundations are considered (stiffness_type = 1 and stiffness_type = 2). This table represents the foundation piles parameters, and is associated to the Table 12.2, presented in Section 12.1.

Input	Description	Value	Unit
rho_s	Steel density	8500	$kg{\cdot}m^{-3}$
E_s	Steel Young's modulus	2,10e11	Pa
nu_s	Steel Poisson's coefficient	0,3	-
rho_TP	Transition piece density	8500	$kg{\cdot}m^{-3}$
E_TP	Transition piece Young's modulus	2,10e13	Pa
nu_TP	transition piece Poisson's coefficient	0,3	-

Table 12.4: Base case material inputs

Input	Description	Value	Unit
NL	Number of legs. Can be 3 or 4	4	-
Jh	Jacket height	70	meter
L_bottom	Bottom width	12	meter
L_top	Top width	8	meter
h0	Distance from the seabed to the bottom horizontal member	2	meter
TPL	Distance from the top horizontal member to the transition piece	2	meter
h_tp	Transition piece height	0	meter
Dl_bottom	Outer leg diameter at the sea bed	1,289	meter
Dl_top	Outer leg diameter at the top	1,123	meter
tl_bottom	Leg wall thickness at the sea bed	0,0537	meter
tl_top	Leg wall thickness at the top	0,0312	meter
Fl_leg	Specifies if the legs are flooded or not ('Y' for yes, 'N' for no)	N	-
Fl_brace	Specifies if the brace members are flooded or not ('Y' for yes, 'N' for no)	N	-
BA	Specifies if the batter angle is constant or not ('Y' for yes, 'N' for no)	N	-
Bay_inter	Represents the number of bays in the lower part of the structure if the batter angle is not constant	Y	-
ht	Tower height	70	meter
Dt_bottom	Outer tower diameter at the transition piece	5,5	meter
Dt_top	Outer tower diameter at the top	4	meter
Tt_bottom	Tower wall thickness at the transition piece	0,034	meter
Tt_top	Tower wall thickness at the top	0,02	meter
Bracing_type	Defines the type of bracing(X , Z or K, see section 3.2.3) by entering 'X', 'Z' or 'K'.	X	-
Nb	Represents the number of bays	4	-
Horizontal_member	Defines the presence or not of horizontal members between each bay with the value 'Y' for yes and 'N' for no	N	-
D_brace	Outer brace members diameter	0,732	meter
t_brace	Brace members thickness at the top	0,020	meter

Table 12.5: Base case geometric inputs

Input	Description	Value	Unit
Lf	Pile length	30	meter
Df	Pile outer diameter	1,22	meter
t_fun	Pile wall thickness	0,01	meter
Delta_z	Step interval for the p-y and t-z curves computation	1	meter
F_x	Static load at the top of each pile in the x direction	10000	N
F_y	Static load at the top of each pile in the y direction	10000	N

Table 12.6: Base case foundation pile inputs

12.3. Reference configuration analysis

The reference configuration is modelled in OwjEma. Based on the parameters defined in Section 12.1 and Section 12.2, the structure's natural frequencies are calculated. The first six natural frequencies are presented in Table 12.7. The analysis is done for rigid and stiff foundations. The definition of the input *stiffness_type* is given in Section 4.4 and 7.1.6.

	Natural frequency [Hz]		
Mode number	**stiffness_type = 0**	**stiffness_type = 1**	**stiffness_type = 2**
1	0,304	0,258	0,259
2	0,306	0,260	0,260
3	1,301	1,097	1,105
4	1,495	1,153	1,162
5	1,622	1,258	1,274
6	2,651	2,313	2,333

Table 12.7: Base case natural frequencies

In addition to the modal analysis, some parameters characterizing the concept are computed. These parameters are the structure's mass, the structure's surface, the steel volume, the number of nodes and the number of elements. The structure's surface represents the total outer surface of the elements. This parameter is relevant to estimate the structure's transparency. It has an influence on the scour effect and the hydrodynamics loads applied on the structure. These parameters' values are presented in Table 12.8, and are named the **cost parameters**.

Parameters	stiffness_type = 0	stiffness_type = 1	stiffness_type = 2
Total mass [ton]	886,22	895,91	895,91
Structure surface [m^2] - without foundation	3757,22	3757,22	3757,22
Volume of steel[m^3]	104,26	105,40	105,40
Number of nodes	55	59	59
Number of elements	110	114	114

Table 12.8: Base case cost parameters

The values presented in Table 12.7 and Table 12.8 are considered as a reference. At this point of the study, they are not meaningful, since they need to be compared to the values from other scenarios to be understood properly. This is the objective of the next sections.

12.4. Configuration for three-legged structure

In this section, a three-legged structure is compared to the reference configuration. To model this concept, all the parameters are considered to be the same as the ones from the base case. The only exception is the number of legs, which is changed from four to three.
The natural frequencies and the cost parameters are computed for this scenario. The results are presented in Table 12.9 and Table 12.10.

	Natural frequency [Hz]		
Mode number	**stiffness_type = 0**	**stiffness_type = 1**	**stiffness_type = 2**
1	0,258	0,207	0,207
2	0,259	0,207	0,207
3	0,988	0,944	0,956
4	1,336	1,002	1,008
5	1,435	1,053	1,059
6	2,563	2,243	2,262

Table 12.9: Three-legged case natural frequencies

Parameters	**stiffness_type = 0**	**stiffness_type = 1**	**stiffness_type = 2**
Total mass [ton]	723,77	733,46	733,46
Structure surface [m^2] - without foundation	3071,47	3071,47	3071,47
Volume of steel[m^3]	85,14	86,29	86,29
Number of nodes	44	47	47
Number of elements	85	88	88

Table 12.10: Three-legged case cost parameters

One thing to be noted from this analysis is that the first natural frequency is smaller than the one from the reference configuration. The objective is then to modified the inputs of the three-legged structure to increase the natural frequencies until reaching the same values as in the reference case.
It can also be noted that cost parameter are smaller than in the reference configuration. This makes sense, since the number of legs is reduced, the number of elements decreases, as well as the mass, the amount of steel, the surface and the number of nodes. Logically, this structure is cheaper than the four-legged concept. However, this is not the only criterion of selection. Assuming that the first natural frequency must be equal to 0,304 Hz to withstand the loads, how the cost parameters are going to behave?

12.5. Parameters with a large influence

The parameters increasing the first natural frequency are split in two categories: the parameters with a large influence and the parameters with a small influence. This section focus on the first category.

The first parameter to be modified is the **structure's top and bottom width** (noted L_bottom and L_top in Table 12.5). To increase the natural frequencies, the top and bottom width are increased. The parameters' new values are different according to the type of foundations:
- For stiffness_type = 0: L_bottom = 18,5 m and L_top = 14,5m
- For stiffness_type = 1: L_bottom = 17,4 m and L_top = 13,4m
- For stiffness_type = 2: L_bottom = 17,5 m and L_top = 13,5m

The new natural frequencies and cost parameters are calculated. The results are presented in Table 12.11 and Table 12.12.

	Natural frequency [Hz]		
Mode number	**stiffness_type = 0**	**stiffness_type = 1**	**stiffness_type = 2**
1	0,304	0,258	0,259
2	0,306	0,259	0,260
3	1,303	1,124	1,137
4	1,570	1,192	1,207
5	1,726	1,227	1,246
6	2,712	2,316	2,343

Table 12.11: Influence of structure width on three-legged case natural frequencies

Parameters	stiffness_type = 0	stiffness_type = 1	stiffness_type = 2
Total mass [ton]	779,85	779,31	780,23
Structure surface [m^2] - without foundation	3410,60	3348,76	3354,32
Volume of steel[m^3]	91,74	91,68	91,79
Number of nodes	44	47	47
Number of elements	85	88	88

Table 12.12: Influence of structure width on three-legged case cost parameters

With this larger width, the structure is less transparent and more impacted by the hydrodynamic loads. However, all the cost parameters are lower than the ones from the reference configuration. The increase of the top and bottom width is considered as realistic. However, it can be combined to other parameters to optimized the three-legged structure.

The next parameters to be tested are the **legs diameter and wall thickness**, noted Dl_bottom, Dl_top, tl_bottom and tl_top in Table 12.5.They are all increased with the same proportion. The modified values are:
- For stiffness_type = 0: Dl_bottom = 1,882 m Dl_top = 1,640 m tl_bottom = 7,8 cm tl_top = 4,6 cm (+ 46%)
- For stiffness_type = 1: Dl_bottom = 1,637 m Dl_top = 1,426 m tl_bottom = 6,8 cm tl_top = 4,0 cm (+ 27%)
- For stiffness_type = 2: Dl_bottom = 1,663 m Dl_top = 1,449 m tl_bottom = 6,9 cm tl_top = 4,0 cm (+ 29%)

In the case of stiff foundations, the foundation wall thickness needs to be increase by 4 cm to support the new structure weight. The result of this concept analysis are presented in Table 12.13and Table 12.14.

	Natural frequency [Hz]		
Mode number	**stiffness_type = 0**	**stiffness_type = 1**	**stiffness_type = 2**
1	0,304	0,258	0,259
2	0,306	0,259	0,260
3	1,077	0,987	0,998
4	1,459	1,135	1,440
5	1,567	1,194	1,199
6	2,528	2,297	2,311

Table 12.13: Influence of legs diameter on three-legged case natural frequencies

Parameters	stiffness_type = 0	stiffness_type = 1	stiffness_type = 2
Total mass [ton]	1030.97	941.41	955.68
Structure surface [m^2] - without foundation	3437,66	3286,41	3302,33
Volume of steel[m^3]	121,29	110,75	112,43
Number of nodes	44	47	47
Number of elements	85	88	88

Table 12.14: Influence of legs diameter on three-legged case cost parameters

The structure mass is significantly increased, as well as the structure surface. Moreover, the new values of the legs diameter and wall thickness are really high and look unrealistic. This scenario should be combined to another to be feasible.

In order to reduce the augmentation of the legs diameter and wall thickness, the brace members and the tower are also increased. Ergo, in this scenario, **the diameter and the wall thickness of all the structure's members** are increased by the same percentage. As for the previous case, the foundations' wall thickness are increased by 4 cm to support the new members' mass. The modified parameters are: Dl_bottom, Dl_top, tl_bottom, tl_top, Dt_bottom, Dt,top, Tt_bottom, Tt_top, D_brace and t_brace. The increased percentage applied to these parameters are:
- For stiffness_type = 0: +14%
- For stiffness_type = 1: +9,5%
- For stiffness_type = 2: +9,5%
The results are presented in Table 12.15 and Table 12.16.

	Natural frequency [Hz]		
Mode number	**stiffness_type = 0**	**stiffness_type = 1**	**stiffness_type = 2**
1	0,304	0,258	0,258
2	0,306	0,259	0,259
3	1,180	1,075	1,086
4	1,495	1,209	1,216
5	1,575	1,265	1,273
6	2,991	2,593	2,616

Table 12.15: Influence of member diameter and wall thickness on three-legged case natural frequencies

Parameters	**stiffness_type = 0**	**stiffness_type = 1**	**stiffness_type = 2**
Total mass [ton]	940,61	914,68	914,68
Structure surface [m^2] - without foundation	3501,47	3363,26	3363,26
Volume of steel[m^3]	110,66	107,61	107,61
Number of nodes	44	47	47
Number of elements	85	88	88

Table 12.16: Influence of member diameter and wall thickness three-legged case cost parameters

This scenario increases significantly the amount of steel and the surface of the structure. The increase of elements' diameter and wall thickness are more realistic than in the previous case. However, the increase of the structure's surface is huge and may leads to a problem when considering the hydrodynamic loads.

In the previous scenarios, the elements' diameter has been increased, causing an augmentation of the structure's surface. What if only the **wall thickness of the members is increased**? Consequently, in this scenario the hydrodynamic loads applied on the structure remains the same. The parameters concerned are tl_bottom, tl_top, Tt_bottom Tt_top and t_brace. They are increased by:
- For stiffness_type = 0: +54%
- For stiffness_type = 1: +38%
- For stiffness_type = 2: +38%
Again, for the stiff foundations cases, the pile wall thickness are increased by 4 cm. The results are presented in Table 12.17 and Table 12.18.

	Natural frequency [Hz]		
Mode number	**stiffness_type = 0**	**stiffness_type = 1**	**stiffness_type = 2**
1	0,304	0,258	0,258
2	0,306	0,259	0,259
3	1,196	1,096	1,108
4	1,422	1,149	1,156
5	1,493	1,197	1,204
6	2,850	2,510	2,533

Table 12.17: Influence of member wall thickness on three-legged case natural frequencies

Parameters	stiffness_type = 0	stiffness_type = 1	stiffness_type = 2
Total mass [ton]	1100,09	1036,51	1036,51
Structure surface [m^2] - without foundation	3071.47	3071.47	3071.47
Volume of steel[m^3]	129,42	121,94	121,94
Number of nodes	44	47	47
Number of elements	85	88	88

Table 12.18: Influence of member wall thickness three-legged case cost parameters

The structure's surface remains the same. This is not the case for the other cost parameters which are highly increased. Moreover, the increased percentage applied to the members' wall thickness is really high and can leads to manufacturing problems. Therefore, this scenario, as all the other above, should be combined to other parameters to obtain an optimal three-legged structure design.

12.6. Parameters with a small influence

The parameters considered in this section are the inputs that doesn't affect enough the structure to obtain the required first natural frequency. Nevertheless, these parameters have an influence and can be combined to obtained an optimal structure design at small cost.

The program offers the possibility to add an **horizontal member** between the bays. This parameter, noted Horizontal_member in Table 12.5, increases the natural frequency of the structure. However, this augmentation is small. As an example, for rigid foundation, the new first natural frequency is 0,262 Hz when it was 0,258 Hz before. The downside of the presence of these new members is the increase of the structure's mass and surface. The cost/benefice ratio is not in the favour of the horizontal member and should therefore be excluded of the final concept design.

According to Table 3.2, the steel density can be reduced to 7800 kg·m^3. Here again, the increase is not important, from 0,258Hz to 0,260 Hz in the case of rigid foundation. Also, changing the steel quality can have un-expecting impacts on the structure and should be considered carefully when calculating the jacket's resistance.

The number of bay have an influence on the natural frequencies. However, to increase the natural frequency, the number of bay needs to be reducing, according to the OwjEma simulations. This option leads to a possible problem of structure integrity and might be dangerous.

The last parameter that can be changed is the brace pattern. In the current scenario, the brace pattern has an X shape. However, since the diagonal and the K brace shapes seem to reduce the natural frequencies, this parameter is not modified.

12.7. Optimized scenario

Based on all the simulations from the previous sections, an optimal scenario is established. The modified parameters are presented in Table 12.19.

Input	stiffness_type = 0	stiffness_type = 1	stiffness_type = 2
L_bottom [m]	15	14,4	14,4
L_top [m]	11	10,4	10,4
Dl_bottom [m]	1,4179	1,289	1,289
Dl_top [m]	1,2353	1,123	1,123
tl_bottom [m]	0,0650	0,070	0,070
tl_top [m]	0,0378	0,040	0,040
t_brace [m]	0,0242	0,026	0,026
Tt_bottom [m]	0,0411	0,044	0,044
Tt_top [m]	0,0242	0,026	0,026
tf [m]	-	0,02	0,02

Table 12.19: Optimal three-legged scenario inputs

The natural frequencies and the cost parameters are calculated for each foundation type (rigid and stiff). The results are listed in Table 12.20 and Table 12.21.

	Natural frequency [Hz]		
Mode number	stiffness_type = 0	stiffness_type = 1	stiffness_type = 2
1	0,304	0,258	0,258
2	0,306	0,259	0,259
3	1,188	1,133	1,142
4	1,512	1,155	1,168
5	1,622	1,183	1,194
6	2,794	2,463	2,492

Table 12.20: Three-legged structure optimized natural frequencies

Parameters	stiffness_type = 0	stiffness_type = 1	stiffness_type = 2
Total mass [ton]	918,49	963,70	963,70
Structure surface [m^2] - without foundation	3211,27	3119,40	3119,40
Volume of steel[m^3]	108,06	113,38	113,38
Number of nodes	44	47	47
Number of elements	85	88	88

Table 12.21: Three-legged structure optimized cost parameters

The choice of these parameters' value is based mainly on the structure's surface, and then on the structure's mass and the steel's volume. The objective is to obtain a structure's surface smaller than the scenarios previously established.

12.8. Comparison analysis

Once the optimized scenario for a three-legged structure is established, it can be compared to the reference configuration, the four-legged structure. Several parameters must be considered when comparing the two scenarios, such as the amount of steel used, the number of welds, the transport and installation process, the average cost, the structure's transparency and the difference between the higher natural frequencies.

The reference configuration uses less steel than the optimized three-legged structure, respectively 105,40 m^3 and 113,38 m^3 for stiff foundations. This difference is explained by the increased in the structure wall thickness, legs' diameter and base width. Strictly based on the steel, the three-legged structure is more expensive than the reference configuration. However, the steel is not the only criterion considered when designing a jacket. The complexity of the member and the welds have an important role.

In the three-legged scenario, 47 nodes and 88 elements are present, against 59 nodes and 114 elements in the reference configuration. Therefore, if considering only welds at the extremity of the members, 84 welds are performed in the three-legged scenario against 109 in the four-legged case. Even if some welds are more complexed than other, the cost will be higher in the reference configuration. The small amount of members in the optimized scenario reduces the production time and consequently the manufacturing costs.

The transport of both structures is similar. However, the three-legged structure has a advantage over the reference configuration: the number of piles. Since only three piles need to be installed to support the structure, the installation time is considerably reduced, as well as the costs and the risks.

Apart from the manufacturing, transport and installation costs, the influence of the hydrodynamic loads are taken into account. These loads are dependent on the structure's surface. For the three-legged concept the surface is 3119,40 m^2 against 3757,22 m^2 for the reference scenario. Therefore, the three-legged structure is more efficient when considering the hydrodynamics loads. This can be confirmed by computing the equivalent stick model of both scenarios. The results are shown on Figure 12.1 for the equivalent inertia diameter and Figure 12.2 for the equivalent drag diameter. Both figures proved that the three-legged structure is less impacted by the hydrodynamic loads than the four-legged design.

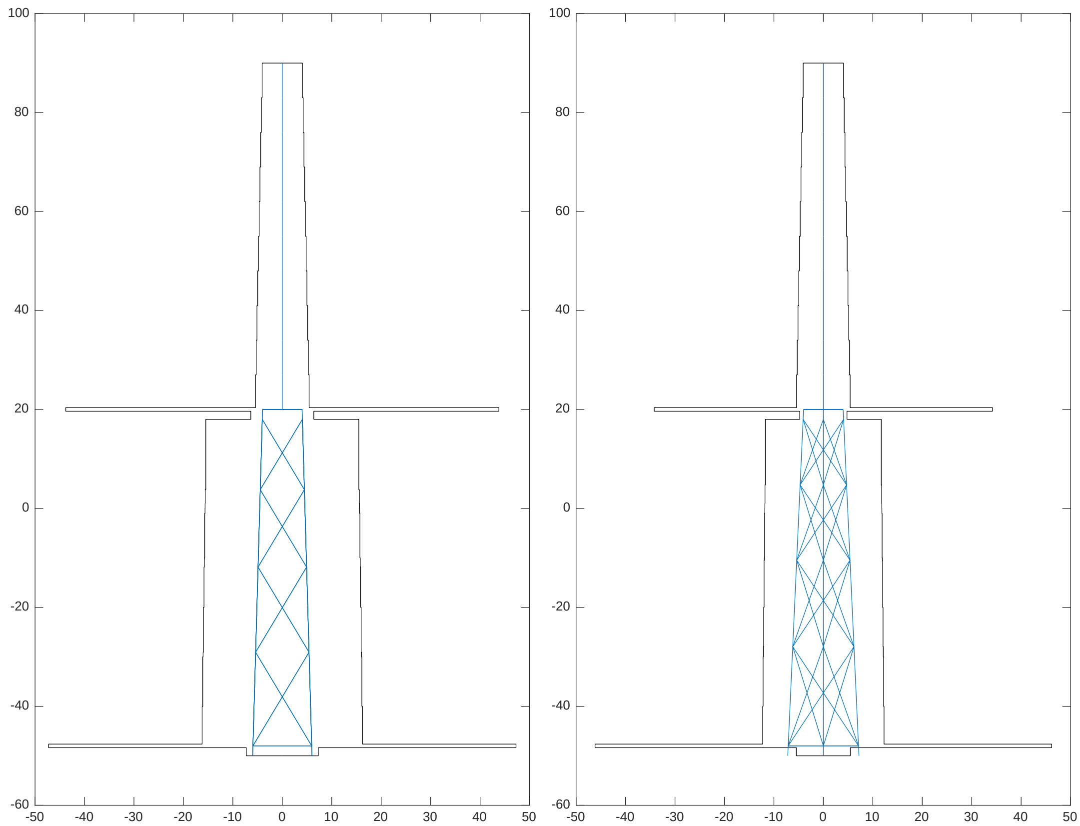

(a) Reference configuration

(b) Optimized configuration

Figure 12.1: Equivalent inertia stick models

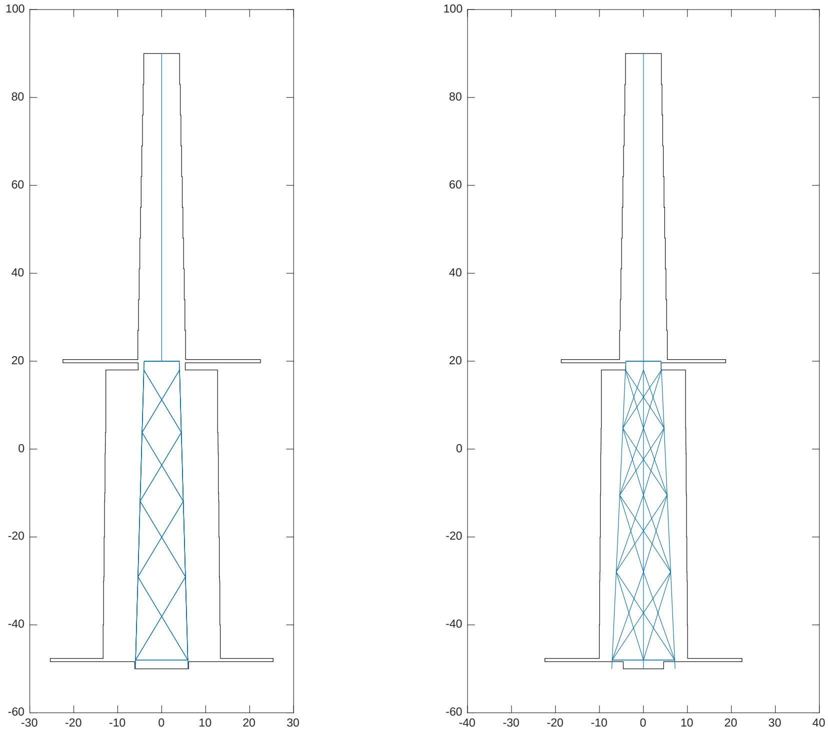

(a) Reference configuration (b) Optimized configuration

Figure 12.2: Equivalent drag stick models

The three-legged model has been designed to have the same first natural frequencies as the reference configuration. But the other natural frequencies are also impacted. Table 12.22 shows the relative error between the natural frequencies from the reference configuration and the ones from the optimized scenario. It can be noted that the higher the modes are, the larger the relative error is. This should be considered carefully when designing the structure. The natural frequencies does not change at the same rate as the other. Therefore, the new configuration might be subject to resonance from harmonic loads that were not impacting the reference structure. If the external loads are known, a clear choice can be made between the four-legged and the three-legged concept.

	Relative error [%]		
Mode number	**stiffness_type = 0**	**stiffness_type = 1**	**stiffness_type = 2**
1	0	0	0
2	0	0,38	0,38
3	9,5	3,28	3,35
4	1,12	0,17	0,52
5	8,49	5,96	6,28
6	5,39	6,49	6,82

Table 12.22: Relative error between the natural frequencies of the reference configuration and the optimized scenario

Based on the previous parameters, the three-legged structure seems to be more relevant than the four-legged. It seems to be less expensive, easier to installed and offer less surface to the hydrodynamic loads. However, there are uncertainties on the higher natural frequencies. If the frequencies of the loads applied on the structure are known, the choice of the concept might change. Without this information, it seems for now that the three-legged concept is the more appropriate.

V

Conclusion

13
Conclusion

13.1. Model objective achieved

The goal of this master's thesis is to design a finite element model for an offshore wind support structure. This model is supposed to represent different lattice structure configurations. Then, with the program, the user should be able to easily conduct sensitivity studies and understand the behaviour of the structure. The main outputs of the model are the eigenfrequencies and the modes shape of the lattice structure.
This model was designed to make the simulations easy to perform, where other programs can appear to be overwhelming for beginners. The program, coded in Matlab, was meant to be intuitive and user-friendly. For this reason, it was decided to make it accessible to anyone with little knowledge of the offshore wind industry. To avoid the "black box" effect, the program returns the details of the steps taken by the algorithm and returns the most relevant possible outputs to understand the model.
The model can be used as a pre-design tool, which implies it must be fast and easy to modified the inputs. This is why the interface offers many options for customizing the lattice structure's design. Since this is a pre-design structure, the model is made Bladed compatible, returning outputs that can be directly implemented in the professional software.
Furthermore, OwjEma returns a more accurate result for modal analysis than Bladed does. This is justified by the fact that Bladed doesn't return natural modes. As a result, the use of OwjEma is more relevant to understand the natural modes and frequencies of a lattice structure.

13.2. Inputs selection

One of the first steps of the project was to select the relevant inputs for the model. As a result, various parameters have been reviewed, such as the different designs of lattice structures, the possible brace patterns, the design of the transition piece and the parameters influencing the mass and the rigidity. Yet, some of the existing designs were out of the study's scope, such as the tripod, the twisted jacket of the full truss concept. Different versions of the foundations have been considered, such as the jacket foundation, the tower foundation and the suction bucket. As the tower structure is more representative of the industry, it was decided to give it more attention.
The overview of the selected inputs is presented on Figure 3.11. The list of the inputs is not exhaustive and can be extended in the future to add more options to the model.

13.3. OwjEma possibility and limitation

With all of these inputs, the model offers various possibilities but also limitations:

- It is possible to model a lot of different lattice structures, to visualized them and calculate their modes and natural frequencies. But this number of possible designs is also one of the limit of the program. The lattice structure can be model only based on existing inputs. In other words, the number of possibilities is not infinite and cannot represent any type of multi-member structures. Nevertheless, this problem can be partially fixed in the future by increasing the number of possibility.

- Another limitation of the model concerns the assumptions made. The transition piece is not entirely modelled, but simplified as a rigid part of the structure. Consequently, the model can not currently give a result to check the effect of the transition piece on the eigenfrequencies.

- Another assumption made with the model is the use of the p-y curves to estimate the equivalent stiffness of the foundation. First, this stiffness has been calculated at the ULS, so it might be overestimated. Also, the equivalent stiffness is considered linear in the model, which can lead to imprecision.

- For now, the model is linear and doesn't take into account the effect of time dynamically. In consequence, it has to be kept in mind that the model only represents a structure at moment in time, not through time.

- Finally, the last part added to the model (the dynamic response analysis), should be developed and checked. For now, this section cannot be used to conduct simulation without major uncertainties. This is where the model shows its limitation. Since the dynamic response analysis is not the initial objective, it should be considered as an extra feature of the program which could be developed later.

13.4. Comparison between three-legged and four-legged structures

The program OwjEma can be used to perform sensitivity studies and optimized a concept. An example of such operation is presented in Chapter 12. A three-legged and a four-legged structure with the same first natural frequency are compared. The objective is to establish which concept is the more appropriate, based on the costs, the installation and the resistance to the loads.
The three-legged concept has been established based on the four-legged structures inputs. Since it is easy to modify the parameters in OwjEma, the inputs of the three-legged structure have been changed until reaching the same first natural frequency of the four-legged design.
The program is used to calculate the mass, the surface and the amount of steel used in both concepts. According to these parameters, an indication on the structures' cost is obtained. A function named equivalent_stick_model.m is used to calculate the equivalent stick model of both designs. Consequently, the influence to the hydrodynamic loads can be visualized.
According to all of these information, the best concept has been chosen. In this scenario, the three-legged structure is more efficient than the four-legged structure.

13.5. Recommendation

Based on the possibilities and limitations detailed in the previous section, some recommendations can be made for further researches:

- Sensitivity studies: the model was designed to represent the modal behaviour of an offshore wind support structure. The initial plan was to be able to conduct studies on the parameters that influence the most the natural frequencies and the shape of the modes. Hence, the model can be used to try to understand the dynamic behaviour of a lattice structure.

- Pre designed function: another characteristic of the model is its possible use as a pre design tool. It can be used to get quick design's proposals and check if these proposals are feasible. Then, based on these results, the established design can be implemented in other software, such as Bladed or Ansys, to perform more advanced research and optimize the design.

- Check the dynamic response: this section has been added to the program as an extra function, representing the next step of the program. Consequently, the dynamic response analysis section could be improved. This section needs to be extensively checked and a way to improve the computational efficiency of the function should be considered.

- Add new functions: based on the previous recommendations, the model can also be extended for other purposes. For now, it correctly describes the modal behaviour of the structure and gives an indication of the dynamic response. Other features may be added, such as the buckling effect or the computation of the resistance at the ULS and FLS .

- Equivalent stiffness non-linearity: the equivalent stiffness is estimated with the p-y and t-z curves. To obtain such results, the user has to enter a static input force. Then rigidity is calculated as a constant value and implemented in the model. Hence, the program does not take into account the non-linear part of the soil. This approximation should be kept in mind and fixed in the future.

- Soil equivalent rotational stiffness: the equivalent soil stiffness only considers the soil's lateral and vertical resistance. However, the rotational stiffness should be also considered for more accurate results. This can be done by modifying the functions soil_boundary_condition.m and p_y_t_z_curves.m.

- Inclined foundation pile: In OwjEma the piles are modelled as vertical beams. This is relevant for a tower substructure, but for a jacket case, the pile should be considered as inclined. This can be done by modifying the angle of the foundation pile in soil_boundary_condition.m and modified the piles' surface in contact with the soil layers.

- Addition of additional masses: It is possible to take into account the additional mass caused by the presence of sacrificial anodes, cables, ladders and other external parameters. Mass can be directly added to the diagonal terms of the global mass matrix. The rows and columns of the mass matrix are those linked to the nodes where the mass is present. This option is not in the program because the ladders, cables, sacrificial anodes and other external masses are specific to each concept. The user can manually decide where to implement these masses, and thus customize the structure.

- Axial load effect: In OwjEma, the effect of the axial load in the member is not considered. But these loads affect the elements' stiffness and consequently the structure's natural frequencies. Therefore, they should be considered when calculating the structure resistance and can be implement to the program in the future.

- Adaptation to the oil industry: the program has been designed for the offshore wind industry. Yet, the core of the code can be used to adapt the OwjEma program to the oil industry. This can be done by making the wind turbine tower really small, with a large diameter and a different density. Or the function FE_tower.m can be deleted to directly add a higher mass to the upper node of the transition piece.

A

START_OwjEma.m script

```
                %%%%%%%%%%%%%%%%%%%%%%%%%%%%%%%%%%%%%%
                %              OwjEma                %
                % FE model of a wind turbine jacket  %
                %       Emeric Descourtieux          %
                %              May 2018              %
                %               V 1.1                %
                %%%%%%%%%%%%%%%%%%%%%%%%%%%%%%%%%%%%%%

clear all
close all

%%%%%%%%%%%%%%%%%%%%%%%%% INPUTS DEFINITION %%%%%%%%%%%%%%%%%%%%%%%%%%%%%%%

% Enter the configuration name :
Inputs = 'Configuration_test.mat' ;
%===========================================================================
%===========================================================================
% Section 1
% Environment inputs

msl = 50;         % Mean sea level - meter
rho_w = 1025;     % Sea water density - kg/m3
splash_zone = 2;  % Amplitude splash zone - meter

u_current = 0;    % Current velocity - m/s
current_dir = 0;  % Current direction - rad. 0 in the x direction, pi/2 in
                  % the y-direction

T = 100;          % Wave period - s
wave_a = 0;       % Wave amplitude - meter
wave_dir = 0;     % Wave direction - rad. 0 in the x direction, pi/2 in
                  % the y-direction


mg_region = 6;    % Marine growth - region :
                  % 1 : Central and Northen North Sea
                  % 2 : Noregian Sea
                  % 3 : Southern North Sea
                  % 4 : Central and Southern California
                  % 5 : Gulf of Mexico
                  % 6 : West Africa

mg = 0;           % Marine growth - meter : if region unknows, enter the
                  % average marine growth here. Otherwise enter 'N'

rho_mg = 1325;    % Marine growth density - kg/m3

%===========================================================================
%===========================================================================
```

```
% Section 2
% Material Properties Inputs

rho_s= 8500;        % Steel density - kg/m3
E_s = 2.10e11;      % Steel Young's modulus - Pa
nu_s = 0.3;         % Steel Poisson's ratio

rho_TP = 8500;      % Transition piece density - kg/m3
E_TP = 2.10e13;     % Transition piece Young's modulus - Pa
nu_TP = 0.3;        % Transition piece Poisson's ratio

%==========================================================================
%==========================================================================
% Section 3.1
% Jacket geometry Inputs
lifetime = 0;        % Lifetime - years (will increase the elements
                     % thickness to prevent corrosion)
L_max = 200;         % Maximum lenght of an element in the FE model - meter

NL = 4;              % Number of legs. Must be 3 or 4

Jh = 70;             % Jacket Height - meter

L_bottom = 12;       % Bottom width - meter
L_top = 8;           % Top width - meter

h0 = 2;              % Distance seabed to bottom brace - meter
TPL = 2;             % Distance top brace to transition piece
h_tp = 0;            % Transition piece height - meter

Dl_bottom = 1.289;   % Bottom Leg diameter - meter (outer diameter)
Dl_top = 1.123;      % Top leg diameter - meter
tl_bottom = 0.0537;  % Bottom Leg thickness - meter
tl_top = 0.0312;     % Top leg tickness - meter

Fl_leg = 'N';        % Flooded leg members. 'Y' for yes, 'N' for no.
Fl_brace = 'N';      % Flooded brace members. 'Y' for yes, 'N' for no.

BA = 'Y';            % Constant batter angle or not : 'Y' / 'N'

%--------------------------------------------------------------------------
% Section 3.2
% Bracing
Nb =4;                    % Number of bay
Brace_pattern = 'X';      % The bracing type, enter 'X', 'Z' or 'K'
Horizontal_member = 'N';  % Enter yes 'Y' or no 'N' for an horizontal
                          % member (only in the case of an X or Z bracing)

D_brace = 0.732;          % Brace diameter - meter
t_brace = 0.020;          % Brace thickness - meter

%--------------------------------------------------------------------------
% Section 3.3
% If the batter angle is constant, do not fill section 3.3, go directly to
% section 4

L_inter = 8;    % Width where the batter angle change - meter
Bay_inter = 3;  % Number of bay before the batter angle change
Jh_inter = 30;  % Height at which the batter angle change - meter
%==========================================================================
%==========================================================================
% Section 4
% Wind turbine inputs

ht = 70;                   % Tower height - meter

Dt_bottom = 5.5;           % Bottom tower diameter - meter
Dt_top = 4;                % Top towt diameter - meter

Tt_bottom = 0.034;         % Bottom tower thickeness - meter
Tt_top = 0.02;             % Top tower thickeness - meter
```

```
M_nacelle = 240;           % Mass nacelle - ton
M_rotor = 110;             % Mass rotor - ton

Rotor_inertia = 38791490; % Rotor moment of inertia - kg/m2
Yaw_inertia = 24000000;   % Yaw moment of inertia - kg/m2

%--------------------For vizualization only-------------------------------

Nacelle_length = 6;        % Nacelle length - meter
Nacelle_height = 2.5;      % Nacelle length - meter
Nacelle_width = 2.5;       % Nacelle length - meter

blade_size = 61;           % Lenght of the blades - meter

%=========================================================================
%=========================================================================
% Section 5.1
% Soil stiffness definition

% Stiffness_type :
% 0 : Rigid foundation     (speed : ++ ; accuracy : --)
% 1 : linear stiffness k0  (speed : -  ; accuracy : +)
% 2 : k_tan                (speed : -- ; accuracy : ++)

stiffness_type = 0;

%-------------------------------------------------------------------------
% Section 5.2
% If Stiffness_type = 0, skip section 5.2. Go directly to section 6

% Foudations inputs

Lf = 30;        % Pile penetration into the seabed - meters
Df = 1.22;      % Pile diameter - meters
t_fun = 0.01;   % Pile tickness - meters

Delta_z = 1;    % Step interval for the p-y curve - meters

Pile_sleeve = 'Y';             % Presence of pile sleeve or not ('Y' or 'N')
Pile_sleeve_mass = 3000;       % Pile sleeve mass - kg
Pile_excentricity = 1;         % Pile distance from the legs - meter

%Soil layer definition.

% sl [Layer ID , Layer type (1 = sand or 2 = clay) , Layer Depth -meter ,
% Density - N/m3 , Friction Angle - deg , Undrained Shear Strength - Pa
% ,Vertical Strain ,  Soil Poisson coefficient ]

sl(1, :) = [1 ,2 , 0 , 8000 , 0  ,25000 , 0.02 , 0.3];
sl(2, :) = [2 ,1 , 2 , 8000 , 30 , 0 , 0 , 0.3];
sl(3, :) = [3 ,2 , 4 , 10000 , 0, 100000 , 0.005 , 0.3];

% Static load at the top of the pile:
Fx = 1000000;     % Newton
Fy = 1000000;     % Newton

%=========================================================================
%=========================================================================
% Section 6
% Plot option

plot_3D = 'Y';         % Enter 'Y' for plotting the volume of the structure.
                       % Otherwise simply enter 'N'
line_plot = 'N';       % Enter 'Y' for plotting the line of the structure.
                       % Otherwise simply enter 'N'

Mode_plot = [1 2 3];   % The modes that will be plotted

Stick_model = 'N';     %  Enter 'Y' for plotting the equivalent stick model.
%=========================================================================
```

```
%==========================================================================
% Section 7
% Modal displacement
modal_displacement_analysis = 'N'; % Selected 'Y' for yes or 'N' for no.

% Ignore the rest of this part if you do not want to calculate the
% modal displacement. Selecting 'Yes' will increase significantely
% the computational time.

force_ampl = 100000;          % The force amplitude on the rotor - Newton
force_freq = 0.3093;          % The force frequency on the rotor - Hertz
force_dir = 0;                % Force direction - rad. 0 in the x direction,
                              % pi/2 in the y-direction

time_simulation = 100;        % The duration of the simulation - second

Node_plot = [55];             % The nodes that will be studied.
Dir_plot  = ['x','y','z'];    % The direction that will be studied.
                              % Enter 'x' for the x-direction and 'y' for the
                              % y-direction.


Displacement_plot = 'Y';     % Enter 'Y' if you want to plot the diplacement
                             % the velocity and the acceleration of the
                             % selected node in the selected direction.
                             % Otherwise enter 'N'.

Force_plot = 'Y';            % Enter 'Y' if you want to plot the force of
                             % the selected node in the selected direction.
                             % Otherwise enter 'N'.

Moment_plot = 'Y';           % Enter 'Y' if you want to plot the moment of
                             % the selected node in the selected direction.
                             % Otherwise enter 'N'.
Stress_plot = 'Y';           % Enter 'Y' if you want to plot the moment of
                             % the selected node in the selected direction.
                             % Otherwise enter 'N'.

%%%%%%%%%%%%%%%%%%%%%% END OF THE INPUTS DEFINITION %%%%%%%%%%%%%%%%%%%%%%
%% FE model
% !!! DO NOT MODIFY THIS SECTION !!!
save (Inputs,'msl','rho_w','lifetime','u_current','current_dir','T','wave_a','wave_dir',
'mg','mg_region','rho_mg','splash_zone','L_max','NL','BA','Nb','Jh','h0','TPL','h_tp',
'L_bottom','L_top','Dl_bottom','Dl_top','tl_top','tl_bottom','Fl_leg','Fl_brace',
'D_brace','t_brace','Brace_pattern','Horizontal_member','L_inter','Bay_inter','Jh_inter',
'ht','Dt_bottom','Dt_top','Tt_bottom','Tt_top','M_nacelle','M_rotor','Rotor_inertia',
'Yaw_inertia','rho_s','E_s','nu_s','rho_TP','E_TP','nu_TP','Lf','Df','t_fun',
'sl','Delta_z','stiffness_type','Fx','Fy','Mode_plot','plot_3D','line_plot',
'modal_displacement_analysis','force_ampl','force_freq','force_dir','Node_plot',
'Dir_plot','Displacement_plot','Force_plot','Moment_plot','time_simulation','Stress_plot',
'Nacelle_length','Nacelle_height','Nacelle_width','blade_size','Stick_model');
clearvars -except Inputs
[Bladed_member, Bladed_nodes, Bladed_material,Bladed_stiffness_foundation,
Modes,Eigenfrequencies,M_glob, C_rayleigh , K_glob, C_drag] = FE_model_builder(Inputs);
```

Bibliography

[1] The world factbook - cia. URL https://www.cia.gov/library/publications/the-world-factbook/fields/2233.html.

[2] Tripod support structures. URL http://www.4coffshore.com/windfarms/tripod-support-structures-aid7.html.

[3] Jacket or lattice structures. URL http://www.4coffshore.com/windfarms/jacket-or-lattice-structures-aid5.html.

[4] Cone - mathworks file exchange. URL https://nl.mathworks.com/matlabcentral/fileexchange/21951-cone?focused=5104620&tab=function.

[5] Vesta164 8mw. URL https://www.4coffshore.com/windfarms/turbine-mhi-vestas-offshore-wind-v164-8.0-mw-tid89.html.

[6] *DNVGL-RP-C205 Envirenmental conditions and envirenmental loads.* DNV GL AS, April 2007.

[7] *DNVGL-ST-0126 Support Structures for Wind Turbines.* DNV GL AS, April 2016.

[8] *DNVGL-OS-B101 Metallic materials.* DNV GL AS, July 2015.

[9] *DNVGL-RP-0416 Corrosion protection of wind turbines.* DNV GL AS, March 2016.

[10] *DNVGL-OS-J101 Design of Offshore Wind Turbine Structures.* DNV GL AS, October 2007.

[11] Yong Bai and Qiang Bai. *Subsea pipelines and risers.* Elsevier, 2005.

[12] M Bax, David Short, and David Short. *Underwater inspection.* CRC Press, 1988.

[13] Kok Hon Chew, EYK Ng, Kang Tai, Michael Muskulus, and Daniel Zwick. Offshore wind turbine jacket substructure: A comparison study between four-legged and three-legged designs. *J. Ocean Wind Energy*, 1(2):74–81, 2014.

[14] Indrajit Chowdhury and Shambhu P Dasgupta. Computation of rayleigh damping coefficients for large systems. *The Electronic Journal of Geotechnical Engineering*, 8(0):1–11, 2003.

[15] Wybren De Vries, NK Vemula, P Passon, T Fischer, D Kaufer, D Matha, B Schmidt, and F Vorpahl. Support structure concepts for deep water sites. *Delft University of Technology, Delft, The Netherlands, Technical Report No. UpWind Final Report WP4*, 2:167–187, 2011.

[16] L Gaul. The influence of damping on waves and vibrations. *Mechanical systems and signal processing*, 13(1):1–30, 1999.

[17] Cliff Gerwick. *Construction of marine and offshore structures.* CRC press, 2007.

[18] Ali Akbar Golafshani and Amin Gholizad. Friction damper for vibration control in offshore steel jacket platforms. *Journal of Constructional Steel Research*, 65(1):180–187, 2009.

[19] Yu-Hung Lin Shiu-Wu Chau I-Wen Chen, Bao-Leng Wong and Hsin-Haou Huang. Design and analysis of jacket substructures for offshore wind turbines. *Energies*, 2 April 2016.

[20] Madjid Karimirad. *Offshore energy structures: for wind power, wave energy and hybrid marine platforms.* Springer, 2014.

[21] RF Kristensen, Kim Lau Nielsen, and Lars Pilgaard Mikkelsen. Numerical studies of shear damped composite beams using a constrained damping layer. *Composite structures*, 83(3):304–311, 2008.

[22] Janusz S Przemieniecki. *Theory of matrix structural analysis.* Courier Corporation, 1985.

[23] Lymon C Reese and William F Van Impe. *Single piles and pile groups under lateral loading.* Crc Press, 2010.

[24] Ramesh Singh. *Corrosion Control for Offshore Structures: Cathodic Protection and High-Efficiency Coating.* Gulf Professional Publishing, 2014.

[25] Jean-Charles Massabuau Sirina Yark. Etat des connaissances des anodes sacrificielles en mer. *Cahier des expertises*, October 2016.

[26] B Mutlu Sumer, Jørgen Fredsøe, Klavs Bundgaard, et al. Global and local scour at pile groups. In *The Fifteenth International Offshore and Polar Engineering Conference*. International Society of Offshore and Polar Engineers, 2005.